REMARKS

Claims 1-3, 6-22 and 24-34 are pending; claims 20, 21, 25, 28 and 29 have been withdrawn from consideration; upon entry of this amendment, claims 35, 36 and 37 will be added; claims 1-19, 22-24, 26, 27 and 30-34 have been rejected.

Claims 1, 2, 7-17, 24, 32-34 have been amended and new claims 35, 36 and 37 have been added.

The amendments and new claims are supported as follows:

Claim 1: at least at pages 7-10 of the specification.

Claim 2: at least at page 11 of the specification.

Claim 35: at least at pages 26-28 of the specification.

Claim 36: at least at pages 26-28 of the specification.

Claim 37: at least at claim 1 as originally filed.

The specification has been amended as follows.

Paragraphs 32, 93, 101, and 104 are amended to properly designate trademarks.

Paragraphs 162-164, 167-168, 170-171 and 174, and Table 7 are amended to correct printing errors, where question marks should be "Å" or "→."

Support for the amendments can be found in the parent application as shown in the following chart:

Current Application	Parent application
¶162	¶137
¶163	¶138
¶164	¶139
¶167	¶142
¶168	¶143
Table 7	Table 7
¶170	¶145
¶171	¶146
¶174	¶148, lines 20-21.

Further description has been added after paragraph 92. Support for the amendment can be found at least at page 3082, column 2 to 3083, column 1; page 2830, column 2, last paragraph; page 2829, column 1; 2644, column 1, first full paragraph; page 2579, last paragraph;

page 2579, last paragraph; page 2365, column 2, last paragraph; page 2361, column 2 and page 2363, column 1; page 2359, column 2 - 2360, column 1; page 2359, column 1 of DeVita *et al.*, which is incorporated by reference at page 69, paragraph 181, and page 26, paragraph 93 of the specification. No new matter is added.

I. Partial Withdrawal of Election/Restriction Requirement Acknowledged

Applicants acknowledge Examiner's rejoinder of claims 19, 22, 24, 26, 27 30, 31 and 34, drawn to a method using the composition of Group I. Office Action, paragraph 6. The claims of both Groups I and II (claims 1-3, 6-19, 22-24, 26, 27 and 30-34) are under consideration. New claims 35 and 36 are included within Group III, and thus, should also be under consideration. Applicants further acknowledge that the Examiner withdraws the species requirement from the claims of Group II. Office Action, paragraph 6. In addition, Applicants acknowledge that the Examiner rejoins gemcitabine as a species of Group I. Office Action, paragraph 6.

II. Priority Acknowledged

Applicants assert that claims 2, 17, 23, 30 and 32-34 are at least entitled to the benefit of the filing date of the instant application.

III. Specification

A. Paragraphs 32, 93, 101 and 140 of the Specification Are Proper

At paragraph 9 of the Office Action, the Examiner objects to the specification alleging the term "Bexxar" is a trademark and should be indicated as such. Applicants amend paragraphs 32, 93, 101 and 140 of the specification to identify "Bexxar" as a trademark.

Accordingly, the objection is overcome.

B. Paragraphs 162-164, 167-168, 170-171 and 174, and Table 7, of the Specification Are Proper

The Examiner objects to several paragraphs of the specification for containing misplaced question marks. The question marks are printer errors and should be "Å" or "→." Paragraphs

162-164, 167-168, 170-171 and 174, and Table 7, of the specification have been appropriately amended.

C. & D. Claims 2, 17 and 30 Are Proper

The Examiner alleges that the specification fails to provide "proper antecedent basis" for the following secondary agents: thalidomide, vincristine, interferon alpha-2α, carmustine, pamidronate, prednisone, erythropoietin and bisphosphonate. The Examiner asserts that the specification improperly incorporates by reference, via DeVita *et al.*, the noted secondary agents.

The specification has been amended to include specific reference to thalidomide, carmustine, pamidronate, prednisone, erythropoietin and bisphosphonate, as supported by DeVita *et al.*, which is expressly incorporated by reference at page 69 of the specification.

At page 5 of the Office Action, the Examiner asserts, "Applicant is cautioned that introduction of less than the entirety of the above reference into the specification would be considered new matter," however it is unclear on what basis the Examiner makes this assertion. No statute, case law, regulation or directive suggests such a policy, and, in fact, 37 C.F.R. §1.57(f) implies the exact opposite.

Thalidomide, carmustine, pamidronate, prednisone, erythropoietin and bisphosphonate

Applicants amended claims 2, 17 and 30, and added new claims 32-34 in the Preliminary Amendment filed September 7, 2006, to recite the referenced compounds. Along with the Amendment, Applicants demonstrated support for thalidomide, carmustine, pamidronate, prednisone, erythropoietin and bisphosphonate in DeVita *et al.*, which is cited in paragraph 93 of the specification. The written description relied upon in DeVita *et al.* is incorporated into the description of the specification.

Vincristine and interferon alpha-2a

Applicants disagree that the specification fails to provide proper antecedent basis for vincristine and interferon alpha-2a.

Vincristine and interferon alpha-2a are clearly supported by the specification, at least at paragraph 91, which recites "[i]n other therapeutic treatments, the antibodies, antibody fragments or conjugates of the invention are co-administered, or administered sequentially, with one or

more additional therapeutic agents. Suitable therapeutic agents include, but are not limited to, cytotoxic or cytostatic agents." In addition, paragraph 83 defines vincristine as a cytotoxic agent, and paragraph 92 defines interferon alpha-2a as a therapeutic agent.

Accordingly, withdrawal of this objection is kindly requested.

IV. Claim Objections

A. Claims 4 and 5 Are Cancelled

At paragraph 10 of the Office Action, the Examiner objects to claims 4 and 5 as being of improper dependent form for failing to further limit the subject matter of a previous claim.

Applicants cancel claims 4 and 5, therefore the objection is moot.

B. Objection to Claim 15 is Overcome

At paragraph 11 of the Office Action, the Examiner has objected to claim 15 as containing an improper Markush group.

Amended claim 15 is in proper Markush group format.

Accordingly, the objection is overcome.

C. Objection to Claims 22, 30, 31 and 34 is Stayed

At section c. on page 7 of the Office Action, the Examiner has objected to claims 22, 30, 31 and 34 as being drawn to a non-elected invention.

Applicants have requested rejoinder of the non-elected claims of Group III (claims 20, 21, 25, 28 and 29), drawn to a method of treating a patient having a cancer using the compositions of Group I. Applicants maintain claims 22, 30, 31 and 34, and their dependency from a non-elected invention, pending further prosecution.

V. Claims 1-3, 6, 8-14, 16-18, 19, 22, 30 and 32-34 Are Definite Under 35 U.S.C. §112, Second Paragraph

At paragraph 13 of the Office Action, claims 1-6, 8-14, 16-18, 19, 22, 30 and 32-34 are rejected under 35 U.S.C. §112, second paragraph, as being indefinite.

A. Claims 1-3, 6, 19, 22 and 32 Are Definite Under 35 U.S.C. §112

In section (a) of the rejection, the Examiner alleges that claims 1-6, 19, 22 and 32 are indefinite because while claim 1 is directed to antibodies (a polypeptide), the claim recites *nucleotide* mutations, deletions and insertions.

Applicants amend claim 1 to delete the recitation of nucleotide mutations, deletions and insertions. Therefore the rejection is overcome.

B. Claims 1-3, 6, 19, 22 and 32 Are Definite Under 35 U.S.C. §112

In section (b) of the rejection, the Examiner alleges that claims 1-6, 19, 22 and 32 are indefinite because while claim 1 recites an antibody having the same amino acid sequence as the EM164 antibody, murine antibodies are comprised of four different chains which each comprise separate amino acid sequences. The Examiner alleges that it is unclear to which of the sequences the claims are directed. The Examiner also alleges that reference to the antibody fragment is unclear.

Applicants amended claim 1 overcomes the first portion of the rejection, since the language objected to by the Examiner is no longer recited in the claim. As to the second portion of the rejection, the claim is clear as written. However, solely for the purpose of advancing prosecution and to better capture the envisioned commercial embodiments, Applicants amend claim 1 to more clearly indicate that the fragments refer to the claimed antibody.

In view of the above remarks and amendments to the claims, the Examiner is requested, respectfully, to reconsider and withdraw this rejection.

C. Claims 2, 17 and 30 Are Definite

In section (c) of the rejection, the Examiner notes that claims 2, 17 and 30 contain the trademark/trade names Herceptin, Avastin, Rituxan, Zevalin, Velcade, Tarceva, Cetuximab, Abx-EGF, and that claims 32-34 contain the trademark/trade name VELCADE. The Examiner asserts that the use of a trademark or trade name in a claim renders the claim indefinite.

Applicants amend claims 2, 17, 30 and 32-34 to delete recitation of the noted terms from the claims. Accordingly, the rejection is overcome.

D. Claims 8-14 and 16 Are Definite

In section (d) of the rejection, the Examiner alleges that the recitation in claims 8-14 and 16 of "represented by" renders the claims indefinite.

Without agreeing with the Examiner, solely to advance prosecution, Applicants amend claims 8-14 and 16 to replace "represented by" with "of."

Accordingly, the rejection is overcome.

E. Claims 4 and 5 Are Cancelled

In section (e) of the rejection, the Examiner alleges that claims 4 and 5 are indefinite because while claims 4 and 5 recite process limitations, the claim from which they depend (claim 1) is a product claim.

Applicants cancel claims 4 and 5, therefore the rejection is moot.

F. Claim 32 is Definite

In section (f) of the rejection, the Examiner alleges that the limitation in claim 32 of "the method of claim 1" renders the claim indefinite because claim 1 is a product claim and not a method claim.

Applicants amend claim 32 to recite "the composition of claim 1."

Accordingly, the rejection is overcome.

VI. Rejection of Claims 1-19, 22, 32 and 33 Under 35 U.S.C. §112, First Paragraph, is Moot in Part and Traversed in Part

A.

At paragraph 15 of the Office Action, claims 1-19, 22, 32 and 33 are rejected under 35 U.S.C. §112, first paragraph, as allegedly lacking written description support in the specification.

1. Rejection of Claims 1-6, 19, 22 and 32 Under 35 U.S.C. §112, First Paragraph is Overcome

The Examiner notes that claims 1-6, 19, 22 and 32 are directed to functional equivalents or variant antibodies having at least one amino acid mutation, deletion or insertion, compared to murine antibody EM164.

Without agreeing with the Examiner and solely to advance prosecution, Applicants amend claim 1, therefore the rejection is overcome.

2. Rejection of Claims 7-18 and 33 Under 35 U.S.C. §112, First Paragraph

a. At page 10 of the Office Action, the Examiner alleges that claims 7-18 and 33 are directed to antibodies or fragments that do not necessarily bind to any one antigen.

Without agreeing with the Examiner and solely to advance prosecution, Applicants amend claims 7-18 and 33 to specifically recite antigen specificity. Accordingly, the rejection is overcome.

b. The Examiner asserts that the specification teaches antibodies and fragments that bind IGF-IR, comprising each of the six CDRs of EM164, but alleges that Applicants fail to describe any such antibody lacking one or more of the CDRs but retaining the binding specificity.

Applicants amend claim 7 to recite three sequential CDRs. Applicants find support for amended claim 7 in at least paragraph 74 of the specification.

Accordingly, withdrawal of this aspect of the rejection is kindly requested.

c. The Examiner notes that while the specification teaches antibodies and fragments that bind IGF-IR, it allegedly fails to describe any other heavy or light chain variable regions that are 90-95% identical to the heavy and light chains of one of SEQ ID NOs:7-13 that retain the binding activity.

Applicants disagree with the Examiner's position and traverse the rejection. Applicants assert that the specification includes specific examples of sequence homologues. For example, claim 15 recites four homologues of the light chain, and claim 16 recites one heavy chain homologue. The specification provides adequate written description of the homologues at least at paragraph 67.

In addition, Applicants assert that the claims in the instant application are directed to a composition comprising (a) an antibody . . . and (b) a therapeutic agent. The specification exemplifies the antibody as at least an isolated antibody that binds to IGF-IR (e.g., EM164).

EM164 was sequenced and humanized and was determined to have heavy chain variable region sequences which are set forth in SEQ ID NOS.:7 (murine) and 9 (humanized), and light chain variable region sequences which are set forth in SEQ ID NOS:8 (murine) and 10 (humanized). The specification also teaches antibodies or fragments thereof produced by, at least, mutation, deletion and/or insertion within the variable and/or constant region sequences that flank a particular set of CDRs (paragraph 68) or polypeptides (e.g., antibodies) with amino acids substantially the same as the amino acid sequence of the variable or hypervariable regions of the antibodies of the invention (paragraph 71). Furthermore, the specification teaches that "[t]he variability is not usually evenly distributed through the variable domains of the antibodies. It is typically concentrated in three segments called complementarity determining regions (CDRs) or hypervariable regions both in the light chain and the heavy chain variable domains." See paragraph 68, column 6, lines 4-9. The CDR sequences are taught at least by SEQ ID NOS:1-6 and are encompassed in the heavy chain and the light chain variable region sequences set forth. The specification teaches mutation, deletion and/or insertion within the variable and/or constant region sequences that flank a particular set of CDRs (paragraph 63) and teaches an assay for determining binding activity of the antibody to the IGF-IR (for example, see paragraph 117 under the title "Binding Characterization of EM164 Antibody").

Furthermore, the claims are directed to encompass an antibody with the same specificity as EM164, wherein said antibody has in the heavy chain variable region at least 90% sequence identity to an amino acid sequence set forth in SEQ ID NOS:7 or 9 or in the said light chain variable region at least 90% sequence identity to an amino acid sequence set forth in SEQ ID NOS:8 or 10 and specifically bind to IGF-IR.

The invention has at least two additional aspects, the first being an antibody which comprises a heavy chain variable region defined by at least SEQ ID NOS:7 or 9 or a light chain variable region defined by at least SEQ ID NOS:8 or 10 and the second being an antibody in which the heavy chain variable regions retain the specificity of at least SEQ ID NOS:7 or 9 or the light chain variable regions which retain the specificity of at least SEQ ID NOS:8 or 10.

The specification teaches an antibody having a heavy chain variable region defined by at least SEQ ID NOS:7 or 9 or a light chain variable region defined by at least SEQ ID NOS:8 or 10 or additional EM164 specific antibodies or fragments thereof having 90% identity to the heavy chain variable region defined by at least SEQ ID NOS:7 or 9 or a light chain variable region defined by at least SEQ ID NOS:8 or 10 and having binding affinity to IGF-IR. The procedures for making such antibodies or fragments containing the heavy chain variable region defined by SEQ ID NOS:7 or 9 or a light chain variable region defined by at least SEQ ID NOS:8 or 10 are taught and known in the art. An assay is taught which identifies other antibodies having the claimed IGF-IR binding specificity. Moreover procedures for making antibodies or fragments containing the heavy chain variable region defined at least by SEQ ID NOS:7 or 9 or a light chain variable region defined at least by SEQ ID NOS:8 or 10 which have 90% identity to the heavy chain variable region defined at least by SEQ ID NOS:7 or 9 or a light chain variable region defined at least by SEQ ID NOS:8 or 10, which retain specificity, are known in the art. The specification explicitly states that all varieties must confer binding activity and must have at least 90% identity to the variable regions (paragraph 71).

Accordingly, withdrawal of this rejection is kindly requested.

B. Claims 7, 17, 18 and 33 Are Adequately Supported by the Specification Under 35 U.S.C. §112, First Paragraph

At paragraph 16 of the Office Action, claims 7, 17, 18 and 33 are rejected under 35 U.S.C. §112, first paragraph, as lacking adequate written description support in the specification.

Without agreeing with the Examiner and solely to advance prosecution, Applicants amend claim 7 by deleting recitation of SEQ ID NOS:4-6.

Accordingly, the rejection is overcome.

C Claims 2, 17, 30 and 32-34 Are Supported Under 35 U.S.C. §112, First Paragraph

At paragraph 17 of the Office Action, claims 2, 17, 30 and 32-34 are rejected under 35 U.S.C. §112, first paragraph, as lacking written description support in the specification.

1. With regard to recitation of thalidomide, carmustine, pamidronate, prednisone, erythropoietin and bisphosphonate in the noted claims, the Examiner alleges that the specification does not "particularly point" to disclosures in DeVita *et al.* (cited in paragraph 93 of the specification, incorporated by reference at 69, paragraph 181 of the specification) that describe the noted compounds. As such, the Examiner has taken the position that recitation of these compounds in the rejected claims is an allegedly improper introduction of new matter into the claims.

MPEP §2163.07(b) states that information incorporated by reference is as much a part of the application as filed as if the text was repeated in the application, and should be treated as part of the text of the application as filed. Applicants amendment to the specification includes verbatim relevant portions of DeVita et al., support for which can be found as follows: thalidomide, carmustine, pamidronate, prednisone, erythropoietin and bisphosphonate at least at page 3082, column 2 to 3083, column 1; page 2830, column 2, last paragraph; page 2829, column 1; 2644, column 1, first full paragraph; page 2579, last paragraph; page 2579, last paragraph; page 2365, column 2, last paragraph; page 2361, column 2 and page 2363, column 1; page 2359, column 2 - 2360, column 1; page 2359, column 1, of DeVita *et al.*, respectively.

Accordingly, withdrawal of this rejection is kindly requested.

2. With regard to recitation of interferon alpha-2α and vincristine, the Examiner alleges that recitation of these compounds in the claims lacks support in the specification and thus constitutes new matter. The Examiner further alleges that paragraphs 83 and 92, cited in support of this rejection, only describes the noted compound as a cancer therapeutic agent, and not a second therapeutic agent.

Applicants point to paragraph 91 of the specification which states "[i]n other therapeutic treatments, the antibodies, antibody fragments or conjugates of the invention are co-administered, or administered sequentially, with one or more additional therapeutic agents." Paragraph 92 defines interferon alpha-2a as a therapeutic agent. Paragraph 83 defiines vincristine as a cytotoxic agent.Thus, there is clear support for the recitation of interferon alpha-2a and vincristinein the claims.

Accordingly, withdrawal of this rejection is kindly requested.

D. Claims 1-3, 6, 19, 22-24, 26, 27, 30-32 and 34 Are Enabled Under 35 U.S.C. §112, First Paragraph

At paragraph 18 of the Office Action, claims 1-6, 19, 22-24, 26, 27, 30-32 and 34 are rejected under 35 U.S.C. §112, first paragraph, as allegedly being non-enabled.

The Examiner alleges that claims 1-6, 19, 22-24, 26, 27, 30-32 and 34 are not enabled because the specification lacks complete deposit information for the deposit of antibody EM164, and that a statement by Applicants that (i) the deposit will be replaced if the samples become non-viable, (ii) all restrictions upon public access to the deposit will be irrevocably removed upon the granting of a patent, and (iii) access to the deposit will be assured during pendency of the application, has not been filed.

Applicants provide a copy of the deposit receipt and a signed statement that the deposit is the same as that referenced in the specification and that all restrictions upon public access will be irrevocably removed upon grant of a patent.

Accordingly, withdrawal of this rejection is kindly requested.

E. Rejection of Claims 1-19, 22-27 and 30-34 Under 35 U.S.C. §112, First Paragraph

At paragraph 19 of the Office Action, claims 1-19, 22-27 and 30-34 are rejected under 35 U.S.C. §112, first paragraph, as lacking enablement.

For the following reasons, this rejection is traversed in part and overcome in part.

The Examiner alleges that while the specification is enabling for an antibody or antibody fragment that specifically binds to IGF-IR, comprising all six CDRs of SEQ ID NOs:1-6, it is not enabling for (i) an antibody or fragment that comprises (a) at least one CDR selected from SEQ ID NOs:1-6, (b) all six CDRs, (c) heavy or light chain homologues of 90-95%, or (d) a heavy or light chain represented by SEQ ID NO:7 or 8, wherein the antibody or fragment does not bind IGF-IR, or (ii) an antibody or fragment that binds IGF-IR comprising (a) at least one CDR selected from SEQ ID NOs:1-6, or (b) heavy or light chain homologues of 90-95%.

(i) With respect to (ii), the Examiner alleges that the specification does not provide support for antibodies that "do not bind IGF-IR," Applicants amend claim 7 to recite that the antibodies and epitope binding fragments thereof have the same binding specificity as Murine antibody EM164.

Accordingly, withdrawal of this rejection is kindly requested.

With respect to (ii) (a), Applicants' amended claim 7 recites, the composition of claim 1, wherein said antibody or said fragment comprises a heavy chain variable region and a light chain variable region, wherein said heavy chain variable region comprises three sequential complementarity-determining regions comprising the amino acid sequences of SEQ ID NOs:1-3, respectively.

In addition, Applicants provide the Examiner with a copy of Holt *et al.* which provides a discussion of domain antibodies comprising only the three heavy chain CDRs. Holt *et al.* provides a detailed discussion on domain antibodies (dAbs), teaching that dAbs are antibody fragments consisting of only the variable region of the heavy chain (V_H) that retain the binding activity of the antibody from which they were derived. Holt *et al.* discusses fully human versions of domain antibodies, as well as murine versions. As noted at page 486, col. 2, third full paragraph, both human and mouse dAbs have been prepared that have high antigen specificity and binding affinity. As further noted in the conclusions section at page 489, the ability of dAbs to be affinity-matured by using *in vitro* selection, such as phage display, results in the rapid generation of very specific, high-affinity dAbs.

Applicants also provide the Examiner with copies of Aires da Silva *et al.* (J. Mol. Biol., 340:525-542 (2004)), Tanaka *et al.* (J. Mol. Biol., 331:1109-1120 (2003), and Peterson (Advances in Monoclonal Antibody Technology: Genetic Engineering of Mice, Cells and Immunoglobulins, Peterson NC, ILAR J. 46(3):314-319 (2005)) which further educates the Examiner on these issues.

With respect to (iii) (b), Applicants contend that one of ordinary skill in the art would understand that changes to the heavy and light chain variable regions can easily be made without changing the specificity of the antibody. Applicants refer the Examiner to paragraphs 68 and 75-

76 of the specification which reference a large number of published materials (e.g., journal articles and patents) that teach how changes can be made in an antibody sequence to make the homologues recited in the rejected claims, thus providing the skilled artisan with the tools to make and test the homologues.

More specifically with regard to the EM164 antibody of the instant invention, Example 2 (paragraphs 160-179) of the application teaches a detailed explanation of how to conceive, construct, test and use antibody homologues. Rajpal, *et al.* disclose that comprehensive optimization maps of an antibody site can be developed in facile and rapid manner. Rajpal, *et al.*, page 8466. In view of Applicants' teachings, and the disclosure of Rajpal, *et al.*, one of ordinary skill in the art would appreciate that changes to the heavy and light chain variable regions can easily be made without changing the specificity of the antibody.

Accordingly, withdrawal of this rejection is kindly requested.

VII. The Claims Are Novel Under 35 U.S.C. §102

A. Claims 1, 4-6, 8-14, 16, 19 and 22 Are Novel Under 35 U.S.C. §102(b)

At paragraph 21 of the Office Action, claims 1, 4-6, 8-14, 16, 19 and 22 are rejected under 35 U.S.C. §102(b) as being anticipated by Zia *et al.* (*JCB Suppl.* 24:269-275 (1996)).

The Examiner alleges that Zia *et al.* discloses an antibody (IR-3) that specifically binds IGF-IR, and teaches conjugating the antibody to ^{125}I, where ^{125}I is considered to be a second agent.

Applicants respectfully disagree with the Examiner. Pending claim 1 recites antibodies and fragments thereof which bind IGF-IR and have the same binding specificity as the EM164 antibody. Zia *et al.* disclose an alpha IR-3 antibody with a different specificity as the EM164 antibody. The EM164 anitbody does not agonize the IGF-IR, whereas alpha IR-3 does. For example, Kato *et al.* describe the same alpha IR-3 antibody as inducing receptor autophosphorylation, activating phosphatidylinositol-3-kinase and 2-deoxyglucose uptake, inducing ornithine decarboxylase gene expression, and stimulating thymidine incorporation. (See Kato *et al.*, throughout). Theses results are confirmed by an independent laboratory using the same alpha IR-3, in which antibody alpha IR-3 was capable of mimicking the ability of IGFI

to stimulate three different biological responses in the CHOIGFIR cells. (See Steele-Perkins *et al.*, page 11491). In fact, the investigators concluded that alpha IR-3 stimulated the serine phosphorylation of the receptor (Fig. 5). "This is further evidence that the antibody is capable of stimulating the same responses as IGF-I." Consistent with these prior studies, Zia *et al.* point out that the alpha IR-3 antibody was not potent in inhibiting breast tumors.

Since the alpha IR-3 antibody does not have the same specificity as Applicants' EM164 antibody it cannot anticipate the claims and therefore the rejection should be withdrawn.

The Examiner's assertion that Zia *et al.* have shown the efficacy of ^{125}I-linked to the IR3 antibody is also incorrect. The ^{125}I-linked to IR3 antibody was used for tumor distribution analysis, not efficacy. Since Zia *et al.* do not disclose an antagonist which specifically binds to IGF-I receptor, it cannot anticipate Applicants' claims.

Further, Applicants amendment to claim 1 moots this rejection.

Accordingly, withdrawal of this rejection is kindly requested.

B. Claims 7-11, 16, 19 and 22 Are Novel Under 35 U.S.C. §102(b)

At paragraph 22 of the Office Action, claims 7-11, 16, 19 and 22 are rejected under 35 U.S.C. §102(b) as allegedly being anticipated by Kettleborough (USP 5,844,093; issued December 1, 1998).

The Examiner alleges that Kettleborough teaches an antibody having a CDR identical to the CDR set forth in SEQ ID NO:1.

Applicants assert that SEQ ID NO.:1 and the sequence in Kettleborough are not identical, since SEQ ID NO.:1 is directed to a light chain CDR of an antibody that specifically binds IGF-I receptor, whereas the sequence disclosed by Kettleborough is directed to EGFR.

Applicants also assert that SEQ ID NO.:1 is directed to a heavy chain CDR, whereas the sequence disclosed in Kettleborough is directed to a protein, and is claimed as a variable region of the single chain Fv. Kettleborough does not teach that the 119 amino acid sequence is useful as a heavy chain CDR.

In addition, Applicants' amended claims do not recite a single CDR, but three sequential CDRs. Since Kettleborough teaches only one CDR, it cannot anticipate Applicants' claims.

Accordingly, withdrawal of this rejection is kindly requested.

C. Claims 7-8 and 12-15 Are Novel Under 35 U.S.C. §102(b)

At paragraph 23 of the Office Action, claims 7-8 and 12-15 are rejected under 35 U.S.C. §102(b) as being anticipated by Do Couto (USP 6,309,636; issued October 30, 2001).

The Examiner alleges that Do Couto teaches an antibody having a CDR identical to the CDR set forth in SEQ ID NO:6.

Applicants assert that SEQ ID NO.:6 and the sequence in Du Couto are not identical, since SEQ ID NO.:6 is directed to an antibody that specifically binds IGF-I receptor, whereas the sequence disclosed by Du Couto is directed to a human milk fat globule (HMFG) antigen.

Applicants also assert that SEQ ID NO.:6 is directed to a antibody light chain CDR, whereas the sequence disclosed in Du Couto is directed to a generic protein, and is never recited in any claim. The Du Couto sequence therefore teaches almost nothing. Du Couto certainly does not teach that the 34 amino acid sequence is useful as a light chain CDR.

In addition, Applicants' amended claims do not recite a single CDR, but three sequential CRDs. Since Du Couto teaches only one CDR, it cannot anticipate Applicants' claims.

Accordingly, withdrawal of this rejection of claim 7 is kindly requested.

As to the rejection of claims 8-11, 16, 19 and 22, Kettleborough *et al.* does not recite sequences in Applicant's claims.

Accordingly, withdrawal of this rejection is kindly requested.

As to claims 8 and 12-15, none of these claims is limited to an antibody comprising only SEQ ID NO:6. Do Couto does not recite any sequences recited in claims 8 and 12-15 and therefore cannot anticipate the claims.

Accordingly, withdrawal of this rejection is kindly requested.

D. Claims 8-17, 19 and 33 Are Novel Under 35 U.S.C. §102(b)

At paragraph 24 of the Office Action, claims 8-17, 19 and 33 are rejected under 35 U.S.C. §102(b) as being anticipated by Tan (*Cancer Res.*, Feb. 15, 2002), as evidenced by Queen (USP 5,530,101; issued June 25, 1996).

The Examiner interprets the claims as being drawn to a composition comprising an antibody having an amino acid sequence of at least two consecutive amino acids in length from the CDRs of SEQ ID NOs:1-6 or an amino acid sequence at least two amino acids in length represented by SEQ ID NOs:7-13, and a second agent.

It is very difficult for Applicants to address this rejection as the Examiner does not provide any explanation as to why he has interpreted the claims as encompassing antibodies having amino acids sequences of at least two consecutive amino acids from the sequences set forth in SEQ ID NOs:1-6 and 7-13, and since the Examiner refers to a humanized, anti-Tac antibody in combination with PS-341 (bortezomib) even though an anti-TAC antibody does not appear to be disclosed in Tan *et al.*

Assuming the Examiner is referring to anti-HAT, the Examiner has not demonstrated that the HAT antibody of Tan *et al.* comprises any of the sequences of the antibodies of the pending claims. In fact, Tan et al. do not disclose a single polypeptide sequence. Furthermore, anti-HAT is specific for the alpha domain of IL-2R, not IGF-I receptor. Accordingly, the Examiner clearly has not established that Tan *et al.* teaches each and every limitation of the pending claims.

In addition, Applicants have amended the pending claims to include the same binding specificity as murine antibody EM164. The Examiner provides no evidence that the HAT antibody of Tan binds IGF-IR, nor would the antibody be expected to do so since it is not specific for IGF-IR.

Accordingly, withdrawal of this rejection is kindly requested.

E. Claims 1-3, 6-18, 19, 22, 24, 26, 27, 30 and 31 Are Novel Under 35 U.S.C. §102(a)

At paragraph 25 of the Office Action, claims 1-18, 19, 22, 24, 26, 27, 30 and 31 are rejected under 35 U.S.C. §102(a) as allegedly being anticipated by Maloney *et al.* (*Can. Res.*; August 15, 2003).

The Examiner alleges that Maloney discloses the EM164 antibody in a composition with gemcitabine.

Maloney is the inventor's own work. Applicants submit a Declaration Under 37 C.F.R. §1.132 by Rajeeva Singh and Nancy Dagdigian, executed February 28, 2007, stating that Maloney is a publication of their own work and that the inventorship of the application is correct.

Accordingly, withdrawal of this rejection is kindly requested.

F. Rejection of Claims 1, 4-6, 19 and 22 Under 35 U.S.C. §102(b) is Overcome

At paragraph 26 of the Office Action, claims 1, 4-6, 19 and 22 are rejected under 35 U.S.C. §102(b) as being anticipated by Rohlik *et al.* (*BBRC*; Nov. 30, 1987).

The Examiner alleges that Rohlik teaches an alpha IR-3 antibody with the same binding specificity as the EM164 antibody, and therefore the alpha IR-3 antibody is a functional equivalent of the EM164 antibody recited in claim 1.

Applicants respectfully disagree with the Examiner for the same reasons set forth above, in VII A, incorporated herein. Rohlik discloses an alpha IR-3 antibody with a different specificity as the EM164 antibody.

Since the alpha IR-3 antibody does not have the same specificity as Applicants' EM164 antibody it cannot anticipate the claims and therefore the rejection should be withdrawn.

Accordingly, withdrawal of this rejection is kindly requested.

VIII. Rejections of Claims 1-2 and 32 Under 35 U.S.C. §103 is Traversed

At paragraph 29 of the Office Action, claims 1-2 and 32 are rejected as being unpatentable under 35 U.S.C. §103(a) over Rohlik *et al.* (*BBRC*; Nov. 30, 1987) in view of Teicher *et al.* (*Clin. Can Res.*; Sept. 1999).

The Examiner alleges that Rohlik teaches an alpha IR-3 antibody with the same binding specificity as the EM164 antibody, and therefore the alpha IR-3 antibody is a functional equivalent of the EM164 antibody recited in claim 1. The Examiner further alleges that Teicher teaches the proteasome inhibitor PS-341 (bortezomib), and that it would have been *prima facie* obvious to make a composition comprising the alpha IR-3 antibody and PS-341 for use in the inhibition of growth of MCF-7 cells.

Applicants respectfully disagree with the Examiner for the same reasons set forth above, in VII F, incorporated herein. Rohlik discloses an alpha IR-3 antibody with a different specificity as the EM164 antibody.

Since the alpha IR-3 antibody does not have the same specificity as Applicants' EM164 antibody it cannot anticipate the claims and therefore the rejection should be withdrawn.

Accordingly, withdrawal of this rejection is kindly requested.

IX. Double Patenting

A. Provisional Rejection of Claims 1-18, 23 and 32-33 is Stayed

At paragraph 31 of the Office Action, claims 1-18, 23 and 32-33 are provisionally rejected on the grounds of non-statutory obviousness-type double patenting as being unpatentable over claims 1-27 of the co-pending parent application (appln. no. 10/170,390), in view Teicher *et al.*

Both applications are pending therefore the Examiner is requested to hold the rejection in abeyance.

B. Provisional Rejection of Claims 19, 22, 24, 26, 27, 30 and 34 is Stayed

At paragraph 32 of the Office Action, claims 19, 22, 24, 26, 27, 30 and 34 are also provisionally rejected on the grounds of non-statutory obviousness-type double patenting as being unpatentable over claim 30 of the parent application, in view Teicher *et al.*

The Examiner alleges that claim 30 of the parent application encompasses the scope of claims 19, 22, 24, 26, 27, 30 and 34 of the instant application.

Because both applications are pending the rejection is stayed.

In view of the above, reconsideration and allowance of this application are now believed to be in order, and such actions are hereby solicited. If any points remain in issue which the Examiner feels may be best resolved through a personal or telephone interview, the Examiner is kindly requested to contact the undersigned at the telephone number listed below.

The USPTO is directed and authorized to charge all required fees, except for the Issue Fee and the Publication Fee, to Deposit Account No. 19-4880. Please also credit any overpayments to said Deposit Account.

Respectfully submitted,

/William J. Simmons/

William J. Simmons, Ph.D.
Registration No. 59,887

SUGHRUE MION, PLLC
Telephone: (202) 293-7060
Facsimile: (202) 293-7860

WASHINGTON OFFICE
23373
CUSTOMER NUMBER

Date: April 16, 2007

PATENT APPLICATION

IN THE UNITED STATES PATENT AND TRADEMARK OFFICE

In re application of

Rajeeva Singh et al. Confirmation No. 3309

Appln. No.: 10/729,441 Group Art Unit: 1643

Filed: December 8, 2003 Examiner: B. Duffy

For: ANTI-IGF-I RECEPTOR ANTIBODIES

STATEMENT OF AVAILABILITY

Commissioner for Patents
P.O. Box 1450
Alexandria, VA 22313-1450

Sir:

We, ImmunoGen, Inc., do depose, declare and state that:

We are the Assignee of the entire right, title and interest of the invention described and claimed in the above-identified application, as evidenced by the Assignment recorded on May 4, 2006, at REEL 017861, FRAME 0081.

We agree that upon allowance and issuance of the above-identified application into a United States Patent, all restrictions on availability of:

Murine hybridoma cell line EM164 (ATCC Deposit No. PTA-4457)

which is designated in the specification of the above-identified application and deposited at the American Type Culture Collection, P.O. Box 1549, Manassas, VA 20108, on June 14, 2002, will be irrevocably removed.

The deposit was accepted by the American Type Culture Collection under the terms of the Budapest Treaty on June 14, 2004. A copy of the deposit receipt is being filed herewith, or has been previous filed in this application.

We hereby declare that all statements made herein of our own knowledge are true and that all statements made on information and belief are believed to be true; and further that these statements were made with the knowledge that willful false statements and the like so made are punishable by fine or imprisonment, or both, under Section 1001 of Title 18 of the United States

Code, and that such willful false statements may jeopardize the validity of this application or any patent issuing thereon.

ImmunoGen, Inc.

Date: 2/23/07

Name: W. Blattler

Name: Walter A. Blattler, Ph.D.
Title: Vice-President, Science and Technology

ATCC

10801 University Blvd • Manassas, VA 20110-2209 • Telephone: 703-365-2700 • FAX: 703-365-2745

BUDAPEST TREATY ON THE INTERNATIONAL RECOGNITION OF THE DEPOSIT OF MICROORGANISMS FOR THE PURPOSES OF PATENT PROCEDURE

INTERNATIONAL FORM

RECEIPT IN THE CASE OF AN ORIGINAL DEPOSIT ISSUED PURSUANT TO RULE 7.3 AND VIABILITY STATEMENT ISSUED PURSUANT TO RULE 10.2

To: (Name and Address of Depositor or Attorney)

ImmunoGen, Inc.
Attn: Rajeeva Singh
128 Sidney Street
Cambridge, MA 02139

Deposited on Behalf of: ImmunoGen, Inc.

Identification Reference by Depositor:	**Patent Deposit Designation**
Mouse Hybridoma: EM164	PTA-4457

The deposit was accompanied by: __ a scientific description _ a proposed taxonomic description indicated above.

The deposit was received June 14, 2002 by this International Depository Authority and has been accepted.

AT YOUR REQUEST: X We will inform you of requests for the strain for 30 years.

The strain will be made available if a patent office signatory to the Budapest Treaty certifies one's right to receive, or if a U.S. Patent is issued citing the strain, and ATCC is instructed by the United States Patent & Trademark Office or the depositor to release said strain.

If the culture should die or be destroyed during the effective term of the deposit, it shall be your responsibility to replace it with living culture of the same.

The strain will be maintained for a period of at least 30 years from date of deposit, or five years after the most recent request for a sample, whichever is longer. The United States and many other countries are signatory to the Budapest Treaty.

The viability of the culture cited above was tested June 18, 2002. On that date, the culture was viable.

International Depository Authority: American Type Culture Collection, Manassas, VA 20110-2209 USA.

Signature of person having authority to represent ATCC:

Marie Harris

Marie Harris, Patent Specialist, ATCC Patent Depository

Date: July 15, 2002

cc: Susan J. Mack, Esq.
(Ref: Docket or Case No.: A8338)

Advances in Monoclonal Antibody Technology: Genetic Engineering of Mice, Cells, and Immunoglobulins

Norman C. Peterson

Abstract

The ability to produce antibodies that are directed against specific antigens has played a crucial role in advancing scientific discoveries. Recombinant technologies have extended the application of antibodies beyond the research laboratory and into the clinic for the treatment of cancer and other diseases. Creative approaches using these technologies have been used to reduce the antibody to its minimal functional size, and/or make them bifunctional (immunotoxins), bispecific, or less immunoreactive (humanized). Additionally, mice that are engineered to generate antibodies of human genomic origin have been used to produce therapeutic antibodies and are being further developed. As the research and clinical demands for antibodies continue to increase, the development of improved resources (cell lines and animals) to improve production efficiency, generate larger repertoires, and deliver greater yields of antibodies is being explored, and advances in this area are discussed further in this review.

Key Words: antibody; apoptosis; hybridoma; immunotherapy; single chain Fv; tissue culture

Introduction

Soon after it was realized that antibodies with desired specificity could be mass-produced, the concept that they could be used as "magic bullets" to target disease-associated proteins was born. The development of technology to clone and sequence immunoglobulin genes provided the tools necessary to construct antibody-based molecules and fusion proteins for the treatment and diagnosis of cancer, rheumatoid arthritis, and infectious diseases. In 2003, the US Food and Drug Administration approved 14 antibody-based pharmaceuticals, of which 70 were in late-stage clinical trials (Phase II+) and > 1000 were in preclinical development (reviewed in Stockwin and Holmes 2003).

Additional growth in the area of hybridoma and monoclonal antibody production technology is projected as genomic and proteomic high-throughput programs identify new proteins that will require immunoanalyses and/or purification for further characterization. Although standard procedures for generating antibodies of desired specificity have been used for approximately 30 yr, the development of more efficient techniques and resources would be a boon for biomedical research.

Antibody Engineering

Early studies demonstrated that when monoclonal antibodies (MAbs[1]) directed against tumor cell antigens were injected into mouse models, they inhibited the growth of tumors expressing the targeted antigens (Drebin et al. 1988). Although somewhat effective in human clinical trials, the neutralizing effects of the human antimouse antibodies that were elicited in response to the administration of these mouse-derived proteins reduced their effectiveness as diagnostic and therapeutic agents and raised concerns over the risk of treatment-associated anaphylaxis (Ritter et al. 2001). "Humanization" of the mouse-derived MAbs has been the most widely used strategy to reduce their immunogenicity for therapeutic purposes in people. To humanize a mouse MAb, its modeled structure is compared with that of human immunoglobulin (Ig[1]) protein structures (allotypes) to identify the closest match. Recombinant approaches are then used to graft the complementarity (or specificity)-determining regions (CDRs[1]) from the mouse-derived hybridoma Ig cDNA to the corresponding regions of the matched human Ig cDNA. The CDRs (described below), which give the antibody its affinity, are relatively small, hence the newly formed recombinant protein produced from the expression of this construct has the specificity of the mouse Ig but is less likely to be recognized as being foreign by the human immune system.

Because of their large size, it is often difficult to manipulate and express antibody genes. To overcome this limitation, various recombinant antibody-like forms and peptides have been produced using a reductionist's approach (reviewed in Peterson (1996) (Figure 1). The smallest functional unit of an antibody to be produced has been the CDR peptides (Figure 1C). Depending on which CDR is

During the preparation of this article, Norman C. Peterson, D.V.M., Ph.D., Dipl. ACLAM, was an Assistant Professor in the Department of Comparative Medicine, The Johns Hopkins University, Baltimore, Maryland. At the time of publication, Dr. Peterson had assumed the new position of Laboratory Animal Veterinarian at MedImmune, Gaithersburg, Maryland.

[1]Abbreviations used in this article: CDR, complementarity-determining region; CHO, Chinese hamster ovary; ETA, exotoxin A; Ig, immunoglobulin; MAb, monoclonal antibody; scFv, single chain fragment variable; Ig, immunoglobulin; TSA, transitional state analogue; VH, variable heavy; VL, variable light.

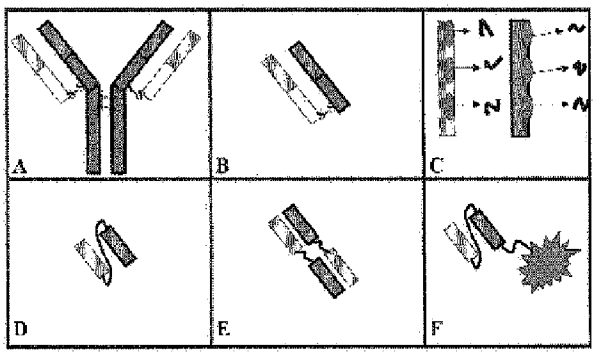

Figure 1 Schematic of antibody-derived molecules. (A) Antibodies (immunoglobulin G) are naturally produced by B cells and are composed of two heavy and two light chains joined by disulfide bonds. The variable regions (variable heavy [VH] and light [VL]) are stippled. (B) Fabs were the first small antibody forms made by proteolytic digestion with papain. (C) The VH and VL regions each contain three complementarity-determining regions whose sequences can be used to synthesize CDR peptides. (D) In a single chain fragment variable (scFv) molecule, the VH and VL regions are held together by a glycine-serine linker (dark line). (E) Diabodies form when the linker spanning the VH and VL is shortened. (F) scFv-toxin fusion protein.

produced, it can vary in length from eight to 20 amino acids. The CDRs may be thought of as fingertips, which make contact with an object, and the framework regions of an antibody chain as being analogous to the hand and fingers, which hold things in place. The affinity of a CDR is tested by its ability to compete with the parental antibody at its binding site. Berezov and colleagues (2001) demonstrated that a peptide designed from the sequence of the third CDR of an anti-Her2/neu antibody heavy chain sequence was able to bind to the receptor and disable its tyrosine kinase activity. Another biologically active peptide derived from an antineurokinin receptor antibody by Wijkhuisen and coworkers (2003) was capable of antagonizing substance P-induced cAMP production. These results among others exemplify the potential for antibodies to provide a scaffold from which small molecule therapeutics and diagnostic compounds can be made (Murali and Greene 1998).

Because an antibody uses multiple CDRs to bind to an epitope and peptides lack three-dimensional structure, antibody-based peptides have significantly less affinity than their multivalent parental antibodies. This characteristic may consequently limit their practical application. Recombinant approaches have led to the development of single chain fragment variables (scFvs[1]), which are monovalent and about one third the size of an antibody (Figure 1D). The Fv section of an antibody is limited to that portion of the heavy and light chains that each contain the three CDRs and framework regions. It is smaller than a Fab (Figure 1B) in that the scFv does not include the first constant region with disulfide bounds that link the heavy and light chains together. The recombinant single chain is formed by the tandem arrangement of the heavy chain and light chain sequences joined by a flexible linker typically composed of glycines and serines $(gly\text{-}gly\text{-}ser)_5$. When expressed in bacteria or eukaryotic cells, the scFv folds into a conformation that is similar to the respective region of its parental antibody, and it retains comparable affinity to that of a Fab (Kortt et al. 1994).

Once produced, scFvs are amendable to various genetic modifications such as humanization and the production of novel fusion proteins to enhance their potential as therapeutic agents. The latter may be necessary to compensate for their lack of an Fc to stimulate effector function and consequential cell killing. Clinical trials using Pexelizumab, a humanized scFv that binds to the C5 component of complement, has been shown to significantly reduce myocardial infarctions associated with coronary artery bypass graft surgeries in people (Verrier et al. 2004). ScFvs that adhere to various cancer-associated antigens have also been modified to deliver toxins and chemotherapeutics to solid tumors (Figure 1F). By genetically fusing a truncated form of *Pseudomonas aeruginosa* exotoxin A (ETA[1]) to a humanized scFv that has affinity for the proto-oncogenic epithelial cell adhesion molecule, Di Paolo and colleagues (2003) developed an immunotoxin that inhibited the growth of lung, colon, and squamous cell carcinomas in xenografted mice. An additional cysteine residue was placed at the C-terminus of a antiendoglin scFv by Volkel and coworkers (2004) so that it could be chemically coupled to doxorubicin-loaded liposomes for specific delivery to proliferating endothelial cells, such as found in tumors. These examples illustrate the dynamic potential of recombinant antibody-fusion molecules in clinical medicine.

Several IgG/M antibodies have been reported to induce cellular growth/differentiation and apoptosis. These interactions often depend on the antibody being multivalent in order to promote bound receptor aggregation and activation. Reduction of the linker length of the scFvs to between three and 12 residues prevents the monomeric configuration of the scFv molecule and favors intermolecular variable heavy (VH^1)–variable light (VL^1) pairing with the formation of a noncovalent scFv dimer "diabody" (Holliger et al. 1993) (Figure 1E). Further reducing the linker length to fewer than three residues can, in some cases, result in the formation of trimers (Kortt et al. 1997) or even tetramers (Le Gall et al. 1999). Using this approach, Kikuchi and colleagues produced a monovalent scFv and diabody from an anti-CD47 antibody, which induced apoptosis in leukemic cells (Kikuchi et al. 2004). Interestingly, the monovalent scFv (constructed with a longer spacer) had no biological effect, whereas the anti-CD47 diabody acted similarly to its parental antibody and induced apopotosis in leukemic cells that expressed the receptor. By using a synthetic interlocking helix motif, Peterson and Greene (1998) also produced scFvs that formed bivalent dimers. The bacterially expressed bivalent anti-Her2/neu scFv was significantly more effective at causing cell-surface down-modulation of the

oncogenic receptor than the monovalent form of the molecule. Bivalency can also be provided by the fusion of an antireceptor scFv with the receptor's ligand. Bremer and colleagues (2004) used this strategy to cross-link EGP2 (Ep-CAM) receptors, which triggered apoptosis in cancer cells expressing this receptor.

ScFvs of different specificity can also be linked together to produce bispecific antibodies that bind two different receptors on single or different cells. The latter strategy has been commonly used to enhance the activation of T cells in proximity to targeted tumor cells. This approach was used by Korn and coworkers (2004) to produce a bispecific antibody-like form with an antiendoglin scFv (found on proliferating endothelial cell in tumors, mentioned above) and an anti-CD3 scFv, which is a cytotoxic T cell-activating receptor. In tissue culture assays, the diabody facilitated killing of endothelial cells, whereas cells that did not express endoglin were unaffected. Using scFv and ligand sequences, Schmidt and Wels (1996) also constructed a bispecific fusion protein to target both the ErbB-2 and epidermal growth factor receptors (respectively) that are simultaneously expressed in various aggressive adenocarcinomas. This construct also included an ETA sequence, and the bacterially expressed fusion protein inhibited the growth of A431 tumor xenografts in nude mice. From these observations, it would appear that numerous combinations of scFvs and toxins could be made; however, the tendency for many of these synthesized fusion proteins to fold improperly and form aggregates places limitations on these creative designs.

Since the early 1990s, phage display of combinatorial heavy and light chain genes obtained from people and animals have been explored as another means of generating antibody-like molecules (Marks et al. 1991; Pini and Bracci 2000). In this approach, large repertoires of antibody variable region cDNAs are collected from the B cells and combinations of VHs and VLs are expressed in the form of scFvs on the surface of filamentous bacteriophage (Figure 2). This method allows the phages that express scFvs with the appropriate specificity to be panned from antigen-coated plates. The affinity of an scFv may be improved by mutating the CDRs of the construct and then repeating the panning selection procedure. The advantage of this approach is that cancer-specific antibody fragments can be and have been directly isolated from antibody libraries of tumor-infiltrating lymphocytes (Hansen et al. 2001) and lymph nodes (Graus et al. 1998) of cancer patients. The first phage display-derived scFv approved for clinical trial was reported by Chester and colleagues (2000) who used radiolabeled anticarcinoembryonic antigen scFvs to locate colorectal tumors for surgical removal.

The pharmacokinetic values of scFvs differ from those of antibodies and are typically cleared from the system more rapidly. This characteristic may be advantageous in diagnostic imaging applications in that the background noise is reduced by the more rapid clearance of radiolabeled scFvs compared with MAbs. In addition, because of their smaller size, scFvs better penetrate solid tumors.

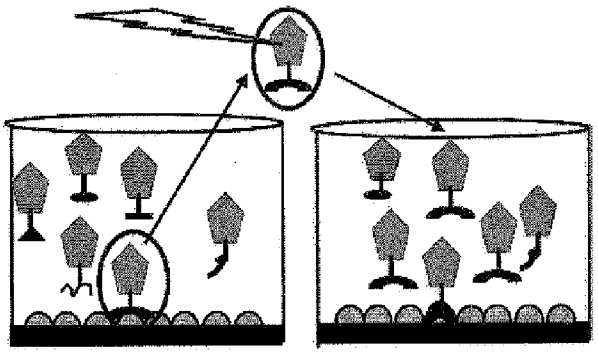

Figure 2 Schematic of combinatorial antibody chain phage display libraries. Bacteriophage are engineered to express combinations of variable heavy and variable light genes on their surface and are incubated with the antigen of interest on a solid support (left panel). Phage particles that adhere to the antigen are selected, propagated, and mutated. The selection procedure is repeated under more stringent conditions in anticipation that the mutagenesis procedures (represented by a bolt) result in increased affinities. Single chain Fvs are then generated from the genetic material of those phage exhibiting the highest affinity.

Mouse Engineering—Human Antibodies

A disadvantage of recombinant phage display is that the production of high-affinity antibody forms is difficult to obtain and the procedures are not familiar to most laboratories, hence the mouse continues to be the most commonly used progenitor of monoclonal antibodies and their derivatives. To avoid the multistep process of producing humanized antibodies to provide immunotherapeutic compounds, the generation of human MAbs directly from genetically engineered mice is continually being developed. This task was impossible until technology to introduce transgenes on yeast artificial chromosomes was developed, enabling the transfer of extremely large human immunoglobulin loci into the mouse germline (Choi et al. 1993). The XenoMouse® (Abgenix, Inc., Fremont, CA) and HuMAb Mouse® (GenPharm-Medarex, San Jose, CA) were the first engineered mice to carry a majority of both the human VH and VL (kappa) repertoire, and in 2002, five fully human MAbs generated from the XenoMouse were used in clinical trials (Kellermann and Green 2002). Ongoing developments are aimed at increasing the antibody repertoire even further by introducing the human Ig lambda chain locus into these mice (Nicholson et al. 1999). Microcell-mediated chromosome transfer has also been successfully utilized to transfer chromosome fragments containing human Ig genes into mice (Tomizuka et al. 1997) and cattle (Kuroiwa et al. 2002), and these genetically engineered animals may have

potential as additional sources of human MAbs and polyclonal antibodies, respectively.

Mouse Engineering—Production Technologies

The application and advancement of most of the technologies discussed above depend on the generation of an immune response to a specific antigen and the ability to harness the B cell component of that response for continued production and further testing. In 1975, Kohler and Milstein first reported that B cells harvested from an immunized mouse could be immortalized by fusing them with established myeloma cell lines derived from the BALB/c mouse (Kohler and Milstein 1975). The BALB/c mouse and its derived cell lines are still the current primary resource used for the generation of Mab-producing hybridoma cells. However, evidence presented in the remaining sections of this review suggests that the use of some spontaneous mutant and genetically modified mouse strains and cell lines may improve the efficiency of hybridoma/MAb production technology.

One such strain is the MRL/MpJ-lpr/lpr mouse, which has a spontaneously formed defect in the apoptosis regulatory gene *Fas*. Expression of the defected *Fas* leads to polyclonal B cell lymphoproliferation and hypergammaglobulinemia in these mice. After experiencing difficulty producing antibodies that catalyzed esterolytic activity in BALB/c mice, Takahashi and coworkers (2000) immunized MRL/MpJ-lpr/lpr mice with a transitional state analogue ($TSA^{\dagger}$). They found that this strain produced eight times as many catalytic antibody-secreting clones as similarly immunized BALB/c mice. They speculated the TSA may be recognized as a self-antigen, and hence reactive B cells were selectively eliminated in the BALB/c mice, whereas the apoptosis-resistant MRL/MpJ-lpr/lpr cells escaped this negative selection. The advantage of using this mouse strain for the generation of antibodies to other antigens, particularly those that are not very immunogenic, awaits further investigation.

The effects of antiapoptotic gene expression on B cell longevity was further demonstrated by the prolonged IgG and IgM serum titers to sheep red blood cells in inoculated Bcl-2 transgenic mice (Strasser et al. 1991). In addition, the numbers of splenocytes obtained from B galactosidase-immunized Bcl-2 transgenic mice were subsequently increased by two to five fold compared with wild-type BALB/c mice (Knott et al. 1996). When the splenocytes from these B galactosidase-immunized transgenic mice were used to produce hybridomas, 48% of the wells plated with the fused Bcl-2 expressing spleen cells produced B galactosidase-specific MAbs compared with only 14% of the wild-type splenocyte fusions. These results suggest that apoptosis inhibitory genes (endogenous and transgenic) may improve the efficiency of hybridoma production by increasing the numbers and repertoire of B cells obtained from each immunized mouse.

Pasqualini and Arap (2004) recently demonstrated that it may soon be possible to produce monoclonal antibodies without fusing them with myeloma cells. They demonstrated that splenocytes obtained from bacteriophage-immunized transgenic mice, H-2kb-tsA58 "Immorto-Mouse" (Charles River Breeding Laboratories, Wilmington, MA), could survive clonal selection and produce bacteriophage-specific MAbs in vitro. The key to this finding was that this mouse contains a recombinant construct that places the large T-antigen under the control of a temperature-sensitive mutant of the SV40 promoter, and thus when the splenocytes are grown at 33°C, the gene is expressed and the cells are immortalized. Additional studies are needed to determine whether this strategy will also be successful and practical in producing antibodies to additional antigens.

Myeloma and Hybridoma Cell Engineering

The expression of antiapoptotic genes affects the mouse's immune response to antigens, but does expression of these genes provide any advantage to the cells' survivability and production characteristics in vitro? Similar to the experiments using apoptosis-resistant splenocytes described above, Ray and Diamond (1994) and Kilpatrick and coworkers (1997) demonstrated that a larger repertoire of hybridoma cell lines were obtained when exogenous Bcl-2-expressing myelomas were used in fusions instead of their parental controls. These results can most likely be attributed to the protective effect of Bcl-2 expression on populations of hybridomas that would otherwise be destined for apoptosis and lost during the fusion process. Although postfusion Bcl-2 expression was not analyzed in these cells, the expression of exogenous Bcl-2 in other hybridoma cell lines was shown to suppress cell death rates under conditions of low cell density (Simpson et al. 1999), nutrient deprivation (Chung et al. 1998; Simpson et al. 1998), and increased intracellular acidity (Ishaque and Al-Rubeai 1998). In another set of studies, the increased survivability of Bcl-2 transfected hybridomas translated into increased monoclonal antibody yields (Itoh et al. 1995; Simpson et al. 1997). However, an advantage in MAb production was not noted in Bcl-2 transfected cells in two other independent studies (Bierau et al. 1998; Simpson et al. 1999).

When the genetic components of apoptosis-resistant (P3X63Ag8.653) and -susceptible (SP2/0 and D5) myeloma cell lines were compared, Bcl-XL, a protein related to Bcl-2, was found to be elevated (Gauthier et al. 1996). Similarly, we found that viability, maximal cell density, and MAb yields were markedly improved in 5-day batch cultures when Bcl-xl expression was restored to a hybridoma cell line that had been deficient in its expression (Peterson and Servinsky, submitted). These observations raise the prospects that strategies to identify and restore the expression of deficient genes that are important regulators of cell viability, such as Bcl-xl, may be an effective means to optimize MAb production.

Recently, it was demonstrated that deletion of a 60-amino acid unstructured loop from Bcl-2 and Bcl-xl enhanced the ability of the protein to prevent apoptosis (Chang et al. 1997; Figueroa et al. 2001). Chinese hamster ovary (CHO^1) cells that expressed the deletion mutant form of Bcl-2 (Bcl-2 delta) were also more resistant to Sindbis virus-mediated apoptosis than the parental cell line (Figueroa et al. 2001). As a result of this difference, higher yields of a heterologous protein encoded on the Sindbus virus were obtained from the Bcl-2 delta-expressing cell line. Additionally, Bcl-2 delta-expressing CHO cells adapted to serum deprivation better than the full-length Bcl-2-expressing CHO cells (Chang et al. 1997). Expression of a deletion mutant form of Bcl-xl (Bcl-xl delta) was also better at preventing apoptosis caused by IL-3 withdrawal in an immature B cell line than the full-length protein (Chang et al. 1997). Bcl-2 delta and Bcl-xl delta expression also inhibited apoptosis in two hybridoma cell lines that were studied in my laboratory; however, increases in batch MAb yields varied among the clones analyzed (N.C.P. and Servinsky, submitted). These results are similar to those obtained with the full-length Bcl family genes discussed above and are most likely attributed to the modifying effects of the backgrounds of each of the cells.

An alternative approach to increasing cell longevity in batch cultures is to decrease the cell's production of lactic acid, which when accumulated can lead to apoptosis. By using homologous recombination to partially disrupted lactic acid dehydrogenase A expression, Chen and colleagues were able to select a hybridoma cell clone that produced 50% less lactic acid than its parental cell (Chen et al. 2001). In batch culture, cells achieved a higher density and viability, and the amount of antibody harvested from 5-day cultures was three times greater than that obtained from the parental cell cultures. As additional information about cell metabolism and protein production is gained, additional targets will be identified for modification to maximize in vitro MAb yields.

Concluding Remarks

Despite numerous reports of the potential for alternative mouse strains and modified cell lines to enhance MAb production technologies, the commonly accepted resources have not changed. This situation may be due in part to the inconsistent gains in increased MAb yields obtained from cultures of genetically modified cell lines. Unfortunately, reported comparisons have not involved sufficient trials with different cell lines, animals, and/or antigens to make generalized conclusions, and experiments have been performed independently with no standardization.

To evaluate effectively whether the use of genetically modified mice or cell lines can significantly improve MAb production technology, it is necessary to invest considerable effort and resources to test these resources on a larger scale under consistent, defined conditions. Academic hybridoma production centers are ideally suited to perform this task because they receive numerous antigens for custom antibody production. Additional fusions using some of the genetically modified mice or cell lines discussed above could be included with each antigen submitted, and the success rates (positive clones) and MAb production yields obtained from the alternative and conventional approaches could be compared. Given that some academic hybridoma centers perform more than 30 fusions per year, sufficient trials could be included at these centers to evaluate the practical application of these alternatives effectively. Once completed, results should be publicized to avoid future duplication of efforts and to promote the use of these newly developed resources. This endeavor would be very worthwhile because even modest gains in the development of resources to increase fusion efficiencies and/or increases in MAb yields would have a significant impact, given the large-scale use of this technology.

In keeping with a philosophy of developing alternatives to animals (Russell and Burch 1959), innovations to increase the efficiency of hybridoma production would also reduce the number of animals needed per immunization (reduction). In addition, advances in in vitro MAb production technologies would further deflate the popularity of in vivo approaches (replacement).

References

Berezov A, Zhang HT, Greene MI, Murali R. 2001. Disabling erbB receptors with rationally designed exocyclic mimetics of antibodies: Structure-function analysis. J Med Chem 44:2565-2574.

Bierau H, Perani A, al-Rubeai M, Emery AN. 1998. A comparison of intensive cell culture bioreactors operating with hybridomas modified for inhibited apoptotic response. J Biotechnol 62:195-207.

Bremer E, Kuijlen J, Samplonius D, Walczak H, de Leij L, Helfrich W. 2004. Target cell-restricted and -enhanced apoptosis induction by a scFv:sTRAIL fusion protein with specificity for the pancarcinoma-associated antigen EGP2. Int J Cancer 109:281-290.

Chang BS, Minn AJ, Muchmore SW, Fesik SW, Thompson CB. 1997. Identification of a novel regulatory domain in Bcl-X(L) and Bcl-2. Embo J 16:968-977.

Chen K, Liu Q, Xie L, Sharp PA, Wang DI. 2001. Engineering of a mammalian cell line for reduction of lactate formation and high monoclonal antibody production. Biotechnol Bioeng 72:55-61.

Chester KA, Bhatia J, Boxer G, Cooke SP, Flynn AA, Huhalov A, Mayer A, Pedley RB, Robson L, Sharma SK, Spencer DI, Begent RH. 2000. Clinical applications of phage-derived sFvs and sFv fusion proteins. Dis Markers 16:53-62.

Choi TK, Hollenbach PW, Pearson BE, Ueda RM, Weddell GN, Kurahara CG, Woodhouse CS, Kay RM, Loring JF. 1993. Transgenic mice containing a human heavy chain immunoglobulin gene fragment cloned in a yeast artificial chromosome. Nat Genet 4:117-123.

Chung JD, Sinskey AJ, Stephanopoulos G. 1998. Growth factor and bcl-2 mediated survival during abortive proliferation of hybridoma cell line. Biotechnol Bioeng 57:164-171.

Di Paolo C, Willuda J, Kubetzko S, Lauffer I, Tschudi D, Waibel R, Pluckthun A, Stahel RA, Zangemeister-Wittke U. 2003. A recombinant immunotoxin derived from a humanized epithelial cell adhesion molecule-specific single-chain antibody fragment has potent and selective antitumor activity. Clin Cancer Res 9:2837-2848.

Drebin JA, Link VC, Greene MI. 1988. Monoclonal antibodies specific for the neu oncogene product directly mediate anti-tumor effects in vivo. Oncogene 2:387-394.

Figueroa B Jr, Sauerwald TM, Mastrangelo AJ, Hardwick JM, Betenbaugh MJ. 2001. Comparison of Bcl-2 to a Bcl-2 deletion mutant for mammalian cells exposed to culture insults. Biotechnol Bioeng 73:211-222.

Gauthier ER, Piche L, Lemieux G, Lemieux R. 1996. Role of bcl-X(L) in the control of apoptosis in murine myeloma cells. Cancer Res 56:1451-1456.

Graus YF, Verschuuren JJ, Degenhardt A, van Breda Vriesman PJ, De Baets MH, Posner JB, Burton DR, Dalmau J. 1998. Selection of recombinant anti-HuD Fab fragments from a phage display antibody library of a lung cancer patient with paraneoplastic encephalomyelitis. J Neuroimmunol 82:200-209.

Hansen MH, Nielsen H, Ditzel HJ. 2001. The tumor-infiltrating B cell response in medullary breast cancer is oligoclonal and directed against the autoantigen actin exposed on the surface of apoptotic cancer cells. Proc Natl Acad Sci U S A 98:12659-12664.

Holliger P, Prospero T, Winter G. 1993. "Diabodies": Small bivalent and bispecific antibody fragments. Proc Natl Acad Sci U S A 90:6444-6448.

Ishaque A, Al-Rubeai M. 1998. Use of intracellular pH and annexin-V flow cytometric assays to monitor apoptosis and its suppression by bcl-2 over-expression in hybridoma cell culture. J Immunol Methods 221: 43-57.

Itoh Y, Ueda H, Suzuki E. 1995. Overexpression of bcl-2, apoptosis suppressing gene: Prolonged viable culture period of hybridoma and enhanced antibody production. Biotechnol Bioeng 48:118-122.

Kellermann SA, Green LL. 2002. Antibody discovery: The use of transgenic mice to generate human monoclonal antibodies for therapeutics. Curr Opin Biotechnol 13:593-597.

Kikuchi Y, Uno S, Yoshimura Y, Otabe K, Iida S, Oheda M, Fukushima N, Tsuchiya M. 2004. A bivalent single-chain Fv fragment against CD47 induces apoptosis for leukemic cells. Biochem Biophys Res Commun 315:912-918.

Kilpatrick KE, Wring SA, Walker DH, Macklin MD, Payne JA, Su JL, Champion BR, Caterson B, McIntyre GD. 1997. Rapid development of affinity matured monoclonal antibodies using RIMMS. Hybridoma 16: 381-389.

Knott CL, Reed JC, Bodrug S, Saedi MS, Kumar A, Kuus-Reichel K. 1996. Evaluation of Bcl-2/B cell transgenic mice (B6) for hybridoma production. Hybridoma 15:365-371.

Kohler G, Milstein C. 1975. Continuous cultures of fused cells secreting antibody of predefined specificity. Nature 256:495-497.

Korn T, Muller R, Kontermann RE. 2004. Bispecific single-chain diabody-mediated killing of endoglin-positive endothelial cells by cytotoxic T lymphocytes. J Immunother 27:99-106.

Kortt AA, Lah M, Oddie GW, Gruen CL, Burns JE, Pearce LA, Atwell JL, McCoy AJ, Howlett GJ, Metzger DW, Webster RG, Hudson PJ. 1997. Single-chain Fv fragments of anti-neuraminidase antibody NC10 containing five- and ten-residue linkers form dimers and with zero-residue linker a trimer. Protein Eng 10:423-433.

Kortt AA, Malby RL, Caldwell JB, Gruen LC, Ivancic N, Lawrence MC, Howlett GJ, Webster RG, Hudson PJ, Colman PM. 1994. Recombinant anti-sialidase single-chain variable fragment antibody. Characterization, formation of dimer and higher-molecular-mass multimers and the solution of the crystal structure of the single-chain variable fragment/sialidase complex. Eur J Biochem 221:151-157.

Kuroiwa Y, Kasinathan P, Choi YJ, Naeem R, Tomizuka K, Sullivan EJ, Knott JG, Duteau A, Goldsby RA, Osborne BA, Ishida I, Robl JM. 2002. Cloned transchromosomic calves producing human immunoglobulin. Nat Biotechnol 20:889-894.

Le Gall F, Kipriyanov SM, Moldenhauer G, Little M. 1999. Di-, tri- and tetrameric single chain Fv antibody fragments against human CD19: Effect of valency on cell binding. FEBS Lett 453:164-168.

Marks JD, Hoogenboom HR, Bonnert TP, McCafferty J, Griffiths AD, Winter G. 1991. By-passing immunization. Human antibodies from V-gene libraries displayed on phage. J Mol Biol 222:581-897.

Murali R, Greene MI. 1998. Structure-based design of immunologically active therapeutic peptides. Immunol Res 17:163-169.

Nicholson IC, Zou X, Popov AV, Cook GP, Corps EM, Humphries S, Ayling C, Goyenechea B, Xian J, Taussig MJ, Neuberger MS, Bruggemann M. 1999. Antibody repertoires of four- and five-feature translocus mice carrying human immunoglobulin heavy chain and kappa and lambda light chain yeast artificial chromosomes. J Immunol 163:6898-6906.

Pasqualini R, Arap W. 2004. Hybridoma-free generation of monoclonal antibodies. Proc Natl Acad Sci U S A 101:257-259.

Peterson NC. 1996. Recombinant antibodies: Alternative strategies for developing and manipulating murine-derived monoclonal antibodies. Lab Anim Sci 46:8-14.

Peterson NC, Greene MI. 1998. Bacterial expression and characterization of recombinant biologically active anti-tyrosine kinase receptor antibody forms. DNA Cell Biol 17:1031-1040.

Pini A, Bracci L. 2000. Phage display of antibody fragments. Curr Protein Pept Sci 1:155-169.

Ray S, Diamond B. 1994. Generation of a fusion partner to sample the repertoire of splenic B cells destined for apoptosis. Proc Natl Acad Sci U S A 91:5548-5551.

Ritter G, Cohen LS, Williams C, Jr, Richards EC, Old LJ, Welt S. 2001. Serological analysis of human anti-human antibody responses in colon cancer patients treated with repeated doses of humanized monoclonal antibody A33. Cancer Res 61:6851-6859.

Russell WMS, Burch RL. 1959. The Principles of Humane Experimental Technique. London: Methuen & Co., LTD. [Reissued: 1992. Universities Federation for Animal Welfare, Herts, England.] Online (http://altweb.jhsph.edu/publications/human-exp/het=toc.htm).

Schmidt M, Wels W. 1996. Targeted inhibition of tumour cell growth by a bispecific single-chain toxin containing an antibody domain and TGF alpha. Br J Cancer 74:853-862.

Simpson NH, Milner A, Al-Rubeai M. 1997. Prevention of hybridoma cell death by BCL-2 during suboptimal culture conditions. Biotechnol Bioeng 54:1-16.

Simpson NH, Singh RP, Emery AN, Al-Rubeai M. 1999. Bcl-2 overexpression reduces growth rate and prolongs G1 phase in continuous chemostat cultures of hybridoma cells. Biotechnol Bioeng 64:174-186.

Simpson NH, Singh RP, Perani A, Goldenzon C, Al-Rubeai M. 1998. In hybridoma cultures, deprivation of any single amino acid leads to apoptotic death, which is suppressed by the expression of the bcl-2 gene. Biotechnol Bioeng 59:90-98.

Stockwin LH, Holmes S. 2003. Antibodies as therapeutic agents: Vive la renaissance! Expert Opin Biol Ther 3:1133-1152.

Strasser A, Whittingham S, Vaux DL, Bath ML, Adams JM, Cory S, Harris AW. 1991. Enforced BCL2 expression in B-lymphoid cells prolongs antibody responses and elicits autoimmune disease. Proc Natl Acad Sci U S A 88:8661-8665.

Takahashi N, Kakinuma H, Hamada K, Shimazaki K, Yamasaki Y, Matsushita H, Nishi Y. 2000. Improved generation of catalytic antibodies by MRL/MPJ-lpr/lpr autoimmune mice. J Immunol Methods 235:113-120.

Tomizuka K, Yoshida H, Uejima H, Kugoh H, Sato K, Ohguma A, Hayasaka M, Hanaoka K, Oshimura M, Ishida I. 1997. Functional expression and germline transmission of a human chromosome fragment in chimaeric mice. Nat Genet 16:133-143.

Verrier ED, Shernan SK, Taylor KM, Van de Werf F, Newman MF, Chen JC, Carrier M, Haverich A, Malloy KJ, Adams PX, Todaro TG, Mojcik CF, Rollins SA, Levy JH. 2004. Terminal complement blockade with pexelizumab during coronary artery bypass graft surgery requiring cardiopulmonary bypass: A randomized trial. JAMA 291:2319-2327.

Volkel T, Holig P, Merdan T, Muller R, Kontermann RE. 2004. Targeting of immunoliposomes to endothelial cells using a single-chain Fv fragment directed against human endoglin (CD105). Biochim Biophys Acta 1663:158-166.

Wijkhuisen A, Tymciu S, Fischer J, Alexandrenne C, Creminon C, Frobert Y, Grassi J, Boquet D, Conrath M, Couraud JY. 2003. Pharmacological properties of peptides derived from an antibody against the tachykinin NK1 receptor for the neuropeptide substance P. Eur J Pharmacol 468: 175-182.

A general method for greatly improving the affinity of antibodies by using combinatorial libraries

Arvind Rajpal*†‡, Nurten Beyaz*‡, Lauric Haber*‡, Guido Cappuccilli*, Helena Yee*, Ramesh R. Bhatt*‡, Toshihiko Takeuchi*‡, Richard A. Lerner‡§, and Roberto Crea*‡¶

*Bioren Inc., 100 Glenn Way, Suite 1, San Carlos, CA 94070; and §Department of Chemistry, The Scripps Research Institute, 10550 North Torrey Pines Road, La Jolla, CA 92037

Contributed by Richard A. Lerner, April 29, 2005

Look-through mutagenesis (LTM) is a multidimensional mutagenesis method that simultaneously assesses and optimizes combinatorial mutations of selected amino acids. The process focuses on a precise distribution within one or more complementarity determining region (CDR) domains and explores the synergistic contribution of amino acid side-chain chemistry. LTM was applied to an anti-TNF-α antibody, D2E7, which is a challenging test case, because D2E7 was highly optimized (K_d = 1 nM) by others. We selected and incorporated nine amino acids, representative of the major chemical functionalities, individually at every position in each CDR and across all six CDRs (57 aa). Synthetic oligonucleotides, each introducing one amino acid mutation throughout the six CDRs, were pooled to generate segregated libraries containing single mutations in one, two, and/or three CDRs for each V_H and V_L domain. Corresponding antibody libraries were displayed on the cell surface of yeast. After positive binding selection, 38 substitutions in 21 CDR positions were identified that resulted in higher affinity binding to TNF-α. These beneficial mutations in both V_H and V_L were represented in two combinatorial beneficial mutagenesis libraries and selected by FACS to produce a convergence of variants that exhibit between 500- and 870-fold higher affinities. Importantly, these enhanced affinities translate to a 15- to 30-fold improvement in *in vitro* TNF-α neutralization in an L929 bioassay. Thus, this LTM/combinatorial beneficial mutagenesis strategy generates a comprehensive energetic map of the antibody-binding site in a facile and rapid manner and should be broadly applicable to the affinity maturation of antibodies and other proteins.

look-through mutagenesis | maturation | mutagenesis | TNF-α

Nowadays one can create antibodies *in vitro* by methods that duplicate most aspects of the natural immune system (1, 2). For instance, combinatorial antibody libraries allow one to obtain numbers of antibodies that greatly exceed the diversity of the natural repertoire and are not limited by the phenomenon of immune tolerance. In addition, multiple display technologies are available to link recognition and replication such that improved antigen-binding clones can be enriched, recovered, and retrieved. One significant aspect of the natural immune system not yet duplicated by current methods is the use of the powerful evolutionary principle of mutation and selection to achieve affinity maturation. However, as we can now create very large numbers of antibodies *in vitro*, it should be possible to duplicate or even improve on nature's affinity maturation process by the use of a precise selection process based on chemical principles that optimize the interactions between antibody and antigen. Here, we describe a method where such a chemical approach is used to dramatically increase the affinity of an antibody. To demonstrate the substantial power of this method, we chose an antibody whose affinity had already been optimized by several orders of magnitude.

Current antibody affinity maturation methods belong to two mutagenesis categories: stochastic and nonstochastic. Error-prone PCR, mutator bacterial strains (3), and saturation mutagenesis (4–7) are typical examples of stochastic mutagenesis methods. When applied to multiple positions within multiple complementarity determining regions (CDRs) these stochastic strategies fail to provide practical comprehensive mutagenic coverage because the size of any resulting complete library typically exceeds the limitations of all current physical display systems. Nonstochastic techniques often use alanine-scanning or site-directed mutagenesis to generate limited collections of specific variants.

Look-through mutagenesis (LTM) was developed to provide a comprehensive optimization map of the antibody-binding site in a facile and rapid manner. For LTM, nine amino acids, representative of the major side-chain chemistries provided by the 20 natural amino acids, were selected (Fig. 1) to dissect the functional side-chain contributions to binding at every position in all six CDRs of the antibody (Fig. 1). LTM generates a positional series of single mutations within a CDR where each "wild type" residue is systematically substituted by one of nine selected amino acids. Mutated CDRs are combined to generate combinatorial single-chain variable fragment (scFv) libraries of increasing complexity and size without becoming prohibitive to the quantitative display of all variants. After positive selection, clones with improved binding were sequenced, and those beneficial mutations were mapped. To identify synergistic mutations for improved binding, combinatorial libraries (combinatorial beneficial mutations, CBMs) expressing all beneficial permutations were produced by mixed DNA probes, positively selected, and analyzed to identify a panel of optimized scFVs candidates.

The model system used to test the LTM affinity maturation technology was the anti-TNF-α antibody D2E7 (8). Six LTM libraries with single mutations in each individual CDR, 15 LTM libraries with single mutations in two CDRs, and 20 LTM libraries with single mutations in three CDRs were generated for the combined V_H and V_L domains and screened for improved affinity. In this first broad iteration, 38 mutations identified in 21 CDR positions (comprising five of the six CDRs) yielded higher-affinity binders (Table 1). These individual beneficial mutations were combined to generate two sets of CBM libraries (V_H and V_L libraries independently) that were subsequently screened, combined, and further selected for improved binding. Ultimately, 42 clones with dramatically improved binding were characterized and sequenced (Table 2). Among these selected CBM library variants were antibodies that exhibit up to 870-fold enhancement in binding, resulting in low picomolar affinities for TNF-α. Equally important, through the process of generating

Freely available online through the PNAS open access option.

Abbreviations: CDR, complementarity determining region; LTM, look-through mutagenesis; CBM, combinatorial beneficial mutation; SA, streptavidin; PE, phycoerythrin; scFv, single-chain variable fragment.

†Present address: Pfizer Inc., Eastern Point Road, Groton, CT 06340.

‡A.R., N.B., L.H., G.C., H.Y., R.R.B., T.T., R.A.L., and R.C. have a financial interest in Bioren, Inc.

¶To whom correspondence should be addressed. E-mail: crea@biorenInc.com.

www.pnas.org/cgi/doi/10.1073/pnas.0503543102

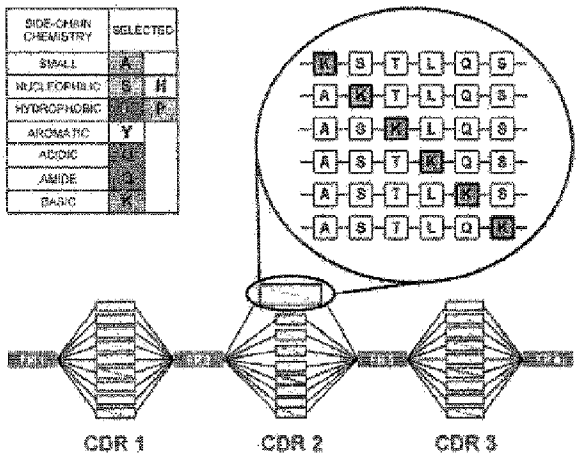

Fig. 1. Triple LTM example. Nine amino acids, representative of the 20, were selected for the LTM process based on their side-chain chemical functionalities (*Inset Left*). Discrete CDR oligonucleotides are synthesized to produce a mutagenized CDR with one target amino acid mutation at each CDR position (*Inset Right*). In the triple CDR library, all combinations of CDR1, CDR2, and CDR3 oligonucleotides are combined to produce libraries with three simultaneously mutagenized CDRs.

and examining optimized sequences from the LTM diversity libraries a comprehensive map of the D2E7 binding site was quickly delineated.

Materials and Methods

Reagents. Synthetic oligonucleotides were obtained from Syngen (San Carlos, CA). Restriction enzymes were obtained from New England Biolabs. Polymerases and yeast strain EBY100 were obtained from Invitrogen. DNA purification kits were obtained from Qiagen (Valencia, CA). dNTPs were obtained from Fermentas (Hanover, MD). TNF-α was obtained from PeproTech (Rocky Hill, NJ), and streptavidin (SA)–phycoerytherin (PE), anti-His-FITC, and Biotin-XX were from Molecular Probes. Endotoxin QCL-1000 kits were purchased from Cambrex (East Rutherford, NJ). All media were prepared according to the vendor's instructions (Invitrogen).

D2E7 scFv Construction and Display. The D2E7 scFv construct was assembled by overlap PCR. Briefly, an equimolar mixture of 30 oligonucleotides (final 0.4 μM) was PCR-assembled by using 0.5 μl of Pfx DNA polymerase (2.5 units per μl) and 5 μl of Pfx buffer (Invitrogen). A second PCR step with oligonucleotide primers to incorporate 5′ BamHI and 3′ NotI restriction sites was used for directional subcloning into modified yeast display vector pYD1 (Invitrogen). The modified construct ultimately incorporated a C-terminal hexahistidine and c-myc epitope tag for purification and detection, respectively. After sequence verification the construct served as the template for subsequent LTM libraries.

TNF-α Biotinylation. Briefly, 300 μl of TNF-α (1 mg/ml) was added to 30 μl of 1 M sodium bicarbonate buffer (pH 8.3) and 5.8 μl of Biotin-XX (20 mg/ml in DMSO). The mixture was incubated for 1 h at room temperature. Unincorporated biotin was removed by microconcentration (Microcon, Millipore), and buffer was exchanged with four volumes of PBS washes. Protein concentration was determined by OD_{280}.

scFv Expression and Display. The D2E7 construct and LTM/CBM variants were transformed into EBY100 yeast and selected in complete supplement mixture, minus tryptophan media. Cultures were then induced by 20% galactose select media for 48 h at 20°C. After induction, cells were washed twice with PBS and resuspended in PBS/0.5% BSA.

LTM Library Construction. Individual oligonucleotides were synthesized to encode each amino acid substitution for each CDR position and provide sufficient overlap for PCR priming from the D2E7 template. Briefly, PCRs containing LTM oligonucleotide mixtures corresponding to individual CDRs were used to amplify LTM-substituted CDR fragments. Next, these PCR products were gel-purified, and equimolar aliquots were combined for megaprime PCR to regenerate full-length scFv. To generate combinatorial LTM libraries for multiple CDRs we followed the protocol described above, except instead of using the parental D2E7 construct as PCR template a previously generated single or double CDR LTM library was used instead.

Magnetic Bead LTM Library Selection. Briefly, 1×10^7 cells were incubated for 2 h at room temperature with biotinylated TNF-α (final concentrations of 50, 0.5, and 0.1 nM), pelleted, and bound to 1×10^8 SA beads (Spherotech, Libertyville, IL). The magnet was applied, and cells were washed with PBS/0.5% BSA. The beads were directly resuspended into 2 ml of glucose selective media and grown for 2 days at 30°C, shaking at 300 rpm.

FACS Sorting of scFv Libraries. After scFv induction, cells were incubated with 400 nM biotin–TNF-α for 3 h at room temperature under shaking. Cells were washed with two volumes of PBS, then resuspended in PBS/BSA containing 1 μM TNF-α, and incubated at 25°C for an additional 24–70 h. After this chase, the cells were washed twice with PBS/BSA buffer, then labeled with SA–PE (2 mg/ml) and anti-His–FITC (25 nM) for 30 min on ice, washed, and resuspended as described. The D2E7 bearing yeast were used to set a threshold for sorting improved clones from the LTM library. Cells expressing the scFv fusion (FITC-positive) that displayed greater binding to biotin–TNF-α (PE signal) were bulk-sorted. After collecting these clones, we performed a postsort flow cytometry analysis to confirm enrich-

Table 1. LTM mutations that yield higher affinity for TNF-α

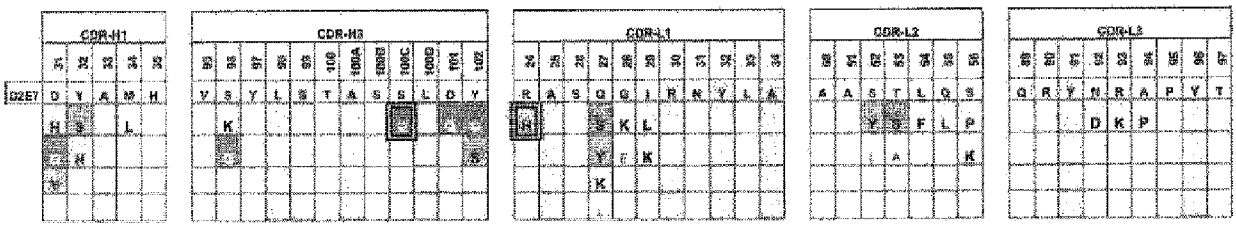

In gray are amino positions where no LTM substitutions are observed. In color are amino acid positions that were combined in the CBM process. Highlighted positions are derived from magnetic bead selections. Amino acid positions are numbered according to Kabat *et al.* (34).

Table 2. Sequence of CBM clones displaying higher affinity for TNF-α

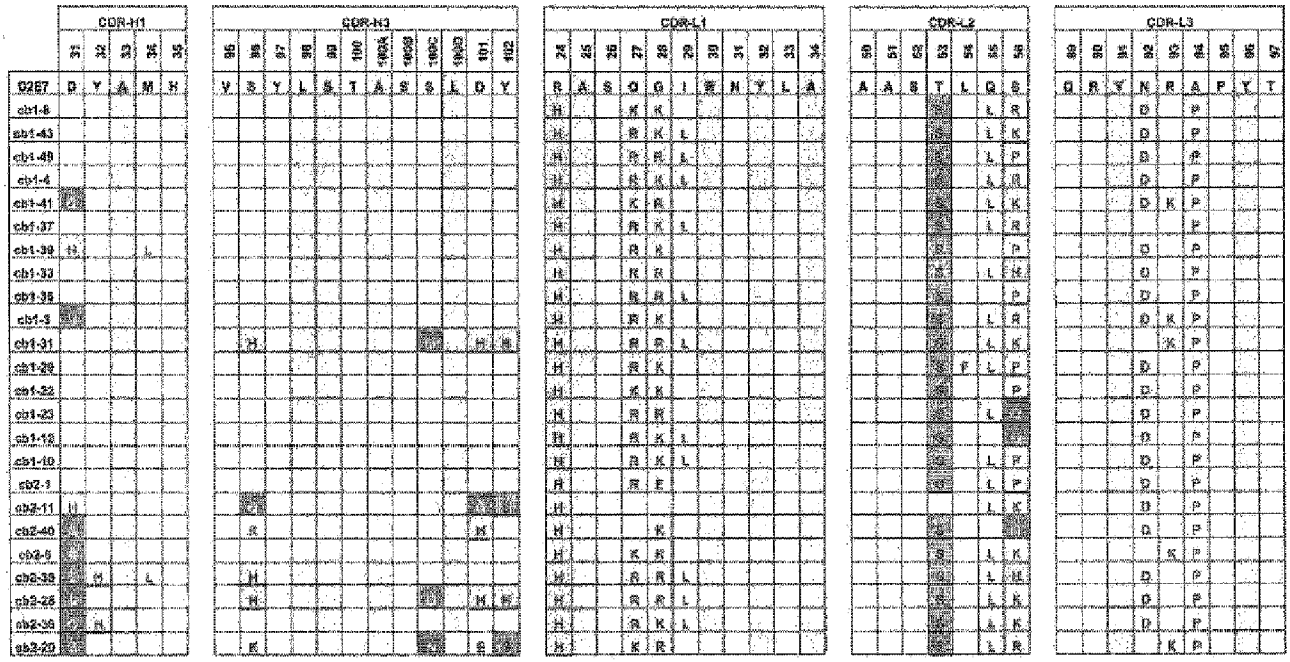

ment. Bulk-sorted clones were then propagated in 10% glucose select media at 30°C for 48 h and then plated on solid media for clonal segregation.

CBM Library Construction. Twenty nine selected beneficial D2E7 CDR mutations obtained through the LTM screen were used to combinatorially construct CBM libraries by the use of degenerate CDR oligonucleotides. They were CDR H1 (ctgggttcaccttt-gac BAK YMT GCT MTG CAT tgggtccgacaagcgccag), CDR H3 (gtatattactgtgcaaag GTG MRY TAC TTA TCA ACA GCT TCT MRK CTA SAK YMK tgggggcaaggcactctag), CDR L1 (gacagagtaacaataacgtgt CRT GCA TCT HRK RRA MWA AGA AAT TAT CTC GCA tggtatcaacagaagccg), CDR L2 (cacctaagctgttaatttat GCC GCC TMT WCT TTW CWA MVK ggtgtgccttctaggtttag), and CDR L3 (gacgttgcaacatattactgt CAA AGA TAC RAT ARA SCT CCA TAT ACA ttcggtcaaggtacta-aagtc). Degenerated oligos were used to separately produce heavy- and light-chain CBM libraries by PCR (V_H CBM-V_L parental and V_H parental-V_L CBM). These two scFv libraries were subjected to a single round of dissociation-kinetics FACS selection, yielding two enriched populations (V_H CBM-rd1-V_L parental and V_H parental-V_L CBM-rd1) The CBM-rd1 heavy and light chains were then PCR-amplified and used to generate three additional libraries (V_H CBM-rd1-V_L CBM, V_H CBM-V_L CBM-rd1, and V_H CMB-rd1-V_L CBM-rd1). Those three libraries were finally pooled and subjected to two additional rounds of FACS-based selection.

Expression and Purification of D2E7 Variants. All scFvs were subcloned into pBAD (Invitrogen) and secreted into the *Escherichia coli* periplasm of LMG194 cells (Invitrogen) with a C-terminal 6×His-Myc epitope tag. Individual colonies were grown at 37°C to OD_{600} 1–2 in RM media (M9 salts/2% Casamino acids/0.2% glucose/1 mM $MgCl_2$), then diluted 100-fold into LB media and grown at 37°C to OD_{600} 0.5 and then induced with arabinose (final concentration of 0.0002%) overnight at room temperature. Subsequently, bacteria were harvested by centrifugation, hypertonically lysed by resuspending the cell pellet in 1/25th volume sucrose buffer (20% sucrose/30 mM Tris, pH 8.0/1 mM EDTA), and incubated for 1 h on ice. Cells were then gently collected by centrifugation, resuspended (equal in volume to sucrose buffer) in BBS buffer (200 mM boric acid/160 mM NaCl/10 mM EDTA), and incubated overnight at 4°C. EDTA was then removed from the sucrose and BBS buffers by dialysis or through chelation with four mole equivalents of $MgSO_4$ and then purified by nickel chelate chromatography (Qiagen) and eluted with PBS containing 250 mM imidazole. Samples were then concentrated by using ultra-free concentrators (Amicon) and exchanged into citrate buffer (20 mM sodium citrate, pH 5.5) by using a PD-10 size exclusion column (Amersham Pharmacia). The resulting eluate was purified to homogeneity by using cation exchange chromatography on a mono S column (Amersham Pharmacia). After cation exchange, the resulting protein was buffer-exchanged into PBS by using a PD-10 column. For cell-based assays, endotoxin was removed by reisolation from an endotoxin-free PBS-equilibrated superdex 75 column that had been previously treated with 1 M NaOH. Resulting endotoxin levels were <2.5 units per mg for all samples, as assayed by an endotoxin kit (Cambrex).

BIAcore Assay. Binding affinities ($K_D = k_d/k_a = k_{off}/k_{on}$) of the scFv antibodies were measured by using a BIAcore 3000 surface plasmon resonance system (BIAcore, Neuchatel, Switzerland). TNF-α was immobilized on a CM5 chip according to the manufacturer's instructions. scFv samples in concentrations between 30 pM and 1 nM were injected over the TNF surfaces with a 10-min association phase followed by a 3-h dissociation phase. All experiments were carried out at 25°C. Binding data were fit to a simple 1:1 interaction model to extract binding constants by using CLAMP (9). For the TNF-β cross-reactivity experiment, TNF-α and TNF-β were immobilized to ≈1,000 response units as above, and the chips were subjected to a solution containing 100 nM scFv in running buffer.

Cell Culture. L929 cells were propagated in Eagle's minimal essential medium, supplemented with 2 mM L-glutamine, and

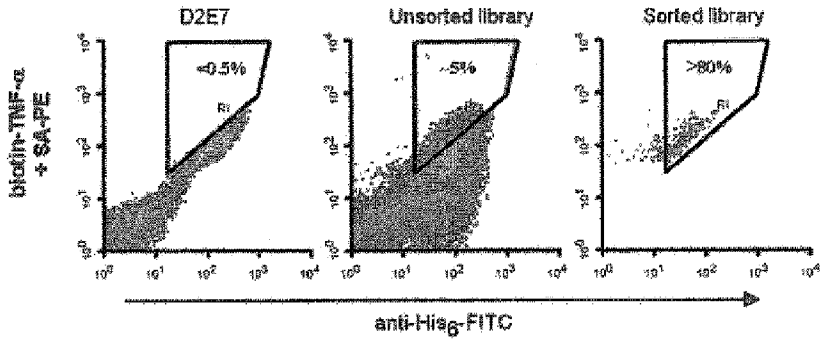

Fig. 2. Dot plot of yeast displayed anti-TNF-α scFv. (*Left*) D2E7 staining was used to thresholds for improved binders. (*Center*) The LTM libraries. Shown is FACS profile for the unsorted library. (*Right*) The dot plot profile for the sorted library.

Earle's balanced salt solution adjusted to contain 1.5 g/liter sodium bicarbonate, 0.1 mM nonessential amino acids, 1.0 mM sodium pyruvate, 10% FBS, and 50 μg/ml gentamycin. Cells were maintained throughout the study at 37°C and 5% CO_2.

TNF-α Neutralization Assay. A total of 35,000 L929 cells in complete growth media were added to each well of a 96-well plate and grown overnight. For inhibition studies scFvs were preincubated with TNF-α (350 pg/ml) at room temperature for 30 min. Just before TNF-α treatment, growth media were removed and replaced with 0.5 volume Eagle's minimal essential medium containing 10% FBS and 1 μg/ml actinomycin D. The TNF-α–scFvs complexes were next added to the plate immediately after changing the media so that the cells were exposed to actinomycin D for no longer than 15 min. Next, the L929 cells were incubated for 20–24 h at 37°C. The next day, 20 μl of WST-1 was added to each well and incubated for an additional 4 h at 37°C, and OD_{450} were then read. IC_{50}s were determined from these readings by using PRISM 3.02 software (GraphPad, San Diego). Each measurement was performed in quadruplicate, and each experiment was performed a minimum of two times.

Results

Design and Yeast Display of D2E7 scFv. The D2E7 scFv was designed starting from a published sequence by using codons optimized for both *Saccharomyces cerevisiae* and *E. coli* usage (10) and constructed by assembly PCR. In the D2E7 scFv the C terminus of V_H was fused to the N terminus of V_L by a $(Gly_4–Ser)_3$ linker. The scFv was displayed as a fusion to the C terminus of the yeast extracellular protein Aga2p. We found the displayed scFv fusion bound TNF-α with an EC_{50} of 13.5 nM (data not shown).

LTM Library Construction. In LTM, only one wild-type amino acid is substituted per CDR with a selected amino acid (Fig. 1). In total, nine selected amino acids were chosen to produce individual CDR LTM libraries. The individual CDR libraries were then combined to generate 15 double (two CDRs simultaneously mutated per clone) and 20 triple (three CDRs mutated) LTM libraries (Fig. 2). By design, the most diverse triple LTM library contained 1.4×10^6 distinct scFv mutants. As the number of mutants for four, five, and six mutated CDRs would exceed the practical limits of yeast display, we restricted the complexity of the LTM libraries to any three of the light- and heavy-chain CDRs. The final LTM library thus is made of 6 single, 15 double, and 20 triple LTM libraries. To assess library integrity and diversity we sequenced and analyzed ≈200 random clones (data not shown). In general, we found that the libraries were highly diverse with an extremely low number of contaminating wild-type clones. We did notice increased error rates that correlated to the increasing complexity of each library. This finding is not surprising as the aggregation of errors in template libraries is cumulatively propagated in the generation of subsequent more complex libraries.

Isolation of Improved Binding Clones from LTM Libraries. Initially, an equilibrium magnetic bead-based method was used and only resulted in a modest 2-fold increased affinity. Further improvements by this selection strategy were inherently limited by low signal-to-noise ratios as equilibrium selection methods require antigen levels in the range of the antibody K_D (<1 nM).

However, because most affinity maturation techniques yield optimization of the dissociation rate constant, k_{off} (5, 11, 12), a pulse–chase strategy was used to select for clones that display slower dissociation kinetics than the parent molecule. We accomplished this selection by labeling the yeast cell surface-displayed libraries with biotin-TNF-α and chasing with unlabeled TNF-α. Subsequent FACS sorting enabled the enrichment of slower dissociating clones. As expected, a bulk of the library displayed unproductive low-expressing, fast-dissociating constituents. However, a significant number of mutants displayed improved binding compared with D2E7 (Fig. 2).

After three rounds of sorting the single, double, and triple libraries separately, we combined these enriched libraries and conducted an additional two rounds of selections. Finally, 210 colonies were analyzed for dissociation kinetics and sequenced. Thirty-two unique clones (Table 1) displayed slower dissociation kinetics (dissociation profiles for some of these are shown in Fig. 3). In all, we found 14 positions in the CDRs (one in CDRH1, three in CDRH2, four in CDRH3, four in CDRL1, and two in CDRL3) that were never mutated and were termed as the primary binding architecture. Mutations conferring higher affinity were characterized as beneficial mutations and mutations that did not alter affinity were characterized as neutral mutations.

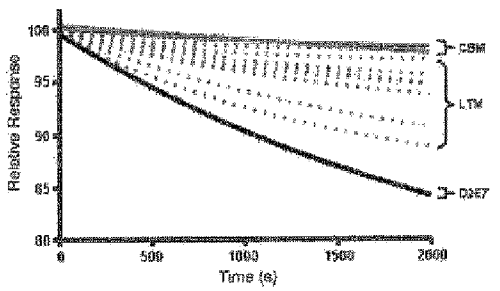

Fig. 3. BIAcore dissociation profiles of D2E7, LTM (broken lines), and CBM clones.

Table 3. BIAcore parameters for WT, LTM, and CBM clones

scFv	k_{on} ($\times 10^6$ $M^{-1}s^{-1}$)	Error	k_{off} ($\times 10^{-5}$ s^{-1})	Error	K_D, pM	Relative K_D improvement
D2E7	1.12	0.02	107.000	0.1	955 ± 17	
A1	11.1	0.3	2.086	0.004	1.88 ± 0.05	500
cb2–44	5.8	0.4	0.637	0.01	1.10 ± 0.08	870
cb1–3	7.1	0.1	0.770	0.02	1.08 ± 0.02	870
cb2–6	4.0	0.9	0.0454	0.02	1.1 ± 0.3	870

A1 sequence has D2E7 mutations: CDRH1:D31Q, CDRH3:S99P, CDRL1:G28E.

Generating and Screening CBM Libraries. An amino acid map of all clones that confer higher affinity (or slower dissociation rates) was compiled for each of the CDR sequences (Table 1). Mutations observed in multiple clones were selected and combined into CBM libraries to explore the synergistic potential among these individual mutations. Degenerate oligonucleotides encoding the selected amino acid mutations, in addition to the wild-type amino acid, were synthesized and assembled to produce these libraries. The use of degenerate nucleotides not only reduces the number of oligonucleotides necessary to introduce the selected mutations, but also allows the introduction of yet another aspect of natural evolution into the process (Table 4, which is published as supporting information on the PNAS web site). Because of the practical display limitations of *S. cerevisiae*, scFv libraries were built separately for the V_H (diversity of 2×10^5) and V_L (diversity of 6×10^5) domains. After three rounds of selection the V_H and V_L libraries were combined by PCR, and the resulting libraries were pooled for two rounds of additional selection. From 68 selected mutants, we found a total of 58 mutants that displayed slower dissociation rates than D2E7. A total of 14 positions in CDRH1, CDRH2, CDRH3, CDRL1, and CDRL3 were mutated. From sequence analysis of the 42 unique clones we discovered a dramatic substitution pattern (Table 2). Only seven positions in V_H CDRs are mutated with little convergence in type of mutation. However, in V_L CDRs there is remarkable convergence of mutations. Four positions in the CDR L1 were mutated repeatedly with a strict requirement for His-24, two positively charged residues Lys-27 and Arg-28 in the middle, followed by a conservative change in hydrophobic Ile-29 to Leu-29. Three mutations in CDR L2 were also detected in the majority of the clones. The first change is a conservative change from Thr-53 to Ser-53 followed by a less conservative Gln-55 to Leu-55. There is little convergence in the type of mutation in position 56 in the CDR, suggesting a less stringent requirement in this position. Two positions (92 and 94) in the middle of CDRL3 were mutated in almost all instances, whereas an Arg-93 to Lys-93 conservative mutation was observed in only some of the clones. Interestingly, the selection of a Pro-94–Pro-95 sequence in this CDR suggests dramatic changes in secondary structure in this region.

Determining Affinities of Improved Clones. Several selected clones from the LTM and CBM libraries were expressed as scFvs in *E. coli*. Affinity measurements for these clones were determined by surface plasmon resonance (Fig. 3; values for kinetic and equilibrium parameters are in Table 3). Remarkably, in the CBM clones there is dramatic improvement in both k_{on} and k_{off}. In fact, the highest affinity clone displays a 20-fold improvement in k_{on} and 10-fold in k_{off}.

L929 *in Vitro* Neutralization Assay. Next, we tested the neutralization activity of the affinity-enhanced CBM clones by using a TNF-α-responsive L929 cell-based bioassay. By this assay we found the bioactivity of the parent D2E7 (105 pM) consistent with previous reports (8), whereas the IC_{50} values for our CBM-optimized clones (3–6 pM) demonstrated 15- to 30-fold enhancement in neutralization (Fig. 4).

Discussion

Antibodies have become an increasingly important class of therapeutic molecules for numerous indications, including cancer, organ rejection, antiviral prophylaxis, rheumatoid arthritis, psoriasis, and Crohn's disease (13). High affinity and specificity are critical parameters to their therapeutic utility. To generate Abs of clinical utility with the highest affinity possible, a facile and comprehensive affinity maturation method is needed.

Numerous protein engineering and mutagenesis strategies have been used for the enhancement of antibody affinity (3, 5, 6, 11, 14–29). For small regions (<8–10 aa), saturation mutagenesis is typically used to produce all combinations of the 20 naturally occurring amino acids. However, this process becomes impractical beyond eight to 10 positions because of library display capacities (30). Affinity maturation of antibodies involving 60 positions (six CDR loops) would yield unmanageably large libraries ($>10^{78}$) that are impossible to produce and screen with current expression-display systems. As a result, some researchers have limited saturation mutagenesis to one or two CDRs, such as CDR L3 and H3, because a majority of binding energy is thought to be contributed by these two CDR loops (19). Reduced codon complexity to limit library diversity has also been proposed (15, 20, 31). Alternatively, specific residues among the six CDRs are selected based on their propensity for somatic hypermutation (6, 29). Although these strategies can result in significant affinity enhancement, none comprehensively interrogate all six CDR positions in a precise and informative fashion. Other stochastic methods used for maturation (21, 23) are also limited because of the inherent randomness in such mutagenesis strategies. Although improved properties might be obtained through

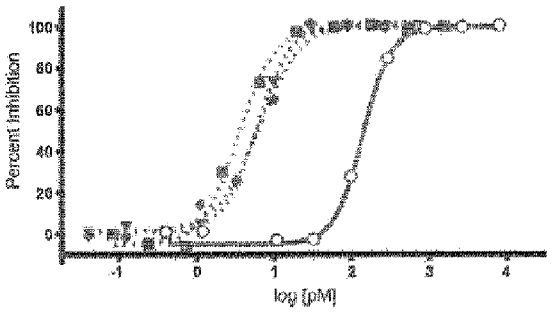

Fig. 4. Affinity-matured anti-TNF-α antibodies have improved neutralizing abilities. L929 cells were treated with actinomycin and TNF-α, as indicated for 24 h, in the absence and presence of purified anti-TNF-α scFv antibodies. WST-1 was added and incubated for an additional 4 h, and OD_{450} was recorded. Fifty percent neutralizing dose values were 141 pM for D2E7 (open green circle), 3.5 pM for A1 (red square), 6.1 pM for cb1-3 (red triangle), and 6.5 pM for cb2-6 (red diamond). Data represent mean ± SEM with each measurement performed in quadruplicate.

these methods, a directed, rational, and informative method based on chemical principles should yield vastly improved variants and informative results about the binding site architecture.

In the present study our approach improved the affinity of an important therapeutic antibody from low nanomolar (1 nM) to low picomolar (1.1 pM). Some of the mutations that we observe that are important to this optimization agree with previous work, in that a significant loss of binding is observed when either Tyr-91 or Tyr-95a in CDRL3 or Leu-98 and Leu-100d in CDRH3 (Table 2) are mutated to alanine (8). However, LTM goes much further in that we identify 10 additional residues as nonenhanceable sites. Although the process of alanine scanning (32, 33) is useful for defining thermodynamic properties of individual positions in the antibody–antigen interface, LTM is better suited for affinity maturation. In LTM, residues important to interaction with antigen and/or overall structure are essentially captured by LTM as a subset of the primary binding architecture, while simultaneously and expeditiously defining mutations that result in improved binding.

The LTM process, in which there is a single amino acid mutation in all positions for each CDR loop, allows the construction of a high-resolution contextual roadmap to rapidly direct further affinity enhancement by combining multiple mutations for synergistic gains. The CBM strategy builds on the LTM process to produce libraries encoding all of the observed beneficial mutations, as well as the parent amino acid sequence, thereby allowing a simultaneous combinatorial "backcross" to occur, thereby eliminating all nonproductive combinations. An advantage of using degenerate oligonucleotides is the incorporation of additional related amino acids during the process, thus allowing further fine-tuning of side-chain interactions. These additional amino acids were allowed and selected in multiple positions, most notably Arg-27 in CDR L1 (see Table 4). As a result, this CBM process produces a convergence of highly optimized activities in the broadest scope of sequence space. The backcross aspect of affinity maturation used here is not part of the process of natural antibody evolution in that, in nature, the recombination event occurs before somatic mutation, and thus further synergy between the two processes is not allowed.

Interestingly, the analysis of the most improved CBM mutants shows a preponderant number of variants in the V_L chain as compared with the V_H. These results may support the notion that the V_H chain has been provided in nature with a more robust optimization strategy than that for the V_L chain (i.e., by VDJ joining). A less optimized V_L chain could in turn be the focus for an expedited affinity maturation path, especially if multiple chemical amino acid contributions can be assessed simultaneously. Thus, our chemical algorithm that allows for both V_H and V_L optimization by a concerted process of recombination and mutation may be more powerful than the genetic algorithm of nature.

We thank Jennifer Jones, Tonia Buechholz, and Randy Shen for technical contributions, Mark Gilbert and Dick Stovel at the Stanford FACS facility (Stanford, CA) for sorting the yeast libraries, David Myszka at Biosensor Tools (Salt Lake City) for BIAcore measurements, and Laurie Goodman at Marin Biologic Laboratories (Tiburon, CA) for cell assays.

1. Huse, W. D., Sastry, L., Iverson, S. A., Kang, A. S., Alting-Mees, M., Burton, D. R., Benkovic, S. J. & Lerner, R. A. (1989) *Science* **246,** 1275–1281.
2. McCafferty, J., Griffiths, A. D., Winter, G. & Chiswell, D. J. (1990) *Nature* **348,** 552–554.
3. Low, N. M., Holliger, P. H. & Winter, G. (1996) *J. Mol. Biol.* **260,** 359–368.
4. Nishimiya, Y., Tsumoto, K., Shiroishi, M., Yutani, K. & Kumagai, I. (2000) *J. Biol. Chem.* **275,** 12813–12820.
5. Yang, W. P., Green, K., Pinz-Sweeney, S., Briones, A. T., Burton, D. R. & Barbas, C. F., 3rd (1995) *J. Mol. Biol.* **254,** 392–403.
6. Chowdhury, P. S. & Pastan, I. (1999) *Nat. Biotechnol.* **17,** 568–572.
7. Chowdhury, P. S. (2002) *Methods Mol. Biol.* **178,** 269–285.
8. Salfeld, J. G., Allen, D. J., Hoogenboom, H. R., Kaymakçalan, Z., Labkovsky, B., Mankovich, J. A., McGuinness, B. T., Roberts, A. J., Sakoralas, P., Schoenhaut, D., *et al.* (2003) U.S. Patent 6,090,382.
9. Myszka, D. G. & Morton, T. A. (1998) *Trends Biochem. Sci.* **23,** 149–150.
10. Nakamura, Y., Gojobori, T. & Ikemura, T. (2000) *Nucleic Acids Res.* **28,** 292.
11. Thompson, J., Pope, T., Tung, J. S., Chan, C., Hollis, G., Mark, G. & Johnson, K. S. (1996) *J. Mol. Biol.* **256,** 77–88.
12. Hawkins, R. E., Russell, S. J. & Winter, G. (1992) *J. Mol. Biol.* **226,** 889–896.
13. Brekke, O. H. & Sandlie, I. (2003) *Nat. Rev. Drug Discov.* **2,** 52–62.
14. Gram, H., Marconi, L. A., Barbas, C. F., 3rd, Collet, T. A., Lerner, R. A. & Kang, A. S. (1992) *Proc. Natl. Acad. Sci. USA* **89,** 3576–3580.
15. Balint, R. F. & Larrick, J. W. (1993) *Gene* **137,** 109–118.
16. Griffiths, A. D., Malmqvist, M., Marks, J. D., Bye, J. M., Embleton, M. J., McCafferty, J., Baier, M., Holliger, K. P., Gorick, B. D., Hughes-Jones, N. C., *et al.* (1993) *EMBO J.* **12,** 725–734.
17. de Kruif, J., Boel, E. & Logtenberg, T. (1995) *J. Mol. Biol.* **248,** 97–105.
18. Crameri, A., Cwirla, S. & Stemmer, W. P. (1996) *Nat. Med.* **2,** 100–102.
19. Schier, R., McCall, A., Adams, G. P., Marshall, K. W., Merritt, H., Yim, M., Crawford, R. S., Weiner, L. M., Marks, C. & Marks, J. D. (1996) *J. Mol. Biol.* **263,** 551–567.
20. Schier, R., Balint, R. F., McCall, A., Apell, G., Larrick, J. W. & Marks, J. D. (1996) *Gene* **169,** 147–155.
21. Wu, H., Beuerlein, G., Nie, Y., Smith, H., Lee, B. A., Hensler, M., Huse, W. D. & Watkins, J. D. (1998) *Proc. Natl. Acad. Sci. USA* **95,** 6037–6042.
22. Chen, Y., Wiesmann, C., Fuh, G., Li, B., Christinger, H. W., McKay, P., de Vos, A. M. & Lowman, H. B. (1999) *J. Mol. Biol.* **293,** 865–881.
23. Wu, H., Nie, Y., Huse, W. D. & Watkins, J. D. (1999) *J. Mol. Biol.* **294,** 151–162.
24. Boder, E. T., Midelfort, K. S. & Wittrup, K. D. (2000) *Proc. Natl. Acad. Sci. USA* **97,** 10701–10705.
25. Daugherty, P. S., Chen, G., Iverson, B. L. & Georgiou, G. (2000) *Proc. Natl. Acad. Sci. USA* **97,** 2029–2034.
26. Maynard, J. A., Maassen, C. B., Leppla, S. H., Brasky, K., Patterson, J. L., Iverson, B. L. & Georgiou, G. (2002) *Nat. Biotechnol.* **20,** 597–601.
27. Short, M. K., Krykbaev, R. A., Jeffrey, P. D. & Margolies, M. N. (2002) *J. Biol. Chem.* **277,** 16365–16370.
28. Graff, C. P., Chester, K., Begent, R. & Wittrup, K. D. (2004) *Protein Eng. Des. Sel.* **17,** 293–304.
29. Ho, M., Kreitman, R. J., Onda, M. & Pastan, I. (2005) *J. Biol. Chem.* **280,** 607–617.
30. Smothers, J. F., Henikoff, S. & Carter, P. (2002) *Science* **298,** 621–622.
31. Chames, P., Coulon, S. & Baty, D. (1998) *J. Immunol.* **161,** 5421–5429.
32. Jones, J. T., Ballinger, M. D., Pisacane, P. I., Lofgren, J. A., Fitzpatrick, V. D., Fairbrother, W. J., Wells, J. A. & Sliwkowski, M. X. (1998) *J. Biol. Chem.* **273,** 11667–11674.
33. Cunningham, B. C. & Wells, J. A. (1989) *Science* **244,** 1081–1085.
34. Kabat, E. A., Wu, T. T., Perry, H. M., Gottesmann, K. S. & Foeller, C. (1991) *Sequences of Proteins of Immunological Interest* (U.S. Department of Health, and Human Services, Bethesda, MD), 5th Ed.

THE JOURNAL OF BIOLOGICAL CHEMISTRY

Vol. 268, No. 4, Issue of February 5, pp. 2655-2661, 1993
Printed in U.S.A.

Role of Tyrosine Kinase Activity in Signal Transduction by the Insulin-like Growth Factor-I (IGF-I) Receptor

CHARACTERIZATION OF KINASE-DEFICIENT IGF-I RECEPTORS AND THE ACTION OF AN IGF-I-MIMETIC ANTIBODY (αIR-3)*

(Received for publication, July 23, 1992)

Hisanori Kato, Teresa N. Faria, Bethel Stannard, Charles T. Roberts, Jr., and Derek LeRoith‡

From the Diabetes Branch, National Institute of Diabetes and Digestive and Kidney Diseases, National Institutes of Health, Bethesda, Maryland 20892

The insulin-like growth factor-I (IGF-I) receptor is a member of a large family of transmembrane signal transducing molecules. The defining characteristic of this class of receptors is the intrinsic tyrosine kinase activity of the cytoplasmic domain. While it has been demonstrated that this tyrosine kinase activity is necessary for the action of a number of transmembrane tyrosine kinase receptors, no evidence of this type has been adduced to date with respect to the signaling requirement of the IGF-I receptor. We have now shown that stably transfected NIH-3T3 cell lines overexpressing human IGF-I receptors display increased responses to IGF-I and an IGF-I-mimetic antibody, αIR-3, in terms of short, intermediate, and long term actions initiated by activation of the IGF-I receptor. These include receptor autophosphorylation, activation of phosphatidylinositol-3-kinase and 2-deoxyglucose uptake, induction of ornithine decarboxylase gene expression, and stimulation of thymidine incorporation. In short term responses, the kinetics seen with αIR-3 were slower than those seen with IGF-I. These effects were severely decreased in clones expressing human IGF-I receptors in which the lysine residue in the ATP-binding site of the tyrosine kinase domain had been mutated to alanine or arginine. This was true for both IGF-I and αIR-3. These results indicate that, for all parameters tested, the tyrosine kinase activity of the IGF-I receptor is necessary for activation of the IGF-I-stimulated signal transduction cascade. Additionally, the effects of αIR-3 also require tyrosine kinase activity.

Insulin-like growth factor-I (IGF[1]-I) is a polypeptide hormone structurally homologous to insulin. IGF-I and insulin have a wide range of functions in common, including stimulation of cell growth and differentiation and the transport and metabolism of glucose (Adamo *et al.*, 1991). These effects are triggered by the binding of these ligands to their specific receptors, the IGF-I receptor and the insulin receptor. Both receptors are heterotetrameric glycoproteins consisting of two extracellular α-subunits and two membrane-spanning β-subunits (Ullrich *et al.*, 1985, 1986; Ebina *et al.*, 1985). As a result of the high degree of homology between the ligands on the one hand and their receptors on the other, IGF-I can also bind to the insulin receptor, albeit with relatively low affinity, and vice versa.

Recent studies have begun to elucidate the structure-function relationships in the insulin receptor. The IGF-I receptor, however, has been studied in less detail and has been discussed primarily by analogy with the insulin receptor. In the case of the insulin receptor, its intrinsic tyrosine kinase activity has been shown to be important in the mediation of many of the biological functions of insulin (Yarden and Ullrich, 1988). Several studies have shown that cells overexpressing insulin receptors mutated at the ATP-binding site in the tyrosine kinase domain (lysine 1018)[2] failed to mediate the action of insulin (Chou *et al.*, 1987; Ebina *et al.*, 1987; McClain *et al.*, 1987). In cells overexpressing insulin receptors that were mutated at one or more of the three major tyrosine phosphorylation sites (tyrosine residues 1146, 1150, and 1151), some of the effects of insulin were impaired (Ellis *et al.*, 1986; Wilden *et al.*, 1990; Murakami and Rosen, 1991). Another study has shown that antibodies directed against the cytoplasmic domain of the insulin receptor blunt the effect of insulin when they are injected into target cells (Morgan and Roth, 1987).

Several lines of evidence, however, have suggested that tyrosine phosphorylation of the insulin receptor may not be essential for all of its functions. First, in some studies, insulin receptors mutated at the cluster of key tyrosines mentioned above apparently function normally in terms of stimulation of DNA synthesis, glycogen synthesis, and amino acid transport (Debant *et al.*, 1988; Wilden *et al.*, 1990; Rafaeloff *et al.*, 1991). Second, Gottschalk (1991) has recently reported that kinase-deficient insulin receptors mediate the activation of pyruvate dehydrogenase by insulin. Other studies suggesting the presence of autophosphorylation-independent insulin receptor signaling pathway(s) have employed insulin-mimetic antibodies. Some antibodies directed against the α-subunit of the insulin receptor have been shown to stimulate a wide spectrum of cellular functions, including glucose and amino acid uptake, thymidine incorporation, and activation of ribosomal protein S6 kinase. While, in some cases, these antibod-

* This work was supported in part by grants from the Juvenile Diabetes Foundation International (to H. K.) and the American Diabetes Association (to C. T. R.). The costs of publication of this article were defrayed in part by the payment of page charges. This article must therefore be hereby marked "*advertisement*" in accordance with 18 U.S.C. Section 1734 solely to indicate this fact.

‡ To whom reprint requests should be addressed. Tel.: 301-496-8090; Fax: 301-480-4386.

[1] The abbreviations used are: IGF, insulin-like growth factor; DMEM, Dulbecco's modified Eagle's medium; BSA, bovine serum albumin; SF-DMEM, serum-free DMEM; Hepes, 4-(2-hydroxyethyl)-1-piperazineethanesulfonic acid; PBS, phosphate-buffered saline; PI3, phosphatidylinositol-3; CHO, chinese hamster ovary; WT, wild-type.

[2] The numbering systems used for the insulin and IGF-I receptors are those of Ullrich *et al.* (1985, 1986).

ies have been shown to stimulate these responses without apparently stimulating tyrosine phosphorylation of the insulin receptor (Zick *et al.*, 1984; Simpson and Hedo, 1984; Ponzio *et al.*, 1988; Hawley *et al.*, 1989; Sung *et al.*, 1989), others have suggested that these antibodies do, in fact, trigger a low level of autophosphorylation of the receptor that is sufficient to activate the post-receptor kinase cascade (Gherzi *et al.*, 1987; Brindle *et al.*, 1990; Steele-Perkins and Roth, 1990a).

In the case of the IGF-I receptor, a monoclonal antibody to the human receptor (αIR-3, Kull *et al.*, 1983) was shown to block the action of IGF-I in some cell lines (Duronio and Jacobs, 1988). However, Steele-Perkins *et al.* (1990a) have shown that this antibody behaves as a partial agonist in CHO cells overexpressing the human IGF-I receptor. Their results demonstrated that αIR-3 stimulated thymidine incorporation, but IGF-I receptor autophosphorylation was not detected *in vivo* (Steele-Perkins *et al.* 1988; Roth *et al.*, 1988), although a very slight increase in receptor phosphorylation was seen using an *in vitro* assay system (Steele-Perkins and Roth, 1990b).

Most cell lines have both IGF-I and insulin receptors. As mentioned above, these two ligands cross-react with each other's receptor. IGF-I-mimetic antibodies should be useful tools to demonstrate that a particular action of IGF-I is mediated via its own receptor, especially in studies in which mutated IGF-I receptors are introduced into cells that have endogenous receptors. In this study, we have assessed the requirement for an active tyrosine kinase domain in the IGF-I signal transduction by the IGF-I receptor and have investigated if the agonist action of αIR-3 requires receptor autophosphorylation, and, by inference, if there are indeed autophosphorylation-independent actions of the IGF-I receptor. To this end, we have established NIH-3T3 mouse fibroblast cell clones overexpressing normal or kinase-deficient human IGF-I receptors and have obtained evidence that receptor autophosphorylation is essential for the biological effects elicited by either IGF-I or αIR-3.

EXPERIMENTAL PROCEDURES

Materials—Recombinant human IGF-I, monoclonal anti-phosphotyrosine antibody, and fetal bovine serum were purchased from Upstate Biotechnology (Lake Placid, NY). Monoclonal anti-human IGF-I receptor antibody (αIR-3) was purchased from Oncogene Science (Manhasset, NY). A human IGF-I receptor cDNA and purified αIR-3 were generously provided by Dr. S. Jacobs (Raleigh, NC). A mouse ornithine decarboxylase cDNA was a gift from Dr. C. Kahana (Rehovot, Israel). Cell culture media and reagents were purchased from Biofluids Inc. (Rockville, MD) and Advanced Biotechnologies (Columbia, MD). Insulin-free bovine serum albumin (BSA, fraction V) was obtained from Armour (Kankakee, IL).

Construction of Expression Plasmids—An *Eco*RI-*Bam*HI fragment of the human IGF-I receptor cDNA containing a complete open reading frame was subcloned into pBluescript II (Stratagene, La Jolla, CA). In order to produce tyrosine kinase-deficient IGF-I receptors, the lysine 1003 residue at the ATP-binding site was substituted by alanine (KA mutant) or arginine (KR mutant). The mutagenized cDNAs were generated by the polymerase chain reaction using a 5′ primer containing a *Bcl*I site in the transmembrane region (5′-CTTCATCCATCTGATCATCGCTCTGCC-3′; the *Bcl*I site is underlined) and mutagenic 3′ primers encompassing both the lysine 1003 codon and an adjacent *Sph*I site. The sequences of the mutagenic primers were 5′-CTCACGCATGCTTGCGGCCTCGTTCACTGTTGCAATGGCCA-3′ for the KA mutant, and 5′-CTCACGCATGCTTGCGGCCTCGTTCACTGTTCTAATGGCCA-3′ for the KR mutant (the *Sph*I sites are underlined and the codons corresponding to amino acid position 1003 are shown in bold). The polymerase chain reaction products were cut with *Bcl*I and *Sph*I and were ligated into an IGF-I receptor cDNA construct partially digested with *Bcl*I and *Sph*I. The sequences of the mutants were confirmed by sequencing. Wild-type (WT) and KA and KR mutant cDNAs in pBluescript II were excised with *Sal*I and *Not*I and cloned into a bovine papilloma virus-derived mammalian expression vector, pBPV (Pharmacia LKB Biotechnology Inc.).

Cell Culture and Transfection—NIH-3T3 mouse fibroblasts were routinely cultured in Dulbecco's modified Eagle's medium (DMEM) supplemented with 10% fetal bovine serum, 100 units/ml penicillin, and 100 μg/ml streptomycin in a humidified atmosphere of 95% air and 5% CO_2 at 37 °C. Plasmid DNAs were prepared using Qiagen plasmid maxi kits (Qiagen, Chatsworth, CA) and each expression plasmid or pBPV without a cDNA insert (20 μg) and pMAMneo (1 μg, Clontech, Palo Alto, CA) were cotransfected by lipofectin using LIPOFECTIN reagent (Bethesda Research Laboratories). Each transfection was performed according to the manufacturer's protocol in 60-mm culture dishes for 24 h, and the cells were then split into 150-mm dishes. The next day, selection by 500 μg/ml G418 (Geneticin, GIBCO) was started. Following 2 weeks of G418 selection, independent colonies were picked using cloning cylinders (Specialty Media Inc., Lavallette, NJ). Clones overexpressing IGF-I receptors were selected by measuring the binding of ^{125}I-IGF-I as described below.

IGF-I Binding Assay—IGF-I binding to whole cells was quantitated using monoiodinated [^{125}I]IGF-I (Amersham Corp.). Confluent cells in 12-well culture plates were washed with 1 ml of binding buffer (100 mM Hepes, pH 7.9, 120 mM NaCl, 5 mM KCl, 1.2 mM $MgCl_2$, 1 mM EDTA, 15 mM sodium acetate, 5 mg/ml BSA) and incubated in 0.5 ml of binding buffer containing 25,000 cpm (approximately 20 pM) of [^{125}I]IGF-I and unlabeled competitor for 5 h at 4 °C. The cells were washed with cold PBS and solubilized in 0.2 N NaOH prior to counting for ^{125}I with a γ-counter (GammaTrac 1290, Tm Analytic, Brandon, FL).

Intact Cell Tyrosine Phosphorylation—Tyrosine phosphorylation of cellular proteins was analyzed by immunoblotting with an anti-phosphotyrosine antibody. Confluent cells in 60-mm dishes were washed twice with serum-free DMEM containing 1% BSA, antibiotics, and 20 mM Hepes, pH 7.5 (SF-DMEM), and incubated in SF-DMEM for 16 h. IGF-I or antibody in fresh medium was added and incubated for the indicated period at 37 °C. The cells were washed rapidly with cold PBS on ice and frozen on liquid N_2 and then thawed on ice. 0.5 ml of lysis buffer (1% Triton X-100, 100 mM NaCl, 50 mM Hepes, pH 7.6, 1 mg/ml bacitracin, 1 mM phenylmethylsulfonyl fluoride, 1 mM sodium orthovanadate, 10 mM NaF, and 10 mM EDTA) was added, and the lysate was cleared by centrifugation (11,000 × *g* for 3 min). The protein content of the lysate was determined by the method of Bradford using a protein assay kit (Bio-Rad), and equal amounts of protein (up to 20 μl of the lysates) were fractionated by SDS-polyacrylamide gel electrophoresis on 7.5% gels. Proteins were then electrophoretically transferred to a polyvinylidene difluoride membrane (Immobilon-P, Millipore Corp., Bedford, MA) with a Hoefer TE42 transfer unit (Hoefer, San Francisco, CA). Tyrosine-phosphorylated proteins were probed with a monoclonal anti-phosphotyrosine antibody and detected by alkaline phosphatase-conjugated anti-mouse immunoglobulin using a ProtoBlot System (Promega, Madison, WI). The dilutions of the first and second antibodies were 1:1000 and 1:7500, respectively.

Thymidine Incorporation—Confluent cells in 12-well plates were grown to quiescence in SF-DMEM for 24 h. IGF-I or αIR-3 in fresh SF-DMEM was added and the cells were incubated for an additional 16 h. One μCi/well of [*methyl*-^{3}H]thymidine (Amersham Corp.) was then added for 1 h. The cells were rinsed twice with ice-cold PBS, twice with ice-cold 5% trichloroacetic acid, and twice with ethanol. The cells were dissolved in 0.3 ml of 1 N NaOH, neutralized with 0.3 ml in HCl, and counted in a liquid scintillation counter.

2-Deoxyglucose Uptake—Confluent cells were washed twice with Krebs-Ringer phosphate buffer containing 1% BSA and 20 mM Hepes, pH 7.4 (DG buffer), and preincubated for 15 min. The cells were then incubated for the indicated period in DG buffer containing IGF-I or αIR-3. Deoxy-D-[1-^{14}C]glucose (0.5 μCi/well) (Amersham Corp.) and 2-deoxy-D-glucose (0.2 mM, final concentration) were added and incubation was continued for 10 min. The cells were washed three times with ice-cold DG buffer containing 0.2 mM phloretin, solubilized with 0.03% SDS, and counted for radioactivity.

Phosphatidylinositol-3-kinase Activity—Phosphorylation of phosphatidylinositol was measured as previously described (Backer *et al.*, 1992) with some modifications. Confluent cells grown in 100-mm dishes were washed twice in SF-DMEM and incubated in SF-DMEM. After 24 h, IGF-I (10 nM) or αIR-3 (50 nM) were added in fresh medium and incubated for the indicated periods at 37 °C. The cells were quickly washed once with ice-cold PBS and twice with wash buffer (20 mM Tris, pH 7.5, 137 mM NaCl, 1 mM $MgCl_2$, 1 mM $CaCl_2$, 100 μM Na_3VO_4). Cells were solubilized in 1 ml of wash buffer

containing 1% Nonidet P-40, 10% glycerol, and 0.35 mg/ml phenylmethylsulfonyl fluoride. The lysate was centrifuged at 12,000 × *g* for 5 min, and tyrosyl phosphoproteins in the supernatant were immunoprecipitated with a monoclonal anti-phosphotyrosine antibody and protein A-sepharose (Pharmacia). The immunoprecipitates were washed once with PBS containing 1% Nonidet P-40 and 100 μM Na_3VO_4, twice with 100 mM Tris, pH 7.5, containing 500 mM $LiCl_2$ and 100 μM Na_3VO_4, and once with 10 mM Tris, pH 7.5, containing 100 mM NaCl, 1 mM EDTA, and 100 μM Na_3VO_4. The pellets were resuspended in 40 μl of 10 mM Tris, pH 7.5, containing 100 mM NaCl and 1 mM EDTA. To each tube was added 10 μl of 100 mM $MnCl_2$ and 20 μg of phosphatidylinositol (Sigma). The phosphorylation reaction was started by the addition of 10 μl of 440 μM ATP containing 30 μCi of [^{32}P]ATP. After 10 min the reaction was stopped by the addition of 20 μl of 8 N HCl and 160 μl of $CHCl_3$/methanol (1:1). The organic phase was extracted and applied to a silica gel thin layer chromatography plate (Merck). Thin layer chromatography plates were developed in $CHCl_3/CH_3OH/H_2O/NH_4OH$ (60:47:11.3:2), dried, and visualized by autoradiography. The spots on the autoradiograph which comigrated with authentic phosphatidylinositol 4-phosphate (Sigma) were quantitated with a phosphorimager (Molecular Dynamics, Sunnyvale, CA).

Measurement of Ornithine Decarboxylase mRNA—A 436-base pair *Pst*I-*Hin*dIII fragment of a mouse ornithine decarboxylase cDNA (Kahana and Nathans, 1985) was cloned into pGEM4Z (Promega), and an antisense RNA probe was transcribed with T7 RNA polymerase. Confluent cells were made quiescent as described above and then cultured for 4 h in the presence or absence of IGF-I (10 nM) or αIR-3 (50 nM). Total RNA was prepared, and 10-μg aliquots were analyzed by a solution hybridization/RNase protection assay performed as previously described (Lowe *et al.*, 1987). Data were quantitated with a Hoefer scanning densitometer (GS-300).

RESULTS

Binding Studies—The number of IGF-I receptors in parental NIH-3T3 cells (3T3), cells cotranfected with the insertless pBPV vector and the neomycin resistance plasmid (Nneo), two clones expressing the wild-type human IGF-I receptor (NWT10, NWT14), and clones of cells expressing mutant IGF-I receptors in which the lysine at position 1003 was substituted by alanine (NKA) or arginine (NKR), were analyzed by Scatchard analyses (Table I). The receptor number in parental NIH-3T3 cells was in accordance with a previous report (Kaleko *et al.*, 1990). However, cells stably transfected with wild-type or mutated human IGF-I receptor cDNAs exhibited elevated numbers of IGF-I receptors. In order to confirm that both the wild-type and mutant IGF-I receptors bound both IGF-I and αIR-3, inhibition of the binding of [^{125}I]IGF-I by 10 nM IGF-I or 50 nM αIR-3 was determined. As αIR-3 does not bind to the mouse IGF-I receptor, no inhibition was observed in 3T3 and Nneo cells. In all cells expressing either wild-type or mutant human IGF-I receptors, αIR-3 inhibited the binding of IGF-I, but inhibition was less potent than the inhibition by IGF-I itself.

TABLE I

Number of IGF-I receptors and inhibition of binding of ^{125}I-IGF-I by 50 nM αIR-3 or 10 nM IGF-I

Equilibrium IGF-I binding assays were done as described under "Experimental Procedures." Approximate number of cell-surface IGF-I receptors/cell were calculated by Scatchard analyses. The dissociation constants (K_d) were 5–10 × 10^{-10} M. The binding of ^{125}I-IGF-I in the presence of 10 nM IGF-I or 50 nM αIR-3 were measured and expressed as the percentage of binding in the absence of competitors.

Cell line	Receptors/cell (×10^5)	Relative binding		
		No competitor	50 nM αIR-3	10 nM IGF-I
			%	
3T3	16	100	102	7
Nneo	9	100	102	10
NWT10	1723	100	74	49
NWT14	1093	100	82	49
NKA	322	100	40	13
NKR	733	100	66	36

Stimulation of Thymidine Incorporation by IGF-I—We next examined the effect of IGF-I on thymidine incorporation (Fig. 1). The cells overexpressing the IGF-I receptor had higher basal levels of incorporation, as discussed below. In both NWT10 and NWT14 cells, 10 nM IGF-I stimulated thymidine incorporation to the same extent as 10% fetal bovine serum. In 3T3, Nneo, NKA, and NKR cells, IGF-I also stimulated thymidine incorporation (3.6-, 3.6-, 1.6-, and 1.8-fold respectively, over the basal level), although this represented less than 10% of the stimulation observed with serum. The stimulation seen in these clones presumably represented activation of the endogenous mouse IGF-I receptor.

Stimulation of Thymidine Incorporation by αIR-3—In order to determine if αIR-3 had IGF-I mimetic effects in NIH-3T3 cells expressing human IGF-I receptors, quiescent cells were exposed to different concentrations of αIR-3, and the stimulation of thymidine incorporation was measured (Fig. 2). At the highest concentration tested (50 nM), high levels of stimulation (5-fold over the control) were observed in the clones expressing the wild-type human IGF-I receptor. In both parental NIH-3T3 and Nneo cells, αIR-3 had no effect, as was expected from the results shown in Table I. In both of the clones expressing kinase-deficient IGF-I receptors, however, αIR-3 failed to stimulate thymidine incorporation.

In Vivo Tyrosine Phosphorylation—Autophosphorylation of the IGF-I receptor and tyrosine phosphorylation of other substrates *in vivo* was examined by Western immunoblotting with an anti-phosphotyrosine antibody. Lysates of cells exposed to IGF-I or αIR-3 were directly applied to SDS-poly-

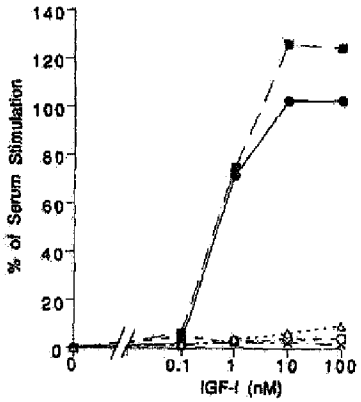

FIG. 1. **IGF-I stimulation of thymidine incorporation.** Confluent monolayers of cells were made quiescent in serum-free media for 24 h and then incubated with the indicated concentrations of IGF-I or 10% fetal bovine serum for 16 h. [^{3}H]Thymidine (1 μCi/ml) was added to for 1 h. Cells were washed and incorporated counts were measured as described under "Experimental Procedures." All assays were carried out in triplicate and the standard errors were within 5%. The data shown are representative of three independent experiments. Although basal and maximum responses tended to vary from experiment to experiment, the stimulation relative to serum stimulation was always consistent. For each cell line, relative stimulation as compared with serum stimulation (percent stimulation) was calculated as follows: percent stimulation = (incorporation in the presence of IGF-I − basal incorporation)/(incorporation in the presence of serum − basal incorporation) × 100. Values for basal incorporation and maximal incorporation induced by IGF-I (basal and maximal (cpm/well)) were, 3T3 (○, 3, 141 and 11,418); Nneo (□, 3,353 and 12,064); NWT10 (●, 43,657 and 470,246); NWT14 (■, 97,481 and 387,180); NKA (△, 10,765 and 17,416); NKR (×, 49,849 and 90,232).

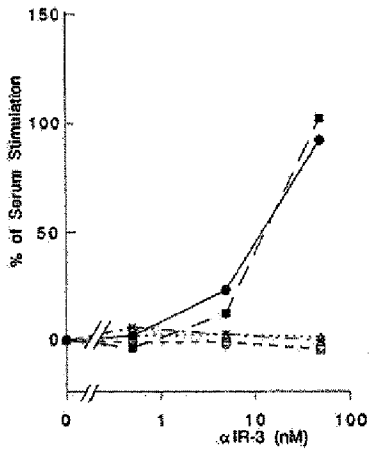

FIG. 2. **αIR-3 stimulation of thymidine incorporation.** Thymidine incorporation after treatment of cells with different concentrations of αIR-3 was measured. Assays were carried out in triplicate as described under Fig. 1. Standard errors were within 5%. The data are representative of two independent experiments. Basic levels of incorporation were basically identical to those shown in Fig. 1. Values represent the percentage of serum stimulation calculated as described under Fig. 1. ○, 3T3; □, Nneo; ●, NWT10; ■, NWT14; △, NKA; ×, NKR.

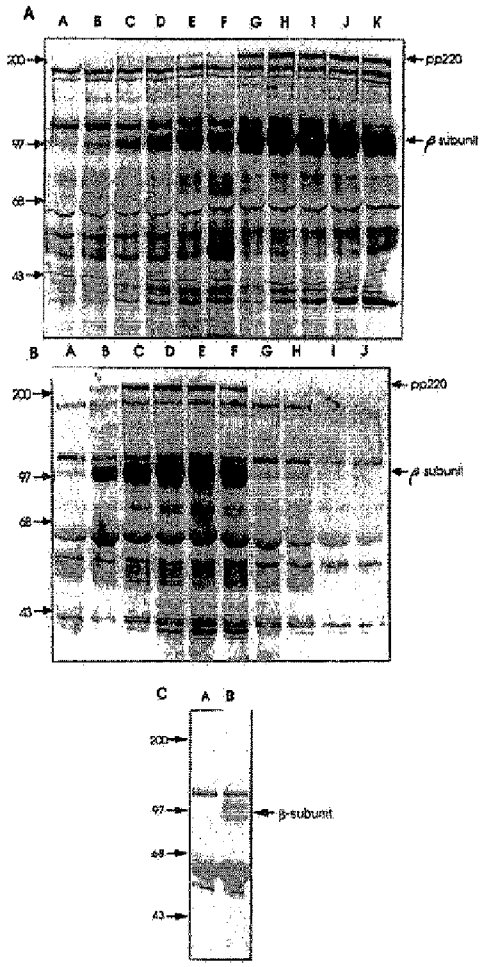

FIG. 3. **Stimulation of tyrosine phosphorylation in intact cells by αIR-3 or IGF-I.** Lysates of cells treated with αIR-3 or IGF-I were directly applied to SDS-polyacrylamide gels, and proteins containing phosphotyrosine were detected with Western immunoblotting as described under "Experimental Procedures." The data are representative of two independent assays. *A*, NWT10 cells were treated with 100 nM αIR-3 (*lanes A-F*) or 100 nM IGF-I (*lanes G-K*) for 0 (*A*), 1 (*B* and *G*), 5 (*C* and *H*), 15 (*D* and *I*) 60 (*E* and *J*) 240 (*F* and *K*) min. *B*, NWT10 cells were treated with 10 nM IGF-I for 0 (*A*), 1 (*B*), 5 (*C*), 15 (*D*), 60 (*E*), 240 (*F*) min or control IgG for 5 (*G*), 60 (*H*) min. NKR cells were treated with 10 nM IGF-I (*I*) or 100 nM αIR-3 (*J*) for 60 min. The result obtained with NKA cells were indistinguishable from those of NKR cells (data not shown). *C*, Nneo cells were treated without (*A*) or with (*B*) 10 nM IGF-I for 60 min. The positions of prestained molecular weight markers (kDa) are indicated.

acrylamide gels. Fig. 3*A* shows the time course of stimulation by the same concentrations (100 nM) of αIR-3 or IGF-I in NWT10 cells. As shown in *lanes G-K*, stimulation of the phosphorylation of the IGF-I receptor β-subunit reached a maximum within 1 min. αIR-3 did stimulate receptor autophosphorylation (*lanes A-F*), although the kinetics were different from IGF-I stimulation. Namely, the increase in the tyrosine phosphorylation of the IGF-I receptor by αIR-3 occurred much slower than that by IGF-I, reaching a maximum after 60 min. *Lanes A-F* of Fig. 3*B* show the stimulation of phosphorylation by 10 nM IGF-I. In this case, the phosphorylation occurred slower than stimulation by 100 nM IGF-I, suggesting that the stimulation by αIR-3 was similar to the stimulation seen with low concentrations of IGF-I. The delayed stimulation by low concentrations of IGF-I and the stable maintenance of a highly phosphorylated level of the receptor (Fig. 3*A*, *lanes G-K*; Fig. 3*B*, *lanes A-F*) are in contrast with our preliminary results in CHO cells overexpressing the IGF-I receptor in which, even at low concentrations of IGF-I (10 nM), receptor autophosphorylation reached a maximum within 1 min and declined rapidly thereafter.[3] Incubation of NWT10 cells with control IgG for 5 or 60 min (Fig. 3*B*, *lanes G* and *H*) did not stimulate autophosphorylation. In NKR cells, neither IGF-I nor αIR-3 caused autophosphorylation (Fig. 3*B*, *lanes I* and *J*). Fig. 3*C* shows the phosphorylation of Nneo cells by IGF-I. Low level of autophosphorylation of the receptor was seen as two separate bands and the molecular weight of the receptor was apparently different from human IGF-I receptor. These bands may correspond to the β-subunits of the IGF-I and insulin receptor or different subtypes of the IGF-I receptor. The latter is favored by the fact that this cell line has 7-fold less insulin receptors than IGF-I receptors (data not shown). In NKR cells (Fig. 3*B*), these bands were not visible. Tyrosine phosphorylation of a 220-kDa protein was markedly stimulated by IGF-I and only slightly by αIR-3.

2-Deoxyglucose Uptake—The effect of IGF-I (10 nM) and αIR-3 (50 nM) on 2-deoxyglucose uptake was examined (Fig. 4). Because αIR-3-induced autophosphorylation of the β-subunit of the IGF-I receptor was slower than that induced by IGF-I, we tested the effect of the length of exposure to ligand. After a short exposure (15 or 30 min) of the cells expressing wild-type human IGF-I receptors, the level of stimulation of 2-deoxyglucose uptake by αIR-3 was about 35% of the stimulation by IGF-I. After 60 min, the stimulation by αIR-3 was 65% of that by IGF-I. These results agree with the kinetics of tyrosine phosphorylation. In Nneo and NKR cells, IGF-I stimulated 2-deoxyglucose uptake less prominently than in NWT10 cells, and αIR-3 did not have any effect in these cells. Stimulation of 2-deoxyglucose uptake in NKR cells by IGF-I required a longer exposure.

[3] H. Kato, manuscript in preparation.

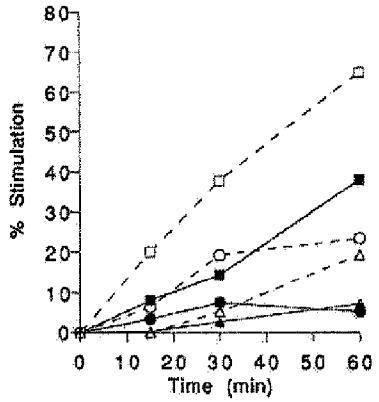

FIG. 4. **Stimulation of 2-deoxyglucose uptake by αIR-3 and IGF-I.** Cells were incubated for the indicated period in the presence of 50 nM αIR-3 or 10 nM IGF-I. Uptake of 2-deoxyglucose in 10 min was measured as described under "Experimental Procedures." The data shown are representative of two experiments. Data are expressed as percent of stimulation over the basal level. The differences in basal uptake/protein content in each cell clone was within 20% at all time points. Assays were done in triplicate and standard errors were within 5% except 15 and 60 min of NWT10 + IGF-I (6.2 and 8.2%) and 30 min of Nneo + αIR-3 (7.9%). ○, Nneo + IGF-I; ●, Nneo + αIR-3; □, NWT10 + IGF-I; ■, NWT10 + αIR-3; △, NKR + IGF-I; ▲, NKR + αIR-3.

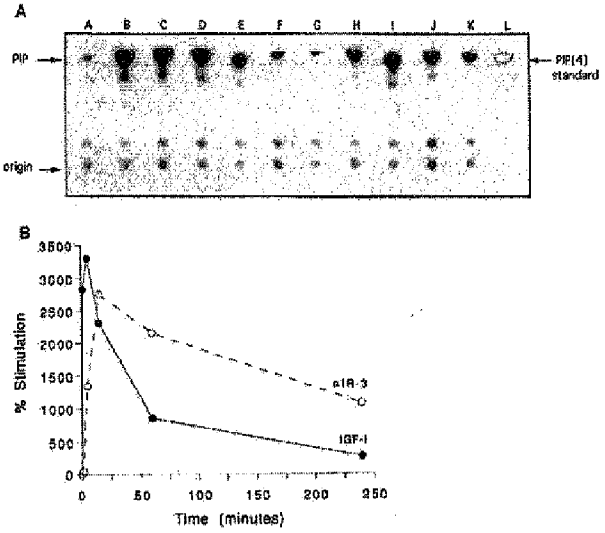

FIG. 5. **Time course of IGF-I and αIR-3 stimulation of PI3-kinase in cells overexpressing the IGF-I receptor.** *A*, PI3-kinase activity in anti-phosphotyrosine immunoprecipitates of NWT10 cells stimulated by 10 nM IGF-I (*lanes B-F*) or by 50 nM αIR-3 (*lanes G-M*). Cells were incubated for 0 (*A*), 1 (*B* and *G*), 5 (*C* and *H*), 15 (*D* and *I*), 60 (*E* and *J*), and 240 (*F* and *K*) min. Phosphatidylinositol 3-phosphate (*PIP*) comigrated with phosphatidylinositol 4-phosphate (*PIP(4)*) standard. *B*, quantitation of the data shown on *A*. Data are expressed as percent of stimulation over the basal level.

Activation of Phosphatidylinositol-3-kinase—The ability of IGF-I (10 nM) and of αIR-3 (50 nM) to stimulate phosphatidylinositol-3 kinase (PI3-kinase) was compared. Lysates of NWT10 cells exposed to IGF-I or αIR-3 were immunoprecipitated with an anti-phosphotyrosine antibody, and PI3-kinase activity in the immunoprecipitate was measured. Both IGF-I and αIR-3 were able to induce PI3-kinase. The time course of this stimulation is shown in Fig. 5. At 5 min (*lane C*), IGF-I induction was maximal and decayed rapidly after this time. The kinetics of stimulation of PI3-kinase by αIR-3 were slightly different: a longer time was necessary to obtain the greatest stimulation, since the maximal activity was observed at 15 min (*lane I*). The rate of decrease of αIR-3-induced PI3-kinase activity was also slower.

The induction of PI3-kinase activity in NWT10, NKR, and Nneo cells after stimulation with either IGF-I or αIR-3 is shown in Fig. 6. In NWT10 cells, PI3-kinase activity was markedly increased by IGF-I and by αIR-3 (11.1- and 8.3-fold, respectively). NKR cells exhibited elevated basal levels of PI3-kinase, and levels after stimulation by αIR-3 were indistinguishable from basal levels . IGF-I had a small effect in Nneo cells but not in NKR cells. These results show that overexpression of both wild-type and kinase-deficient IGF-I receptor caused a constitutive activation of PI3-kinase, although the mutant receptor was not responsive to IGF-I and αIR-3.

Induction of Ornithine Decarboxylase mRNA— Ornithine decarboxylase is a rate-limiting enzyme in the polyamine biosynthetic pathway. Ornithine decarboxylase mRNA levels have been shown to increase greatly after stimulation by various growth factors (Hovis *et al.*, 1986). Manzella *et al.* (1991) have shown that insulin stimulation of NIH-3T3 cells overexpressing insulin receptors increased in ornithine decarboxylase mRNA levels 3.5-fold. We examined the effect of IGF-I and αIR-3 on ornithine decarboxylase mRNA levels in NWT10 and NKR cells. As shown in Fig. 7, IGF-I and αIR-3 markedly increased ornithine decarboxylase mRNA levels in NWT10 cells (by 7.1- and 3.5-fold, respectively). In NKR cells, IGF-I caused a slight increase (1.5-fold). Basal levels were higher in NWT10 cells and NKR cells than in Nneo cells. Similar results were obtained with Northern blotting analyses (data not shown).

DISCUSSION

Overexpression of hormone and growth factor receptors in stably transfected cell lines has proved to be a useful approach

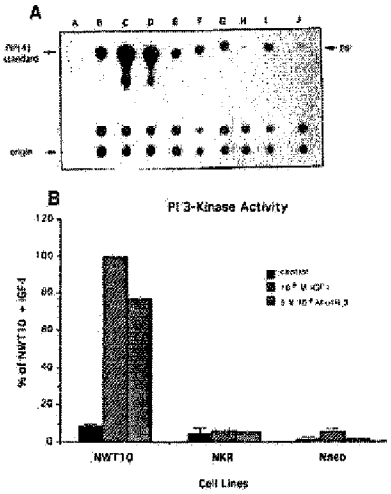

FIG. 6. **IGF-I and αIR-3 stimulation of PI3-kinase in NWT10, NKR, and Nneo cells.** *A*, PI3-kinase activity in anti-phosphotyrosine immunoprecipitates of NWT10 (*B–D*) NKR (*E–F*), and Nneo (*H–J*) cells stimulated by IGF-I (*C*, *F*, and *I*) for 10 min or by αIR-3 (*D*, *G*, and *J*) for 30 min. Control unstimulated cells are shown in *lanes B*, *E*, and *H*. Phosphatidylinositol 3-phosphate (*PIP*) comigrated with phosphatidylinositol 4-phosphate (*PIP(4)*) standard. *B*, quantitation of the data shown on *A*. Data are expressed as percent of NWT10 cells stimulated with IGF-I and represent the average of two separate experiments.

FIG. 7. **Effect of αIR-3 and IGF-I on ornithine decarboxylase mRNA levels.** A solution hybridization/RNase protection assay was performed using an ornithine decarboxylase (*ODC*) antisense RNA probe as described under "Experimental Procedures." Ten μg of total RNA from Nneo cells (*lanes D-F*), NWT10 cells (*lanes G-I*), and NKR cells (*lanes J-L*) incubated without (*lanes D, G,* and *J*) or with (*lanes E, H,* and *K*) 50 nM αIR-3 or with (*lanes F, I,* and *L*) 10 nM IGF-I for 4 h was used in the assay. *Lanes B* and *C* represent probe carried through the assay in the presence of 5 μg of yeast tRNA and subsequently incubated with or without RNase. The autoradiogram shown was exposed for 48 h at −70° C with two intensifying screens. The positions of ^{32}P-labeled pBR322-*Msp*I digest markers (*lane A*) are shown on the left. Relative intensities of the bands (mean of two independent experiments, control:αIR-3:IGF-I) were 1:1.14:3.56 in Nneo cells, 1:3.63:7.08 in NWT10 cells, and 1:0.91:1.42 in NKR cells.

to the investigation of the action of, and structure-function relationships in, their signaling molecules. Previous studies have demonstrated that cells expressing high numbers of IGF-I receptors exhibit elevated DNA synthesis, abrogation of the requirement for other growth factors, and IGF-I-dependent cell transformation (Lammers *et al.*, 1989; Steele-Perkins *et al.*, 1988; Kaleko *et al.*,1990; Chen *et al.*, 1991; McCubrey *et al.*, 1991; Pietrzkowski *et al.*, 1992). In the current study, we have established stably transfected NIH-3T3 cell clones expressing high numbers of human IGF-I receptors. In these clones (NWT10 and NWT14), IGF-I at physiological concentrations stimulated [^{3}H]thymidine incorporation to the same extent as 10% serum (Fig. 1). Additionally, the magnitude of acute responses such as 2-deoxyglucose uptake and PI3-kinase activation was also high in these cells (Figs. 4–6). This system has allowed us to analyze the role of the tyrosine kinase activity of the IGF-I receptor in mediation of IGF-I action and to determine the mechanism by which an IGF-I-mimetic antibody, αIR-3, elicits its biological activity.

Interestingly, in cells overexpressing either wild-type or mutant IGF-I receptors, basal levels of thymidine incorporation, PI3-kinase activity, and ornithine decarboxylase mRNA were higher than in control cells. One possible explanation for this is that overexpression of the IGF-I receptor itself may cause some receptor autophosphorylation-independent, constitutive change in the intracellular environment. This change could be related to the abrogation of requirement of other growth factors for growth stimulation seen in cells overexpressing wild-type receptors (Fig. 1), although more intensive studies are required to elucidate the mechanism and consequences of the elevation of basal levels of various parameters by IGF-I receptor overexpression.

Previous studies using kinase-deficient insulin receptors have demonstrated that most, if not all, of the actions of insulin require an active receptor tyrosine kinase domain (Chen *et al.*, 1987; Ebina *et al.*, 1987; McClain *et al.*, 1987). In intact cells, IGF-I induces autophosphorylation of the IGF-I receptor and the phosphorylation of endogenous substrates such as pp185 (IRS-1), mitogen-activated protein kinase (MAP kinase), and some nuclear proteins (Kadowaki *et al.*, 1987; Oemar *et al.*, 1991; Roth *et al.*, 1991). Consequently, tyrosine kinase activity has generally been considered a requisite for the mediation of IGF-I effects by the IGF-I receptor, although no direct link has been reported previously. Our current studies demonstrate that kinase-deficient IGF-I receptors, in fact, fail to mediate both metabolic and mitogenic actions of IGF-I. Stimulation of [^{3}H]thymidine incorporation, ornithine decarboxylase gene expression, 2-deoxyglucose uptake, and PI3-kinase activation by IGF-I are all decreased in cells expressing high numbers of human IGF-I receptors in which the lysine in the ATP-binding site was mutated to arginine (NKR) or alanine (NKA). This represents the first direct evidence of an absolute requirement for tyrosine kinase activity in the mediation of IGF-I effects by the IGF-I receptor. Rigorously speaking, the loss of receptor responsiveness may be due to lack of autophosphorylation, loss of kinase activity toward other substrates, absence of a conformational change induced by ATP binding, or a combination of these effects. It is therefore theoretically possible that receptor autophosphorylation *per se* is not necessary for receptor activity. However, our preliminary study of another IGF-I receptor mutant in which putative major target residues for tyrosine phosphorylation have been altered suggests that tyrosine phosphorylation of the receptor itself is important.[4]

It has been suggested previously that some actions of insulin which are mediated through the insulin receptor do not occur concomitantly with receptor autophosphorylation. The pertinent studies have generally investigated the effects of insulin-mimetic antibodies (Hawley *et al.*, 1989; Sung *et al.* 1989). We have employed clones overexpressing wild-type and mutant receptors to assess the action of the IGF-I-mimetic antibody αIR-3 and the involvement of tyrosine kinase activity. In cells overexpressing the wild-type human IGF-I receptor, αIR-3 stimulated thymidine incorporation, and the stimulation seen with 50 nM αIR-3 was at least as large as the maximal stimulation seen with IGF-I. In addition to stimulation of thymidine incorporation (a long term action), αIR-3 also increased deoxyglucose uptake and PI3-kinase uptake (short term actions), as well as the level of ornithine decarboxylase mRNA. In these studies we have also shown that αIR-3 induces significant autophosphorylation of the IGF-I receptor, although the kinetics of autophosphorylation are slower than those seen with IGF-I. The effects of αIR-3 on other parameters such as deoxyglucose uptake and PI3-kinase were also slower, consistent with the slower kinetics of autophosphorylation seen with αIR-3. The difference between the kinetics of autophosphorylation induced by IGF-I and by αIR-3 is similar to the phenomenon reported in the case of the insulin receptor (Brindle *et al.* 1990; Steele-Perkins *et al.*, 1990a). The affinity of αIR-3 for the IGF-I receptor has been shown to be lower than that of IGF-I (Steele-Perkins and Roth, 1990b), which may explain the difference in kinetics of activation. The difference in the mechanisms of activation of the receptor by IGF-I and αIR-3, which will be discussed below, could be another explanation for the difference of the kinetics. In intact CHO cells overexpressing human IGF-I receptors, Steele-Perkins *et al.* (1988) demonstrated stimulation of thymidine incorporation and PI3-kinase activation by αIR-3, but did not detect autophosphorylation of the IGF-I receptor. Subsequently, slight increases in IGF-I receptor autophosphorylation could be detected assaying receptors isolated from αIR-3-treated cells using an *in vitro* assay (Steele-Perkins and Roth, 1990b). The low level of αIR-3-induced autophosphorylation seen in this study could be a characteristic of transfected CHO cells as compared to NIH-3T3 cells. Xiong *et al.* (1992) recently demonstrated αIR-3 stimulation of autophosphorylation of the IGF-I receptor isolated from placenta. They, however, reported that αIR-3 itself inhibited thymidine incorporation in NIH-3T3 cells overexpressing human IGF-I receptors. In our hands, even purified αIR-3 from the same source (a gift from Dr. S. Jacobs) also stimu-

[4] H. Kato, T. N. Faria, B. Stannard, C. T. Roberts, Jr., and D. LeRoith, manuscript in preparation.

lated thymidine incorporation (data not shown). Possible explanations for these differences are differences in cell clones and assay conditions such as cell density (confluent *versus* subconfluent). However, the fact that we consistently observed IGF-I-mimetic activities of αIR-3 in all the assays employed demonstrates that αIR-3 does have intrinsic IGF-I-like effects.

The mechanism by which αIR-3 stimulates receptor autophosphorylation is unknown. As has been shown in the case of an insulin-mimetic antibody (Brindle *et al.*, 1990) and suggested in the case of αIR-3 (Xiong *et al.*, 1992), cross-linking of receptors by αIR-3 may induce a conformational change which leads to autophosphorylation. The similarities or differences in signaling pathways activated subsequent to autophosphorylation induced by IGF-I or αIR-3 has yet to be studied. It may be reasonable to assume, however, that they are very similar, as αIR-3 mimics IGF-I in a wide range of actions, both short term and long term. The various effects of αIR-3 were all absent in cells overexpressing lysine mutant receptors, suggesting that the effects of αIR-3, like those of IGF-I itself, require the tyrosine kinase activity of the IGF-I receptor.

In summary, we have shown that the ability of the IGF-I receptor to mediate a range of actions of the IGF-I receptor attributable to IGF-I requires the tyrosine kinase activity of the receptor. Additionally, we have demonstrated that the IGF-I-mimetic antibody αIR-3 stimulates receptor autophosphorylation and that tyrosine kinase activity is required for the various IGF-I-like effects elicited by αIR-3.

Acknowledgments—We thank Dr. S. Jacobs (Burroughs Wellcome Co., NC) for the human IGF-I cDNA and purified αIR-3 and Dr. C. Kahana (Rehovot, Israel) for the mouse ornithine decarboxylase cDNA. We also thank Drs. M. Adamo and D. Accili for critical review of the manuscript and V. Katz for expert secretarial assistance.

REFERENCES

Adamo, M., Roberts, C. T., Jr., and LeRoith, D. (1991) *BioFactors* **3**, 151–157
Backer, J. M., Schroeder, G. G., Kahn, C. R., Myers, M. G., Jr., Wilden, P. A., Cahill, D. A., and White, M. F. (1991) *J. Biol. Chem.* **267**, 1367–1374
Brindle, N. P. J., Tavare, J. M., Dickens, M., Whittaker, J., and Siddle, K. (1990) *Biochem. J.* **268**, 615–620
Chen, S.-C., Chou, C.-K., Wong, F.-H., Chang, C., and Hu, C.-P. (1991) *Cancer Res.* **51**, 1898–1903
Chou, C. K., Dull, T. J., Russell, D. S., Gherzi, R., Lebwohl, D., Ullrich, A., and Rosen, O. M. (1987) *J. Biol. Chem.* **262**, 1842–1847
Debant, A., Clauser, E., Ponzio, G., Filloux, C., Auzan, C., Contreres, J.-O., and Rossi, B. (1988) *Proc. Natl. Acad. Sci. U. S. A.* **85**, 8032–8036
Duronio, V., and Jacobs, S. (1988) *Recept. Biochem. Methodol.* **12B**, 3–18
Ebina, Y., Ellis, L., Jarnagin, K., Edery, M., Graf, L., Clauser, E., Ou, J.-H., Masiarz, F., Kan, Y. W., Goldfine, I. D., Roth, R. A., and Rutter, W. J. (1985) *Cell* **40**, 747–758
Ebina, Y., Araki, E., Taira, M., Shimada, F., Mori, M., Craik, C. S., Siddle, K., Pierce, S. B., Roth, R. A., and Rutter, W. J. (1987) *Proc. Natl. Acad. Sci. U. S. A.* **84**, 704–708
Ellis, L., Clauser, E., Morgan, D. O., Edery, M., Roth, R. A., and Rutter, W. J. (1986) *Cell* **45**, 721–732
Gherzi, R., Russel, D. S., Taylor, S. I., and Rosen, O. M. (1987) *J. Biol. Chem.* **262**, 16900–16905
Gottschalk, W. K. (1991) *J. Biol. Chem.* **266**, 8814–8819
Hari, J., and Roth, R. A. (1987) *J. Biol. Chem.* **262**, 15341–15344
Hawley, D. M., Maddux, B. A., Patel, R. G., Wong, K.-Y., Mamula, P. W., Firestone, G. L., Brunetti, A., Verspohl, E., and Goldfine, I. D. (1989) *J. Biol. Chem.* **264**, 2438–2444
Hovis, J. G., Stumpo, D. J., Halsey, D. L., and Blackshear, P. J. (1986) *J. Biol. Chem.* **261**, 10380–10386
Kadowaki, T., Koyasu, S., Nishida, E., Tobe, K., Izumi, T., Takaku, F., Sakai, H., Yahara, I., and Kasuga, M. (1987) *J. Biol. Chem.* **262**, 7342–7350
Kahana, C., and Nathans, D. (1985) *Proc. Natl. Acad. Sci. U. S. A.* **82**, 1673–1677
Kaleko, M., Rutter, W. J., and Miller, A. D. (1990) *Mol. Cell. Biol.* **10**, 464–473
Kull, F. C., Jr., Jacobs, S., Su, Y.-F., Svoboda, M. E., Van Wyk, J. J., and Cuatrecasas, P. (1983) *J. Biol. Chem.* **258**, 6561–6566
Lammers, R., Gray, A., Schlessinger, J., and Ullrich, A. (1989) *EMBO J.* **8**, 1369–1375
Lowe, W. L., Jr., Roberts, C. T., Jr., Lasky, S. R., and LeRoith, D. (1987) *Proc. Natl. Acad. Sci. U. S. A.* **84**, 8946–8950
Manzella, J. M., Rychlik, W., Rhoads, R. E., Hershey, J. W. B., and Blackshear, P. J. (1991) *J. Biol. Chem.* **266**, 2383–2389
McClain, D. A., Maegawa, H., Lee, J., Dull, T. J., Ullrich, A., and Olefsky, J. M. (1987) *J. Biol. Chem.* **262**, 14663–14671
McCubrey, J. A., Steelman, L. S., Mayo, M. W., Algate, P. A., Dellow, R. A., and Kaleko, M. (1991) *Blood* **78**, 921–929
Morgan, D. O., and Roth, R. A. (1987) *Proc. Natl. Acad. Sci. U. S. A.* **84**, 41–45
Murakami, M. S., and Rosen, O. M. (1991) *J. Biol. Chem.* **266**, 22653–22660
Oemar, B. S., Law, N. M., and Rosenzweig, S. A. (1991) *J. Biol. Chem.* **266**, 24241–24244
Pietrzkowski, Z., Lammers, R., Carpenter, G., Soderquist, A. M., Limardo, M., Phillips, P. D., Ullrich, A., and Baserga, R. (1992) *Cell Growth Differ.* **3**, 199–205
Ponzio, G., Contreres, J. O., Debant, A., Baron, V., Gautier, N., Dolais-Kitabgi, J., and Rossi, B. (1988) *EMBO J.* **7**, 4111–4117
Rafaeloff, R., Maddux, B. A., Brunetti, A., Sbraccia, P., Sung, C. K., Patel, R., Hawley, D. M., and Goldfine, I. D. (1991) *Biochem. Biophys. Res. Commun.* **179**, 912–918
Roth, R. A., Steele-Perkins, G., Hari, J., Stover, C., Pierce, S., Turner, J., Edman, J. C., and Rutter, R. J. (1988) *Cold Spring Harbor Symp. Quant. Biol.* **LIII**, 537–543
Roth, R. A., Yonezawa, K., Pierce, S. and Steele-Perkins, G. (1991) in *Modern Concepts of Insulin-like Growth Factors* (Spencer, E. M., ed) pp. 505–515, Elsevier, New York
Simpson, I. A., and Hedo, J. A. (1984) *Science* **223**, 1301–1304
Steele-Perkins, G., and Roth, R. A. (1990a) *J. Biol. Chem.* **265**, 9458–9463
Steele-Perkins, G., and Roth, R. A. (1990b) *Biochem. Biophys. Res. Commun.* **171**, 1244–1251
Steele-Perkins, G., Turner, J., Edman, J. C., Hari, J., Pierce, S. B., Stover, C., Rutter, W. J., and Roth, R. A. (1988) *J. Biol. Chem.* **263**, 11486–11492
Sung, C. K., Maddux, B. A., Hawley, D. M., and Goldfine, I. D. (1989) *J. Biol. Chem.* **264**, 18951–18959
Ullrich, A., Bell, J. R., Chen, E. Y., Herrera, R., Petruzzelli, L. M., Dull, T. J., Gray, A., Coussens, L., Liao, Y.-C., Tsubokawa, M., Mason, A., Seeburg, P. H., Grunfeld, C., Rosen, O. M., and Ramachandran, J. (1985) *Nature* **313**, 756–761
Ullrich, A., Gray, A., Tam, A. W., Yang-Feng, T., Tsubokawa, M., Collins, C., Henzel, W., Le Bon, T., Kathuria, S., Chen, E., Jacobs, S., Francke, U., Ramachandran, J., and Fujita-Yamaguchi, Y. (1986) *EMBO J.* **5**, 2503–2512
Wilden, P. A., Backer, J. M., Kahn, C. R., Cahill, D. A., Schroeder, G. J., and White, M. F. (1990) *Proc. Natl. Acad. Sci. U. S. A.* **87**, 3358–3362
Xiong, L., Kasuya, J., Li, S.-L., Kato, J., and Fujita-Yamaguchi, Y. (1992) *Proc. Natl. Acad. Sci. U. S. A.* **89**, 5356–5360
Yarden, Y., and Ullrich, A. (1988) *Annu. Rev. Biochem.* **57**, 443–478
Zick Y., Rees-Jones, R. W., Taylor, S. I., Gordon, P., and Roth, J. (1984) *J. Biol. Chem.* **259**, 4396–4400

THE JOURNAL OF BIOLOGICAL CHEMISTRY
© 1988 by The American Society for Biochemistry and Molecular Biology, Inc.

Vol. 263, No. 23, Issue of August 15, pp. 11486-11492, 1988
Printed in U.S.A.

Expression and Characterization of a Functional Human Insulin-like Growth Factor I Receptor*

(Received for publication, February 8, 1988)

George Steele-Perkins, Jennifer Turner‡, Jeffrey C. Edman‡, Joji Hari, Sarah B. Pierce, Cynthia Stover, William J. Rutter‡, and Richard A. Roth§

From the Department of Pharmacology, Stanford University School of Medicine, Stanford, California 94305-5332 and the ‡Hormone Research Laboratory, University of California, San Francisco, California 94143

Stable transfectants of Chinese hamster ovary (CHO) cells were developed that expressed the protein encoded by a human insulin-like growth factor I (IGF-I) receptor cDNA. The transfected cells expressed ~25,000 high affinity receptors for IGF-I (apparent K_d of 1.5×10^{-9} M), whereas the parental CHO cells expressed only 5,000 receptors per cell (apparent K_d of 1.3×10^{-8} M). A monoclonal antibody specific for the human IGF-I receptor inhibited IGF-I binding to the expressed receptor and immunoprecipitated polypeptides of apparent M_r values ~135,000 and 95,000 from metabolically labeled lysates of the transfected cells but not control cells. The expressed receptor was also capable of binding IGF-II with high affinity (K_d ~3 nM) and weakly recognized insulin (with about 1% the potency of IGF-I). The human IGF-I receptor expressed in these cells was capable of IGF-I-stimulated autophosphorylation and phosphorylation of endogenous substrates in the intact cell. This receptor also mediated IGF-I-stimulated glucose uptake, glycogen synthesis, and DNA synthesis. The extent of these responses was comparable to the stimulation by insulin of the same biological responses in CHO cells expressing the human insulin receptor. These results indicate that the isolated cDNA encodes a functional IGF-I receptor and that there are no inherent differences in the abilities of the insulin and IGF-I receptors to mediate rapid and long term biological responses when expressed in the same cell type. The high affinity of this receptor for IGF-II also suggests that it may be important in mediating biological responses to IGF-II as well as IGF-I.

Insulin-like growth factor(s) (IGF)[1] I and II are polypeptide hormones with ~50% amino acid sequence identity with proinsulin (1). Although the IGFs can bind to the insulin receptor, each has its own distinct receptor (2). The IGF-I receptor is structurally similar to the insulin receptor, whereas the IGF-II receptor is quite distinct (2, 3). Both the insulin and IGF-I receptors are synthesized as a single precursor polypeptide of M_r ~180,000 which is glycosylated and cleaved to yield two polypeptides of apparent M_r ~135,000 (the α chain) and 95,000 (the β chain) (4). The α chains of both receptors are predominantly extracellular and are labeled when the radioactive ligands are cross-linked to their respective receptors (5, 6). The β-subunits are transmembrane proteins, and their cytoplasmic domains are tyrosine-specific kinases (6). Although slight differences in the substrate specificities of the two receptor kinases have been described (7), the kinase portions of the two receptors appear to be closely related by various biochemical and immunological criteria (7–9).

The physiological roles for insulin and IGF-I are, however, quite different. Insulin primarily regulates rapid anabolic responses, including glucose uptake into muscle and fat cells, glycogen synthesis in liver and fat synthesis in adipocytes (6, 10). IGF-I, on the other hand, appears to be one of the primary regulators of the growth of organisms (11, 12). Thus, one might predict that the IGF-I receptor kinase might be more potent than the insulin receptor kinase at stimulating long term biological responses in cells, such as DNA synthesis. Conversely, the insulin receptor kinase might be thought of as being more potent at stimulating rapid effects in cells such as glucose uptake.

Recently, Ullrich *et al.* (13) have isolated from human placenta a cDNA clone which they proposed encoded for the IGF-I receptor. This clone was identified by hybridization to an oligonucleotide probe whose sequence was based upon the NH_2-terminal amino acid sequence of the α-subunit of the IGF-I receptor. As expected for the IGF-I receptor, the deduced amino acid sequence of this protein showed similarities in overall structure with the insulin receptor, including encoding for a single polypeptide precursor of M_r = 151,869 with a predicted cleavage site which would yield an α- and β-subunit (13). This predicted β-subunit sequence has a stretch of 24 hydrophobic amino acids which is presumably a transmembrane sequence, and the cytoplasmic domain has a sequence which is homologous to other tyrosine kinases. In agreement with the biochemical and immunochemical data on the IGF-I receptor (7–10), the deduced sequence of the kinase portion of this receptor exhibited the highest homology (84% sequence identity) with the insulin receptor (13). In addition the deduced amino acid sequence contained the sequences of five other peptides generated from the α-subunit of the IGF-I receptor. These results supported the hypothesis that the isolated cDNA encodes for the IGF-I receptor. However, the isolated cDNA was found to hybridize to a mRNA which decreased in abundance during the differentiation of 3T3-L1 preadipocytes to adipocytes (13). Since the levels of the IGF-I receptor protein have been reported to greatly increase during the differentiation of the same cells (14), these results raised the question of whether the isolated cDNA

* This work was supported by National Institutes of Health Grant DK34926 and Research Career Development Award DK01393 (to R. A. R.). The costs of publication of this article were defrayed in part by the payment of page charges. This article must therefore be hereby marked "*advertisement*" in accordance with 18 U.S.C. Section 1734 solely to indicate this fact.

§To whom correspondence should be addressed.

[1] The abbreviations used are: IGF, insulin-like growth factor; CHO, Chinese hamster ovary cells; Hepes, 4-(2-hydroxyethyl)-1-piperazineethanesulfonic acid; SDS, sodium dodecyl sulfate; SSC, saline sodium citrate; EGTA, [ethylenebis(oxyethylenenitrilo)]tetraacetic acid.

does in fact encode for the IGF-I receptor. In addition various forms of the IGF-I receptor have been described in the literature (15–21). These different species of IGF-I receptors vary in their relative affinities for IGF-I and II, the molecular weights of their β-subunits, and their interactions with antibodies.

To characterize further the IGF-I receptor, we have isolated an IGF-I receptor cDNA, transfected Chinese hamster ovary (CHO) cells with this cDNA and isolated cell lines which express the protein encoded by this cDNA. This protein was analyzed for its ability to bind IGF-I and II and insulin and to be recognized by a monoclonal antibody to the human IGF-I receptor. In addition the biological responses mediated by this receptor were compared with the responses stimulated through the human insulin receptor expressed in the same cell type.

EXPERIMENTAL PROCEDURES

Materials—Recombinant IGF-I (22) and IGF-II (23) were the generous gifts of Drs. J. Merryweather (Chiron Corporation) and M. Smith (Eli Lilly), respectively. Ascites and hybridoma supernatants of monoclonal antibody αIR-3 (16) were graciously provided by Dr. S. Jacobs (Wellcome Laboratories) and purified on protein A-Sepharose. Porcine insulin was purchased from Elanco, gel reagents were from Bio-Rad, affinity-purified rabbit anti-mouse IgG was from Pel-Freeze. Other reagents were obtained as previously described (24, 25) or as stated below.

Isolation and Expression of Human Placental IGF-I Receptor cDNA Clones—A full term human placental cDNA library was prepared in λgt10 by published techniques (3). In order to isolate a full length IGF-I receptor cDNA, an oligonucleotide representing bases 136–181 of the published sequence of the human IGF-I receptor cDNA (13) was synthesized. The oligonucleotide (labeled with [γ^{32}P]ATP and T4 polynucleotide kinase) was then used to screen 6×10^5 plaques of the library: hybridization was in 25% formamide, 6 × SSC, and 5 × Denhardt's at 42 °C; washing was with 2 × SSC at 50 °C. Seven clones that hybridized to this probe were plaque-purified. One of these clones had a 5.5-kilobase pair *Eco*RI insert sufficient to encode the entire IGF-I receptor. The restriction map of this insert agreed completely with the published sequence, except that this clone had a substantially longer 5′-untranslated region (600 base pairs in our clone *versus* 45 base pairs in the published sequence). Approximately 80% of our clone has been sequenced, and this sequence agrees entirely with that of the published sequence (13).

Expression constructs were prepared by ligating the 5.5-kilobase pair *Eco*RI insert into the mammalian expression vector, pECE (25). A plasmid with the insert in the proper orientation for SV40 early promoter-dependent transcription was identified by restriction mapping and designated by pE-IGFIR. DNA from pE-IGFIR and a plasmid conferring neomycin-resistance were then cotransfected into CHO cells by calcium phosphate precipitation (25). Twenty-four G418-resistant cell lines were isolated by limiting dilution. Cytoplasmic RNA was prepared from these lines and analyzed by dot-blot hybridization for the presence of human IGFIR transcripts. The line expressing the greatest amount of mRNA was designated CHO-IGFIR and used for the remainder of this study.

Binding Studies—Confluent 24-well culture plates of CHO-IGFIR or CHO cells were washed and incubated with the indicated labeled ligand (50–150 pM) and unlabeled competitor for 5 h at 4 °C in buffer B (100 mM Hepes, pH 7.8, 120 mM NaCl, 1.2 mM $MgSO_4$, 15 mM sodium acetate, 10 mM glucose, and 1% bovine serum albumin). Longer incubations at 4 °C (*i.e.* 8 or 16 h) resulted in less specific binding, in part because of the cells becoming detached from the wells. The cells were solubilized in 0.05% SDS and counted in a γ counter. Washings (2 times) were performed at 4 °C and completed within 3 min, a time such that less than 5% of the specifically bound ligand would dissociate. Labeled ligand was prepared by iodination of recombinant human IGF-I by the use of the Bolton-Hunter reagent (Du Pont-New England Nuclear) (105 Ci/g) or lactoperoxidase (300 Ci/g). Similar results were obtained with both labeled IGF-I preparations.

For measurement of the binding of ^{125}I-IGF-I to the isolated receptor, a plate binding assay was utilized (26). In brief, microtiter wells were sequentially coated with 50 μl of affinity-purified rabbit anti-mouse IgG (40 μg/ml) (Pel Freeze) and 10 nM monoclonal antibody 17A3 and then incubated with 25 μl of a 1:2 dilution of lysate of CHO-IGFIR cells (10^7 cells lysed with 0.5 ml of 2% Triton X-100 in 50 mM Hepes, pH 7.6, 5 mM EDTA, 5 mM EGTA, 150 mM NaCl, 1 mM phenylmethylsulfonyl fluoride, 1 mg/ml bacitracin). After 12 h at 4 °C, wells were washed 3 times, and 25 μl of the mix of labeled (600 pM) and unlabeled ligand were added. After 5 h at 4 °C, wells were washed 4 times and cut out and counted.

Metabolic Labeling—Confluent 100-mm plates of CHO-IGFIR or CHO cells were incubated in methionine- and cysteine-free Dulbecco's modified Eagle's medium containing 10% dialyzed fetal calf serum and 250 μCi of [^{35}S]methionine and cysteine (Tran ^{35}S-label, ICN). After 12 h at 37 °C, complete medium was added to the cells and the incubation continued for an additional 7 h. The cells were then lysed with 2 ml of 2% Triton X-100 in 50 mM Hepes, pH 7.6, 100 mM NaCl, 5 mM EDTA, 5 mM EGTA, 1 mM phenylmethylsulfonyl fluoride, and 1 mg/ml bacitracin. After 1 h at 0 °C, the lysates were centrifuged for 20 min at 3000 rpm and the supernatant immunoprecipitated with 20 μl of protein A-Sepharose (Pharmacia LKB Biotechnologies Inc.) coated with 50 μg of affinity-purified rabbit anti-mouse IgG and either 15 μg of monoclonal antibody or control mouse IgG. After 19 h at 4 °C, the protein A-Sepharose was washed 4 times, and the bound proteins released by heating for 2 min at 100 °C in 1% SDS and 4% β-mercaptoethanol. The released proteins were analyzed on 7.5% polyacrylamide SDS gels.

Biological Assays—For measurements of thymidine incorporation, monolayers of cells in 24-well plates were incubated for 36 h at 37 °C in serum-free Ham's F-12 medium containing 20 mM Hepes, pH 7.3, 100 units/ml of penicillin and 100 μg/ml of streptomycin. Hormones and fresh medium were added, and the cells incubated for an additional 8 h. Cells were then pulsed with 0.75 μCi of [*methyl*-^{3}H] thymidine (ICN) (20 Ci/mmol) for 45 min, washed 2 times, and lysed with 0.075% SDS. Trichloroacetic acid (final concentration, 10%) was added to the lysate, and the resulting precipitate was collected by filtration on Whatman glass fiber filters, washed with 5% trichloroacetic acid, and counted for radioactivity.

For measurements of ligand-stimulated glycogen synthesis, confluent monolayers of cells in 24-well plates were preincubated for 30 min at 37 °C in DB buffer (pH 7.4) containing 140 mM NaCl, 2.7 mM KCl, 1 mM $CaCl_2$, 1.5 mM KH_2PO_4, 8 mM Na_2HPO_4, 0.5 mM $MgCl_2$, and 1% bovine serum albumin. Hormone and 4 μCi of D[6-^{3}H]glucose (0.5 mM, final concentration) (ICN, 25 Ci/mmol) were added and the assay continued for 2 h at 37 °C. After washing the cells 2 times, the cells were lysed by the addition of 750 μl of 30% KOH containing 3 mg/ml carrier glycogen. The mixture was boiled for 30 min, and the glycogen was precipitated by the addition of ethanol (final concentration, 70%). After 16 h at 4 °C, the precipitate was pelleted, washed with 70% ethanol, dissolved in water, and counted for radioactivity.

For measurements of 2-deoxyglucose uptake, confluent monolayers of cells in 24-well plates were washed with DB buffer and then preincubated for 15 min. The assay was initiated by the addition of hormone and 30 min later, 0.25 μCi of deoxy-D-[I-^{14}C]glucose (Pathfinder) in 0.1 mM 2-deoxy-D-glucose. After 10 min at 37 °C, cells were washed with ice-cold buffer containing 200 μM phloretin, solubilized with 0.03% SDS, and the lysates were counted for radioactivity.

Phosphorylation Experiments—Confluent 100-mm plates of CHO-IGFIR cells were washed twice with phosphate-free Krebs-Ringer bicarbonate buffer containing 0.1% bovine serum albumin, 10 mM glucose, and 20 mM Hepes, pH 7.6, and then incubated in 4 ml of the same buffer containing 0.5 mCi carrier-free [^{32}P]orthophosphate (Amersham Corp.). After 2.5 h at 37 °C, the cells were treated with either IGF-I, αIR-3, or buffer. The reaction was stopped after 5 min by rapidly removing the media, washing the cells, and adding 1 ml of lysis buffer (1% Triton X-100, 100 mM NaCl, 50 mM Hepes, pH 7.6, 1 mg/ml bacitracin, 1 mM phenylmethylsulfonyl fluoride, 1 mM sodium vanadate, 10 mM NaF, and 10 mM EDTA). The lysate was cleared by centrifugation (11,000 × *g* for 10 min) and the IGF-I receptor was immunoprecipitated with αIR-3 bound to protein A-Sepharose (Pharmacia LKB Biotechnology Inc.) coated with rabbit anti-mouse IgG. For lysates of cells treated with αIR-3, additional rabbit anti-mouse IgG coated protein A-Sepharose was added to ensure the precipitation of IGF-I receptor complexed with αIR-3. The immunoprecipitates were analyzed by SDS gel electrophoresis and autoradiography. The β-subunit band of the IGF-I receptor was also excised from the dried gel by homogenization in 0.05 M $NaHCO_3$ containing 0.5% SDS and 5% β-mercaptoethanol. The extracted protein was precipitated with 20% trichloroacetic acid and hydrolyzed in 6 N HCl for 2 h at 100 °C. The samples were then lyophilized in a

Speed Vac and the phosphoamino acids were separated by high voltage electrophoresis on thin layer silica gels (0.2-mm thickness, E. Merck) (27).

In vivo tyrosine phosphorylation of the receptor and other proteins were assessed by immunoblotting with anti-phosphotyrosine antibodies. Confluent 100-mm plates of CHO-IGFIR cells were washed and treated with either 10 nM IGF-I or 10 nM αIR-3 in serum-free Ham's F-12 media for 5–15 min. For the experiments shown in this paper, cells were washed and lysed as described above in the phosphorylation studies. In other experiments (not shown), the cells were directly lysed with 2% SDS containing 5% β-mercaptoethanol and loaded onto the SDS-polyacrylamide gels. Lysates (the equivalent of 2×10^6 cells/lane) were electrophoresed on 10% polyacrylamide-SDS gels, transferred to nitrocellulose filters, and probed with antiphosphotyrosine antibodies (28). The bound rabbit immunoglobulin was detected by use of alkaline phosphatase-conjugated anti-rabbit immunoglobulin (Promega Biotech, as detailed in their handbook). In some experiments cells were treated with IGF-I and αIR-3 in the presence of the phosphatase inhibitor 0.5 mM vanadate or 35 μM phenylarsene oxide.

RESULTS

Binding Studies—Chinese hamster ovary cells (called CHO-IGFIR) stably expressing the presumptive IGF-I receptor cDNA (see "Experimental Procedures" for details on this cDNA) were found to specifically bind ~10 times more ^{125}I-IGF-I as the parental CHO cells (Table I). These transfected cells were found to specifically bind approximately the same amount of ^{125}I-IGF-II and ⅙ the amount of ^{125}I-insulin as ^{125}I-IGF-I (Table I). Scatchard analyses of the binding of ^{125}I-IGF-I to CHO-IGFIR indicated the presence of ~25,000 receptors/cell with an apparent K_d of 1.5×10^{-9} M for the hormone (Fig. 1*A*). In comparison the parental CHO cells were found to have ~5,000 IGF-I receptors/cell with an apparent K_d of 1.3×10^{-9} M (Fig. 1*A*).

To verify that the ^{125}I-IGF-I was binding to the human IGF-I receptor, various monoclonal antibodies were tested for their ability to inhibit the binding of ^{125}I-IGF-I to the CHO-IGFIR cells. One monoclonal antibody utilized, αIR-3, recognizes the human IGF-I receptor but does not recognize either the rodent IGF-I receptor or the human insulin and IGF-II receptors (16). At 10 nM this antibody was found to maximally inhibit 70% of the IGF-I binding to CHO-IGFIR cells (Fig. 1*B*). The remaining binding could be due to the endogenous hamster IGF-I receptor. In contrast two monoclonal antibodies to the human insulin receptor (5D9 and MC51) (19) and control IgG at the same concentrations had no effect on the binding of IGF-I to these cells (Fig. 1*B*).

To define further the specificity of the receptor expressed in CHO-IGFIR cells, ^{125}I-IGF-I was incubated with these cells in the presence of increasing concentrations of unlabeled IGF-I, IGF-II, and insulin (Fig. 1*C*). In agreement with the binding studies, IGF-II was found to be only 2–3 times less potent than IGF-I at inhibiting binding, whereas insulin was ~100 times less potent. These results could have been affected by the high levels of endogenous IGF-II receptors in CHO cells (Table I). The IGF-I receptors from the CHO-IGFIR cells were therefore isolated and tested for their relative affinities for IGF-I and II. As with the intact cells, IGF-II was found to be only slightly less potent (<2-fold) than IGF-I at inhibiting the binding of ^{125}I-IGF-I to the purified receptor, whereas insulin was 100 times less potent (Fig. 1*D*).

TABLE I

Binding of labeled insulin, IGF-I, and IGF-II to CHO-IGFIR and CHO cells

Confluent monolayers of cells were incubated for 5 h at 4 °C with 100 pM of labeled ligand in the presence or absence of the indicated competing unlabeled ligand. The cells were washed, lysed, and counted as described under "Experimental Procedures." The specific activities of the ligands were 105, 130, and 102 μCi/μg for IGF-I, -II, and insulin, respectively. Results shown are averages of duplicate wells and the duplicates differed from each other by less than 10%.

^{125}I-Ligand	Competitor	Total ^{125}I-ligand bound	
		CHO-IGFIR cells	CHO cells
		cpm	*cpm*
IGF-I	0	3421	547
IGF-I	100 nM IGF-I	231	216
IGF-II	0	3259	1656
IGF-II	100 nM IGF-II	440	467
Insulin	0	828	332
Insulin	10 μM insulin	247	236

These results indicate that the CHO-IGFIR cells express a receptor with almost equal affinity for IGF-I and II. Similar results were obtained with other preparations of IGF-I and II. For comparison we therefore examined the binding of IGF-I to its receptor in the rat hepatoma cells BRL-3A2 (7) and in fetal human brain. As with the expressed receptor, IGF-II was found to be only 2–3 times less potent than IGF-I at displacing ^{125}I-IGF-I from its receptor in these other tissues.

Metabolic Labeling Studies—To examine the structure of the expressed protein, lysates of metabolically labeled CHO-IGFIR and CHO cells were immunoprecipitated by either control IgG or monoclonal antibodies to the human insulin (19) or IGF-I receptor (16) (αIR-3). Polypeptides of M_r ~135,000 and 95,000 (corresponding to the α- and β-subunits, respectively) were immunoprecipitated from the CHO-IGFIR cells by the monoclonal antibody to the human IGF-I receptor but not by control IgG (Fig. 2). The expressed protein was also not precipitated by the monoclonal antibody to the insulin receptor, which was previously shown to be capable of precipitating the human insulin receptor expressed in CHO cells (29). The antibody to the human IGF-I receptor did not precipitate similar polypeptides from the parental CHO cells, even in greatly overexposed autoradiographs.

Biological Studies—To investigate whether the expressed receptor was functional, the CHO-IGFIR cells were compared to the parental CHO cells for their ability to respond to IGF-I. At 0.3 and 10 nM, IGF-I stimulated thymidine incorporation in the CHO-IGFIR cells ~2- and 4-fold, respectively (Fig. 3*A*). In contrast the parental CHO cells were stimulated 0.5- and 2.5-fold at these concentrations of IGF-I. The increased responsiveness of the transfected cells to IGF-I was consistent with the functioning of the expressed receptor. To further verify that the expressed human IGF-I receptor was mediating this response, we utilized monoclonal antibody αIR-3 which recognizes the human but not the hamster IGF-I receptor (Fig. 2). This antibody was found to stimulate thymidine incorporation in the CHO-IGFIR cells but not in the parental CHO cells (Fig. 3*A*). The maximal response to this antibody was approximately 2-fold and a response was observed at 100 pM. Similar results were obtained with preparations of the antibody isolated from mouse ascites and hybridoma supernatants.

IGF-I was also found to stimulate glycogen synthesis to a greater extent in the CHO-IGFIR cells than in the CHO cells, with responses of 800 and 50% of control at 10 nM IGF-I, respectively (Fig. 3*B*). In addition the monoclonal antibody to the human IGF-I receptor could stimulate this response in the transfected cells but not the parental CHO cells (Fig. 3*B*). As with thymidine incorporation, the maximal response elicited by the antibody was approximately ½ of the response observed with IGF-I. Finally, the two cell types were compared for the ability of IGF-I to stimulate glucose uptake (Fig. 3*C*). Again, IGF-I was more potent in the CHO-IGFIR cells than

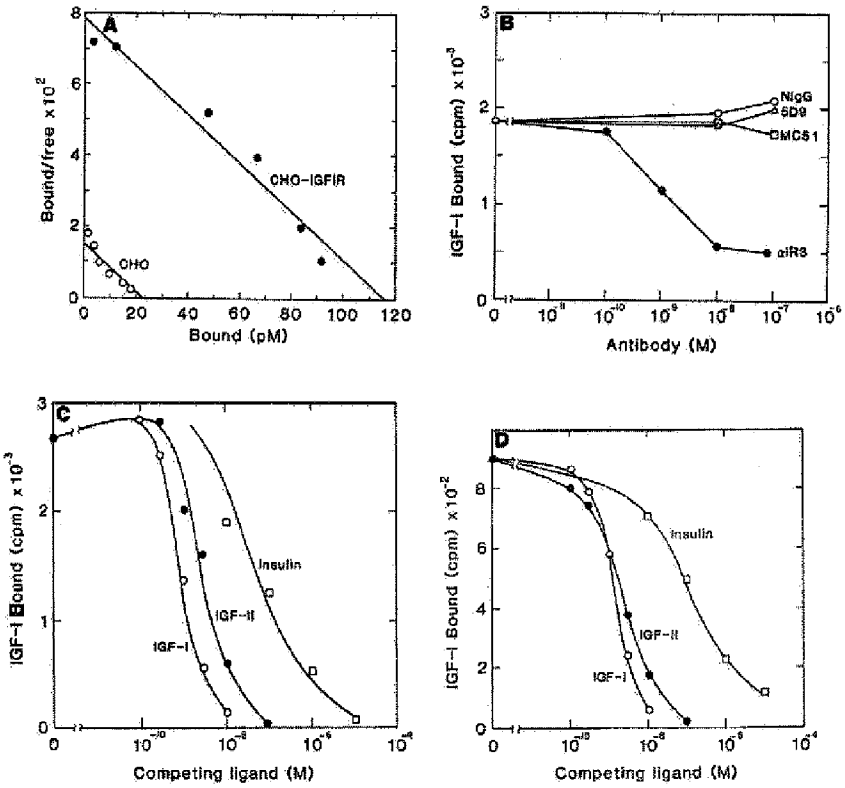

FIG. 1. **IGF-I binding to the expressed IGF-I receptor.** *A*, Scatchard plot of IGF-I binding to either CHO-IGFIR or CHO cells. Duplicate confluent wells of cells were incubated for 5 h at 4 °C with lactoperoxidase-labeled IGF-I, washed, lysed, and counted. Nonspecific binding was determined in the presence of 100 nM IGF-I and was subtracted from all the values. Least squares analysis was used to determine the slope and intercept of the Scatchard plot. *B*, inhibition of IGF-I binding to CHO-IGFIR cells by various monoclonal antibodies and normal IgG (*NIgG*). Binding was performed as in *A* except the ^{125}I-IGF-I was labeled with the Bolton-Hunter reagent. *C*, inhibition of IGF-I binding to CHO-IGFIR cells by insulin, IGF-I, and IGF-II. Binding was performed as in *A*. *D*, inhibition of IGF-I binding to the isolated IGF-I receptor by insulin, IGF-I, and IGF-II. Binding was performed on the IGF-I receptor expressed in CHO-IGFIR cells after adsorption of this receptor onto microtiter wells coated with a monoclonal antibody (17A3) which recognizes the β-subunit of the IGF-I receptor. This antibody does not bind to the IGF-II receptor (24). Comparable lysates of the parental CHO cells had less than 5% of the IGF-I binding of transfected cells.

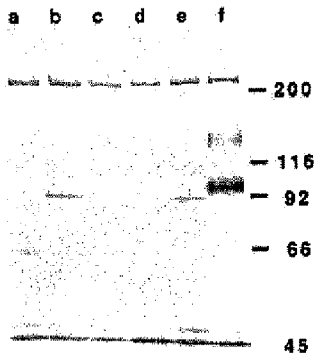

FIG. 2. **Identification of the polypeptide subunits of the expressed human IGF-I receptor.** Metabolically labeled lysates of either CHO (*a–c*) or CHO-IGFIR (*d–f*) cells were immunoprecipitated with either control IgG (*a–d*), monoclonal antibody to the human insulin receptor, MC51 (*b* and *e*) or a monoclonal antibody to the human IGF-I receptor, αIR-3 (*c* and *f*). The immunoprecipitates were analyzed on SDS-polyacrylamide gels and an autoradiograph of the gel is shown. The positions of molecular weight markers (in thousands) are indicated.

in the CHO cells and αIR-3 could only stimulate a response in the transfected cells.

To determine whether the IGF-I receptor had a different potency than the insulin receptor at stimulating responses, the same biological responses were studied in CHO cells expressing the human insulin receptor. These transfected cells have previously been described and shown to have ~15,000 human insulin receptors/cell (29, 30). Insulin maximally stimulates glucose uptake 60–110% over controls in these cells (29, 30), a value close to that found for IGF-I in CHO-IGFIR cells (average stimulation over control cells was 90% in three experiments). At 10 nM, insulin was found to stimulate thymidine incorporation and glycogen synthesis in the CHO-HIR cells 4.5- and 6.5-fold, respectively (Fig. 4), values that were not significantly different from that observed in CHO-IGFIR cells (4- and 8-fold, respectively).

Receptor Phosphorylation—To investigate *in vivo* receptor phosphorylation, CHO-IGFIR cells were labeled with [^{32}P] orthophosphate, treated with IGF-I or αIR-3, lysed, and the lysates were immunoprecipitated and analyzed. IGF-I and αIR-3 were both found to stimulate the *in vivo* phosphorylation of the IGF-I receptor in CHO-IGFIR cells (Fig. 5*A*). As in the biological responses, IGF-I was about twice as potent

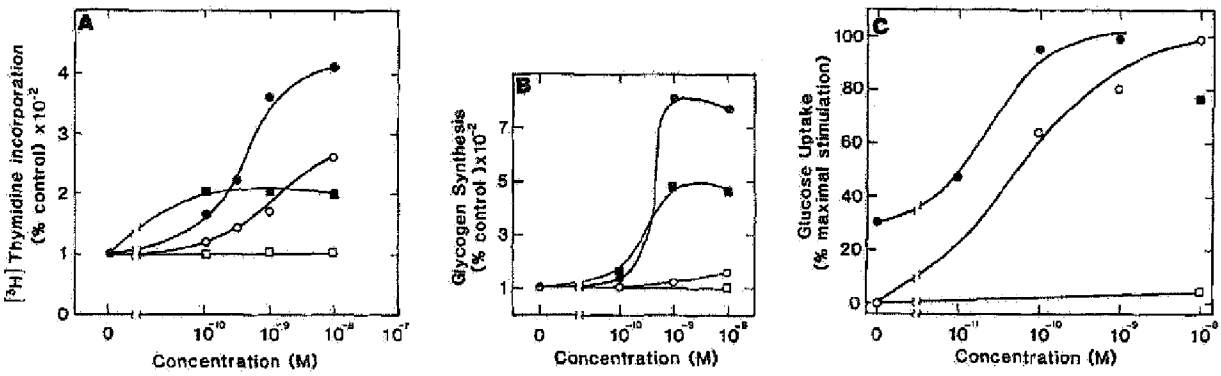

FIG. 3. **Stimulation of biological responses in CHO-IGFIR (*closed symbols*) and CHO (*open symbols*) cells by IGF-I (*circles*) and αIR-3 (*boxes*).** *A*, thymidine incorporation. Cells were incubated with the indicated concentrations of ligands and with [*methyl*-[^{3}H]thymidine as described under "Experimental Procedures." Results shown are averages of triplicate wells and are expressed as percent controls without hormone. The average basal thymidine incorporations in nine experiments were 102 and 60 fmol for the CHO and CHO-IGFIR cells, respectively. *B*, glycogen synthesis. Cells were incubated with the indicated concentrations of ligands and with D-[^{3}H]glucose as described under "Experimental Procedures." Results shown are averages of triplicate wells and are expressed as percent controls without hormone. The average basal incorporations for the CHO-IGFIR and CHO cells were 52 and 60 pmol, respectively, of glucose/4 × 10^5 cells in 2 h. *C*, glucose uptake. Cells were incubated with the indicated concentrations of ligands and with [^{14}C]2-deoxyglucose as described under "Experimental Procedures." Results shown are the averages of three independent experiments and are expressed as the percent maximal stimulation in each experiment. The average maximal stimulations for the three experiments were 92 and 96% for the CHO-IGFIR and CHO cells, respectively, and the average basal 2-deoxyglucose uptake for the two cell types was 1.4 and 1.1 nmol/4 × 10^5 cell in 10 min.

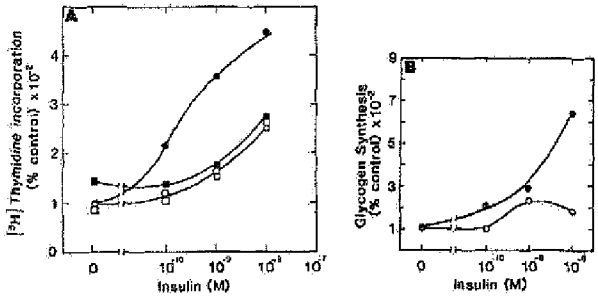

FIG. 4. **Insulin stimulation of biological responses in either CHO cells expressing the human insulin receptor (*closed symbols*) or the parental CHO cells (*open symbols*).** *A*, thymidine incorporation. Cells were incubated with either the indicated concentration of insulin (*circles*) or 30 nM monoclonal antibody to the insulin receptor (5D9) plus the indicated concentration of insulin (*boxes*). Results shown are averages of triplicate wells and are expressed as the percent controls without hormone. The average basal thymidine incorporations were 215 and 201 fmol for the CHO-HIR and CHO cells, respectively. *B*, glycogen synthesis. Cells were incubated with the indicated concentrations of insulin and assayed as described under "Experimental Procedures." Results shown are averages of triplicate wells and are expressed as percent controls without hormone. The average basal glucose incorporations for the CHO-HIR and CHO cells were 54 and 42 pmol, respectively, per 4 × 10^5 cells in 2 h.

as αIR-3. (In three experiments, αIR-3 stimulated ⅓ to ½ as much ^{32}P incorporation into the receptor as IGF-I). Phosphoamino acid analyses, however, indicated that αIR-3 stimulated the phosphorylation of the receptor only on serine residues, whereas IGF-I stimulated the phosphorylation of both tyrosine and serine residues (Fig. 5*B*).

To assess *in vivo* substrates of the IGF-I receptor and to verify the phosphoamino acid analyses, intact cells were treated with either IGF-I or αIR-3, lysed, and the lysates were examined by immunoblotting for the presence of phosphotyrosine-containing proteins. As in the *in vivo* phosphorylation studies, IGF-I but not αIR-3 stimulated the phosphorylation of the receptor on tyrosine residues (Fig. 6). In addition IGF-I but not αIR-3 stimulated the phosphorylation on tyrosine residues of several additional proteins, including proteins of apparent M_r of 150,000 and 40,000 (Fig. 6). As previously reported by Chou *et al.* (31), insulin stimulated the phosphorylation in the CHO-HIR cells of proteins with similar molecular weights (data not shown). The inability to detect proteins phosphorylated on tyrosine residues in CHO-IGFIR cells in response to αIR-3 could have been due to these proteins being insoluble in the Triton X-100 used to lyse the cells. However, the same results were obtained even when the treated cells were directly solubilized with 1% SDS (data not shown). Since a low stoichiometry of tyrosine phosphorylation could be missed in such an experiment, we also treated cells with 35 μM phenylarsine oxide which has been reported to potentiate the ability of insulin to stimulate the phosphorylation of proteins in the intact cell (32). Although IGF-I caused a marked increase in tyrosine phosphorylation of a number of proteins in these cells, we still could not detect any effect of αIR-3 on the tyrosine phosphorylation of any of these proteins (Fig. 6, *lanes d–f*). Similarly, vanadate treatment of the intact cells (33) potentiated the effect of IGF-I on the tyrosine phosphorylation of various endogenous proteins but again no effect of αIR-3 could be detected in these cells (data not shown).

DISCUSSION

The present studies demonstrate that CHO cells transfected with a presumptive IGF-I receptor cDNA with a sequence identical to that reported (13) express a protein which binds ^{125}I-IGF-I with a high affinity (apparent K_d = 1.5 nM) (Fig. 1). Moreover, the expressed protein was recognized by a monoclonal antibody which specifically binds the human IGF-I receptor (16) and has the appropriate structure (Figs. 1 and 2). These results further establish that this cDNA encodes for an IGF-I receptor. Surprisingly, this receptor also recognized IGF-II with high affinity (K_d ~3 nM) (Fig. 1). Although several reports have described IGF-I receptors with almost equal affinities for IGF-I and II (15, 17), most studies have found

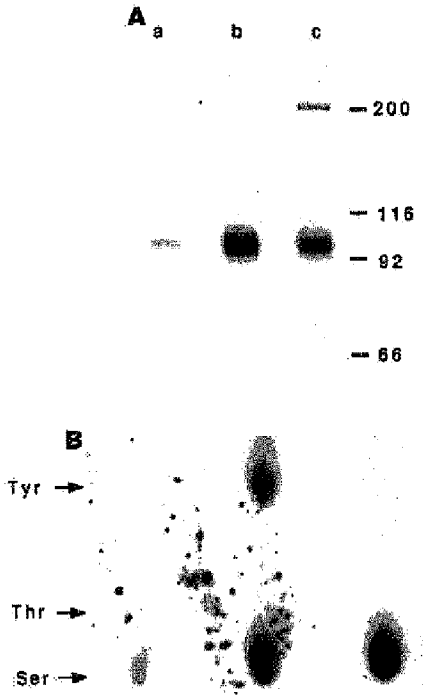

FIG. 5. ***In vivo* receptor phosphorylation.** *A*, stimulation of receptor phosphorylation. CHO-IGFIR cells were labeled with [^{32}P] orthophosphate, treated for 5 min at 37 °C with either buffer (*a*), 10 nM IGF-I (*b*) or 10 nM αIR-3 (*c*), lysed, and the lysates were immunoprecipitated with αIR-3. The immunoprecipitates were analyzed by SDS-polyacrylamide gel electrophoresis and autoradiography. The positions of molecular weight markers (in thousands) are indicated. The phosphorylated band at 200,000 was observed in a second experiment with both IGF-1 and αIR-3 but it was not present in a third experiment. *B*, phosphoamino acid determinations. The phosphorylated β-subunits from (*A*) were hydrolyzed and analyzed by high voltage electrophoresis on thin layer silica gels. The positions of standards (located by ninhydrin staining) are indicated.

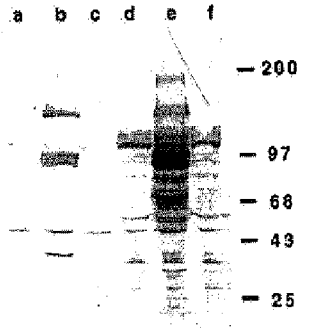

FIG. 6. **Effect of αIR-3 and IGF-I on the phosphorylation of endogenous substrates.** CHO-IGFIR cells were treated for 10 min at 37 °C with either buffer (*a*), 10 nM IGF-I (*b*), or 10 nM αIR-3 (*c*), lysed, and the lysates were analyzed by immunoblotting with anti-phosphotyrosine antibodies. To enhance the detection of endogenous substrates, CHO-IGFIR cells were also treated with 35 μM phenylarsine oxide (31) for 10 min at 37 °C, then either buffer (*d*), 10 nM IGF-I (*e*), or 10 nM αIR-3 (*f*) was added, and after an additional 10 min at 37 °C the cells were processed as above. The positions of prestained molecular weight markers (in thousands) are indicated.

that the IGF-I receptor binds IGF-I with 10–30 times higher affinity than IGF-II (15, 18, 20, 34–38). One explanation for these different results could be the use of partially impure preparations of IGF-II in these latter studies. The present work utilized highly purified recombinant IGF-II (23) which also was almost equipotent with IGF-I in displacing ^{125}I-IGF-I from its receptor in BRL rat hepatomas and in fetal human brain.

It is possible, however, that another IGF-I receptor exists which binds IGF-I more selectively. In several studies the IGF-I receptor β-subunit was found to give two species on SDS-gel electrophoresis (8, 16). In contrast the expressed receptor in CHO-IGFIR cells exhibited only a single β-subunit band on SDS-gel electrophoresis (Fig. 2). In addition a monoclonal antibody (5D9) which recognizes the IGF-I receptor in some tissues (19) did not bind to the expressed receptor (Fig. 1*B*). These results support the hypothesis that another IGF-I receptor type exists, and this species could bind IGF-I with higher selectivity. These two IGF-I receptors could arise from the same gene by differential processing of the mRNA or by a post-translational modification of the protein. The high affinity of the present IGF-I receptor for IGF-II could also be interpreted to mean that this receptor is responsible for mediating the biological responses of cells to IGF-II.

In the present studies the expressed IGF-I receptor was also found to be functionally active. It was capable of mediating long-term (DNA synthesis), intermediate (glycogen synthesis), and rapid effects (glucose uptake) of IGF-I. Evidence that the human receptor was mediating these responses was obtained by the finding that the CHO-IGFIR cells were more responsive to IGF-I than the CHO cells, and that a monoclonal antibody (αIR-3), which is specific for the human IGF-I receptor (16), could stimulate a response in the transfected cells but not the parental cells (Fig. 3). Also of interest was the finding that the IGF-I receptor had about the same potency at stimulating these three responses as the human insulin receptor expressed in the same parental CHO cells (Fig. 4 and Refs. 29–31). These results are consistent with the reports that the major endogenous substrates for the insulin receptor tyrosine kinase are the same as those for the IGF-I receptor (39–41). These results indicate that there are no inherent differences in the abilities of these two receptor kinases to mediate various responses and suggest that the different physiological roles of these two hormones (6, 10–12) are determined by the distribution of the two receptors on different cells and/or the pharmacodynamics of the two hormones.

Quite unexpected was the finding that the monoclonal antibody αIR-3 was capable of mimicking the ability of IGF-I to stimulate three different biological responses in the CHO-IGFIR cells. The antibody was approximately ½ as potent as IGF-I in the maximal responses it could stimulate. This antibody has previously been found to be an antagonist of IGF-I in other cell types (42–46). The mechanism whereby this antibody stimulates a response is unclear. Unlike IGF-I the antibody did not stimulate either the tyrosine phosphorylation of the IGF-I receptor or the tyrosine phosphorylation of the major *in vivo* substrates (Figs. 5 and 6). The antibody did, however, stimulate the serine phosphorylation of the receptor (Fig. 5). This is further evidence that the antibody is capable of stimulating the same responses as IGF-I. These data could be interpreted to mean that the antibody stimulates responses independently of the intrinsic tyrosine kinase activity of the receptor. However, this is unlikely since other antibodies (47, 48) which had been thought to act in this fashion were incapable of stimulating a response in cells

expressing mutated receptors lacking kinase activity (30, 49). Alternately, it is possible that this antibody, like other anti-receptor antibodies (50–53), can efficiently induce the clustering and internalization of the receptor without stimulating its intrinsic tyrosine kinase activity. If the internalized receptor is responsible for mediating the biological responses to hormone, this internalized basally active kinase may be sufficient to induce a partial response. It is also possible that the antibody stimulates a low stoichiometry of receptor tyrosine phosphorylation which is not detected in our assays. However, even when inhibitors of phosphatases or potentiators of phosphorylation were added, we could not detect antibody-stimulated tyrosine phosphorylation of the receptor or other proteins. Finally, it is possible that the antibody induces a conformational change in the receptor which mimics the effect of tyrosine autophosphorylation of the receptor. According to this hypothesis, the autophosphorylation of the β-subunit of the receptor induces a conformational change in the receptor which can activate associated proteins without their being phosphorylated on tyrosine residues. Additional studies on the mechanism whereby this antibody stimulates a response may aid in elucidating how tyrosine kinases transduce their signals.

Acknowledgments—We are grateful to Dr. James Merryweather (Chiron Corp.) for IGF-I, Dr. Michele Smith (Eli Lilly) for IGF-II, Dr. Jean Wang (University of California, San Diego) for the anti-phosphotyrosine antibodies, Dr. Steve Jacobs (Wellcome Labs) for αIR-3, Dr. Anita Payne for a critical reading of the manuscript, and Karen Bird for preparation of the manuscript.

REFERENCES

1. Froesch, E. R., Schmid, C., Schwander, J., and Zapf, J. (1985) *Annu. Rev. Physiol.* **47**, 443–467
2. Rechler, M. M., and Nissley, S. P. (1985) *Annu. Rev. Physiol.* **47**, 425–442
3. Morgan, D. O., Edman, J. C., Standring, D. N., Fried, V. A., Smith, M. C., Roth, R. A., and Rutter, W. J. (1987) *Nature* **329**, 301–307
4. Jacobs, S., Kull, F. C., Jr., and Cuatrecasas, P. (1983) *Proc. Natl. Acad. Sci. U. S. A.* **80**, 1228–1231
5. Czech, M. P. (1982) *Cell* **31**, 8–10
6. Rosen, O. M. (1987) *Science* **237**, 1452–1458
7. Sasaki, N., Rees-Jones, R. W., Zick, Y., Nissley, S. P., and Rechler, M. M. (1985) *J. Biol. Chem.* **260**, 9793–9804
8. Morgan, D. O., Jarnagin, K., and Roth, R. A. (1986) *Biochemistry* **25**, 5560–5564
9. Herrera, R., Petruzzelli, L. M., and Rosen, O. M. (1986) *J. Biol. Chem.* **261**, 2489–2491
10. Kahn, C. R. (1985) *Annu. Rev. Med.* **36**, 429–451
11. Merimee, T. J., Zapf, J., and Froesch, E. R. (1981) *N. Engl. J. Med.* **305**, 965–968
12. Rechler, M. M., Nissley, S. P., and Roth, J. (1987) *N. Engl. J. Med.* **316**, 941–942
13. Ullrich, A., Gray, A., Tam, A. W., Yang-Feng, T., Tsubokawa, M., Collins, C., Henzel, W., Le Bon, T., Kathuria, S., Chen, E., Jacobs, S., Francke, U., Ramachandran, J., and Fujita-Yamaguchi, Y. (1986) *EMBO J.* **5**, 2503–2512
14. Massagué, J., and Czech, M. P. (1982) *J. Biol. Chem.* **257**, 5038–5045
15. Rechler, M. M., Zapf, J., Nissley, S. P., Froesch, E. R., Moses, A. C., Podskalny, J. M., Schilling, E. E., and Humbel, R. E. (1980) *Endocrinology* **107**, 1451–1459
16. Kull, F. C., Jr., Jacobs, S., Su, Y.-F., Svoboda, M. E., Van Wyk, J. J., and Cuatrecasas, P. (1983) *J. Biol. Chem.* **258**, 6561–6566
17. Sara, V. R., Hall, K., Misaki, M., Fryklund, L., Christensen, N., and Wetterberg, L. (1983) *J. Clin. Invest.* **71**, 1084–1094
18. Jonas, H. A., and Harrison, L. C. (1985) *J. Biol. Chem.* **260**, 2288–2294
19. Morgan, D. O., and Roth, R. A. (1986) *Biochem. Biophys. Res. Commun.* **138**, 1341–1347
20. Burant, C. F., Treutelaar, M. K., Allen, K. D., Sens, D. A., and Buse, M. G. (1987) *Biochem. Biophys. Res. Commun.* **147**, 100–107
21. Tollefsen, S. E., Thompson, K., and Petersen, D. J. (1987) *J. Biol. Chem.* **262**, 16461–16469
22. Scheiwiller, E., Guler, H.-P., Merryweather, J., Scandella, C., Maerki, W., Zapf, J., and Froesch, E. R. (1986) *Nature* **323**, 169–171
23. Furman, T. C, Epp, J., Hsiung, H. M., Hoskins, J., Long, G. L., Mendelsohn, L. G., Schoner, B., Smith, D. P., and Smith, M. C. (1987) *Biotechnology* **5**, 1047–1051
24. Morgan, D. O., and Roth, R. A. (1986) *Biochemistry* **25**, 1364–1371
25. Ellis, L., Clauser, E., Morgan, D. O., Edery, M., Roth, R. A., and Rutter, W. J. (1986) *Cell* **45**, 721–732
26. Morgan, D. O., and Roth, R. A. (1985) *Endocrinology* **116**, 1224–1226
27. Hunter, T., and Sefton, B. M. (1980) *Proc. Natl. Acad. Sci. U. S. A.* **77**, 1311–1315
28. Wang, J. Y. J. (1985) *Mol. Cell. Biol.* **5**, 3640–3643
29. Ebina, Y., Edery, M., Ellis, L., Standring, D., Beaudoin, J., Roth, R. A., and Rutter, W. J. (1985) *Proc. Natl. Acad. Sci. U. S. A.* **82**, 8014–8018
30. Ebina, Y., Araki, E., Taira, M., Shimada, F., Mori, M., Craik, C. S., Siddle, K., Pierce, S. B., Roth, R. A., and Rutter, W. J. (1987) *Proc. Natl. Acad. Sci. U. S. A.* **84**, 704–708
31. Chou, C. K., Dull, T. J., Russell, D. S., Gherzi, R., Lebwohl, D., Ullrich, A., and Rosen, O. M. (1987) *J. Biol. Chem.* **262**, 1842–1847
32. Bernier, M., Laird, D. M., and Lane, M. D. (1987) *Proc. Natl. Acad. Sci. U. S. A.* **84**, 1844–1848
33. Tamura, S., Brown, T. A., Whipple, J. H., Fujita-Yamaguchi, Y., Dubler, R. E., Cheng, K., and Larner, J. (1984) *J. Biol. Chem.* **259**, 6650–6658
34. Heaton, J. H., Krett, N. L., Alvarez, J. M., Gelehrter, T. D., Romanus, J. A., and Rechler, M. M. (1984) *J. Biol. Chem.* **259**, 2396–2402
35. Beguinot, F., Kahn, C. R., Moses, A. C., and Smith, R. J. (1985) *J. Biol. Chem.* **260**, 15892–15898
36. Kiess, W., Haskell, J. F., Lee, L., Greenstein, L. A., Miller, B. E., Aarons, A. L., Rechler, M. M., and Nissley, S. P. (1987) *J. Biol. Chem.* **262**, 12745–12751
37. Ewton, D. Z., Falen, S. L., and Florini, J. R. (1987) *Endocrinology* **120**, 115–123
38. Kadowaki, T., Koyasu, S., Nishida, E., Sakai, H., Takaku, F., Yahara, I., and Kasuga, M. (1986) *J. Biol. Chem.* **261**, 16141–16147
39. White, M. F., Maron, R., and Kahn, C. R. (1985) *Nature* **318**, 183–186
40. Izumi, T., White, M. F., Kadowaki, T., Takaku, F., Akanuma, Y., and Kasuga, M. (1987) *J. Biol. Chem.* **262**, 1282–1287
41. Shemer, J., Adamo, M., Wilson, G. L., Heffez, D., Zick, Y., and LeRoith, D. (1987) *J. Biol. Chem.* **262**, 15476–15482
42. Van Wyk, J. J., Graves, D. C., Casella, S. J., and Jacobs, S. (1985) *J. Clin. Endocrin. Metab.* **61**, 639–643
43. Flier, J. S., Usher, P., Moses, A. C. (1986) *Proc. Natl. Acad. Sci. U. S. A.* **83**, 664–668
44. Conover, C. A., Misra, P., Hintz, R. L., and Rosenfeld, R. G. (1986) *Biochem. Biophys. Res. Commun.* **139**, 501–508
45. Rohlik, Q. T., Adams, D., Kull, F. C., Jr., Jacobs, St. (1987) *Biochem. Biophys. Res. Commun.* **149**, 276–281
46. Shimizu, M., Webster, C., Morgan, D. O., Blau, H. M., and Roth, R. A. (1986) *Am. J. Physiol.* **251**, E611–E615
47. Simpson, I. A., and Hedo, J. A. (1984) *Science* **223**, 1301–1303
48. Forsayeth, J. R., Caro, J. F., Sinha, M. K., Maddux, B. A., and Goldfine, I. D. (1987) *Proc. Natl. Acad. Sci. U. S. A.* **84**, 3448–3451
49. Gherzi, R., Russell, D. S., Taylor, S. I., and Rosen, O. M. (1987) *J. Biol. Chem.* **262**, 16900–16905
50. Roth, R. A., Maddux, B. A., Cassell, D. J., and Goldfine, I. D. (1983) *J. Biol. Chem.* 12094–12097
51. Morgan, D. O., Ellis, L., Rutter, W. J., and Roth, R. A. (1987) *Biochemistry* **26**, 2959–2963
52. Forsayeth, J. R., Montemurro, A., Maddux, B. A., DePirro, R., and Goldfine, I. D. (1987) *J. Biol. Chem.* **262**, 4134–4140
53. Russell, D. S., Gherzi, R., Johnson, E. L., Chou, C.-K., and Rosen, O. M. (1987) *J. Biol. Chem.* **262**, 11833–11840

doi:10.1016/j.jmb.2004.04.062 J. Mol. Biol. (2004) 340, 525–542

JMB

Available online at www.sciencedirect.com

SCIENCE DIRECT®

ELSEVIER

Camelized Rabbit-derived VH Single-domain Intrabodies Against Vif Strongly Neutralize HIV-1 Infectivity

Frederico Aires da Silva[1], Mariana Santa-Marta[1], Acilino Freitas-Vieira[1] Paulo Mascarenhas[2], Isabel Barahona[2], José Moniz-Pereira[1] Dana Gabuzda[3,4] and Joao Goncalves[1]*

[1]*URIA – Centro de Patogénese Molecular, Faculdade de Farmácia, Universidade de Lisboa, Lisboa 1649-019 Portugal*

[2]*Instituto Superior de Ciências da Saúde-Sul, Quinta da Granja, Monte da Caparica 2829-511 Caparica, Portugal*

[3]*Department of Cancer Immunology and AIDS, Dana Farber Cancer Institute, Boston MA 02115, USA*

[4]*Department of Neurology Harvard Medical School Boston, MA 02115, USA*

**Corresponding author*

We recently developed a specific single-chain antibody from immunized rabbits to HIV-1 Vif protein that was expressed intracellularly and inhibited reverse transcription and viral replication. The Vif of HIV-1 overcomes the innate antiviral activity of a cytidine deaminase Apobec3G (CEM15) that induces G to A hypermutation in the viral genome, resulting in enhancement of viral replication infectivity. Here, we have developed a minimal scaffold VH fragment with intrabody properties derived from anti-Vif single-chain antibody that was engineered to mimic camelid antibody domains. Non-specific binding of VH by its interface for the light chain variable domain (VL) was prevented through amino acid mutations in framework 2 and 4 (Val37F, G44E, L45R, W47G and W103R). Our results demonstrate that all constructed anti-Vif VH single-domains preserve the antigen-binding activity and specificity in the absence of the parent VL domain. However, only the most highly camelized domains had high levels of intracellular expression. The expression in eukaryotic cells showed that VH single-domains could correctly fold as soluble proteins in the reducing environment. The results demonstrated an excellent correlation between improvements in protein solubility with gradually increasing camelization. Camelized single-domains efficiently bound Vif protein and neutralized its infectivity enhancing function, by reducing late reverse transcripts and proviral integration. The activity of the anti-Vif single-domains was shown to be cell-specific, with inhibitory effects only in cells non-permissive that require Vif for HIV-1 replication. Moreover, cell specificity of anti-Vif intrabodies was correlated with an increase of Apobec3G, which potentiates viral inhibition. The present study strongly suggests that camelization of rabbit VH domains is a potentially useful approach for engineering intrabodies for gene therapy.

Keywords: intracellular antibodies; VH single-domains; camelization; Vif neutralization; HIV infectivity

Introduction

Recombinant antibodies have been usual for an increasing number of applications in the field of biotechnology and medical applications such as diagnosis or therapeutics.[1,2] Recently, recombinant

Abbreviations used: HIV-1, human immunodeficiency virus, type 1; Vif, viral infectivity factor; VL, light chain variable region; VH, heavy chain variable region; VHH, variable domain of heavy chain of heavy chain antibody; scFv, single-chain antibody fragment; ELISA, enzyme-linked immunosorbent assay; CDR, complementarity-determining regions; CAT, chloramphenicol acetyltransferase; IPTG, isopropyl-1-thio-β-D-galactoside; HA, hemagglutinin; CPRG, chlorophenolred-D-galactopyranoside; HRP, horseradish peroxidase.

E-mail address of the corresponding author: joao.goncalves@ff.ul.pt

DNA technology has allowed antibody genes to be manipulated and expressed intracellularly in eukaryotic cells.[3] Intracellularly expressed antibodies, termed intrabodies, consist of engineered single-chain antibodies (scFv) in which the variable domain of the heavy chain (VH) is connected to the light chain (VL) through a peptide linker, preserving the specificity and affinity of the parent antibody.[4,5] Intrabodies have particular promise in the area of functional genomics by directly blocking a protein function or by interfering with protein–protein interactions, thereby contributing to the understanding of a growing number of newly identified proteins.[6,7] In the long term, intrabodies may even find an enormous broad therapeutic application as in gene therapy setting. This new approach has been demonstrated for viral resistance in plants,[8] human immunodeficiency virus (HIV) viral proteins[9–16] and oncogene products.[17–19] Despite such successful results, the efficient cytoplasmic expression of single-chain antibody fragments (scFvs) is generally confronted with folding problems, low solubility, short protein half-life and high tendency for aggregation.[3,17] These problems are most likely caused by the reducing environment of the cell cytoplasm.[3]

The preserved intrachain disulfide bridges of heavy and light chains do not form in scFvs expressed in the cytoplasm, thus resulting in unstable intrabodies that are non-functional inside the cell.[6,7,20] Therefore, only intrinsically very soluble and stable scFv fragments will be able to fold correctly in sufficient amounts to be active as intrabodies.[21] At this time, no rules or consistent predictions can be established about intrabodies that will tolerate the reducing cellular environments.[15,17] Within this context, there is a strong interest in the ability to express functional antibodies in this environment and only recently several different approaches have started to emerge that meet such requirements.[22,23] These approaches include *in vivo* screening for intrabody–antigen interaction based on two hybrid screening[23–25] and construction of antibody libraries using randomized complementarity-determining regions (CDRs) on scFv frameworks that have been selected for high solubility and stability in an intracellular environment.[6,7,17,26]

A promising alternative to conventional intrabodies is the naturally heavy chain antibodies devoid of light chain that were discovered in *Camelidae* (camels, dromedaries and llamas).[27] These antibodies recognize the antigen by one very small single-domain (11–15 kDa), referred to as VHH. The hydrophobic amino acids normally involved in light and heavy chain interactions are replaced by hydrophilic amino acids.[28] Owing to these characteristics, VHH single-domains are easily produced as recombinant proteins in heterologous systems, appear to be more soluble and stable, and do not have a strong tendency to aggregate.[28–33]

The human immunodeficiency virus type-1 (HIV-1) vif gene encodes a 23 kDa protein that is essential for viral replication and spread in peripheral blood lymphocytes and primary macrophages, as well as in some established T-cell lines.[34–38] The action of Vif is essential for the completion of proviral DNA synthesis after virus entry, most likely as a result of its inhibitory effects on the cellular cytidine deaminase Apobec3G (CEM15), which induces G to A hypermutation in the viral genome and leads to activation of DNA repair mechanisms that induce premature degradation of newly synthesized viral DNA.[39,40] We recently demonstrated that anti-Vif intrabodies are an effective approach to inhibit this crucial step of the viral replication cycle. A specific anti-Vif scFv from immunized rabbits was shown to bind Vif intracellularly and inhibit reverse transcription and viral replication.[10]

Recent approaches have been employed to generate VH domains for therapeutic application, including their application as intrabodies.[41,42] Here, VH single-domain antibody fragments derived from rabbit anti-Vif scFv were engineered to obtain minimal scaffold size antigen-binding domains with intrabody properties directed against the HIV-1 Vif protein. To mimic the VHH of *Camelidae*[28–30,43,44] amino acid substitutions were introduced by protein engineering in the anti-Vif VH domain. Our results demonstrate that all anti-Vif VH domains constructed preserve the antigen-binding activity and specificity in the absence of the parent VL domain. However, only the most highly camelized domains are expressed at higher levels intracellularly. These camelized single-domains efficiently bind Vif protein and neutralize its infectivity-enhancing function, by an increase in Apobec3G expression and reduction in proviral integration. Therefore, the present study strongly suggests that camelization of a rabbit VH domain renders it more soluble and enables higher levels of intracellular expression, making these molecules potentially useful as intrabodies.

Results

Rabbit anti-Vif VH domain

We chose the rabbit anti-Vif VH antibody domain as a model system to evaluate single-domains as intrabodies and as a first step towards the design of a rabbit-derived minimal scaffold with intrabody properties. The anti-Vif VH was derived by polymerase chain reaction (PCR) from the anti-Vif scFv gene.[10] The anti-Vif scFv was recently selected from an immunized rabbit library and shown to inhibit HIV-1 reverse transcription and viral replication,[10] which makes this intrabody an excellent scaffold for testing new strategies to improve intrabody properties.

The anti-Vif VH domain was expressed in the periplasm of the non-suppressor *Escherichia coli*

strain TOP10F. After 18 hours of induction, cells were lyzed and the soluble fraction was subjected to immobilized metal affinity chromatography (IMAC). The yield of soluble protein after purification from one liter of bacterial culture was 0.6(±0.1) mg determined by measuring absorbance at $A_{280\ nm}$. The anti-Vif VH domain alone was expressed in the periplasmic space and was purified in soluble form. However, approximately 80% of the total amount of expressed anti-Vif VH domain was also found in an insoluble form as determined by Western blot analysis (Figure 1). This was not surprising, as most isolated VH domains have been found to be insoluble upon periplasmic expression, due to the large hydrophobic surface that is usually covered by the VL domain.[2]

Camelized rabbit anti-Vif VH domain

In order to improve the anti-Vif VH solubility required for making these molecules potential intrabodies, we mutated the exposed hydrophobic surface area contacting the VL domain. Mutations were chosen by comparative analysis with VHH domains of *Camelidae*.[28,30,44] The residues Val37, Gly44, Leu45, and Trp47 are all conserved in rabbit

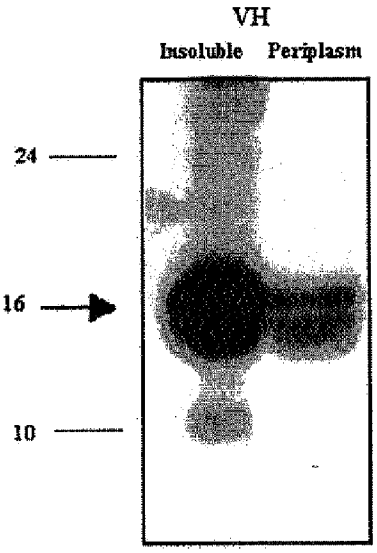

Figure 1. Western blot of soluble and insoluble fractions of anti-Vif VH single-domain fragments in *E. coli* TOP10F strain. *E. coli* TOP10F bacteria expressing anti-Vif VH single-domain after 18 hours by induction with 0.5 mM IPTG at 37 °C. Antibody fragments were extracted from periplasm as described in Materials and Methods. The pellets (insoluble fraction) and the periplasm (soluble fraction) were analyzed by an SDS-PAGE 15% gel, followed by Western blot using the HRP-conjugated anti-HA monoclonal antibody. As shown, more than 80% of VH protein is insoluble. Molecular mass is indicated in kDa.

VH framework 2 and may be involved in interdomain contacts. In original VHH domains of *Camelidae*, these amino acid residues are substituted by hydrophilic residues Phe37, Glu44, Arg45 and Gly47. Trp103 (framework 4) is another residue that is essential for interaction with the VL domain and is highly conserved in VHs. Trp103 is substituted by Arg in ~10% of the VHH domains.[30] The W103R substitution found in the cAB-CA05 VHH that binds specifically to bovine erythrocyte carbonic anhydrase renders the domain more hydrophilic.[30] Therefore, to mimic the VHH of *Camelidae*, single and multiple amino acid substitutions were introduced into the anti-Vif VH domain (Figure 2). The modifications were based on sequences published for single-domain antibody fragments with high conformational stability and solubility[44] and on the human antibody camelization studies done by Davies & Reichmann.[43] We constructed a set of three mutants with gradual increasing camelization. In mutant VH-W, the Trp103 residue in anti-Vif VH framework 4 was substituted by Arg (W103R). In mutant VH-CAM, Val37, Gly44, Leu45 and Trp47 in framework 2 were substituted by Phe37, Glu44, Arg45 and Gly47, respectively. In mutant VH-D, the five mutations described above (V37F, G44E, L45R, W47G and W103R) were all introduced into the anti-Vif VH domain (Figure 2). After introducing these alterations, all three mutants were expressed in the periplasm. Purification yields of soluble protein from one liter of bacterial culture normalized to an A_{550} of 10 were 0.9(±0.1) mg in the VH-W construct, 5(±0.1) mg in VH-CAM, and 8(±0.1) mg in VH-D. All modifications rendered the VH surface less hydrophobic, and aggregation was significantly reduced with gradually increasing camelization (W → CAM → D) (Figure 3A). The W103R mutation in framework 4 had a weaker effect on increasing VH solubility compared to the other mutations. The observed expression yield per liter of shake-flask culture without optimization was relatively high for the two most highly camelized domains. However, these yields were further increased by scaling-up into high-density fermentation conditions (data not shown).

Relative binding affinity of anti-Vif VH single-domain antibodies

To determine the *in vitro* relative affinity of the isolated VH domains for Vif protein, the amounts of anti-Vif VH, VH-W, VH-CAM and VH-D domains were normalized and analyzed by ELISA. As shown in Figure 3B, all of the single-domains had similar binding patterns. Wild-type and single-domain mutants displayed a ~50-fold lower relative affinity for Vif as compared to the parental anti-Vif scFv 4BL. A similar decrease in the relative antigen-binding affinity was demonstrated in previous studies when isolated VH antibody fragments were compared with their parent antibodies.[45,46] In contrast, control experiments

A

	< ------- FRAMEWORK 1 ------>	<--- H1/ CDR1--- >	< - FRAMEWORK 2 >	< ---- H2/ CDR2----->	< ---------- FRAMEWORK 3 - ---------->	<----------H3/ CDR3 ---------->	< FRAMEWORK 4 >
VH anti-Vif	SQSVEESGGRLVTPGTPLTLTCTVS	GFSLYN----YAMS	WVRQAPGKGLEWIG	IISYSG----------NTY	YASWAKGRFTISRTSSTTVDLRITSPTTEDTATYFCAG	AGRDFYTD----------INLWGPGTLVTVSS	
CAb-CA05	QVQLVESGGGSVQAGGSLRISCAAS	GYT---VSTYCMG	WFRQAPGKEREGVA	TIL--GGSTYYGDSVKG	RFTISQDNAKNTVYLQMNSLKP-------EDTAIYYCAG	STVASTGWCSRLRPYD----------EY	RGQGTQVTVSS
Cab-Lys3	DVQLQASGGGSVQAGGSLRISCAAS	GYT---IGPYCMG	WFRQAPGKEREGVA	AINMGGGITYYADSVKG	RFTISQDNAKNTVYLQMNSLEP-------EDTAIYYCAA	DSTIYASYYECGHGLSTGGYGYDS	WGQGTQVTVSS

B

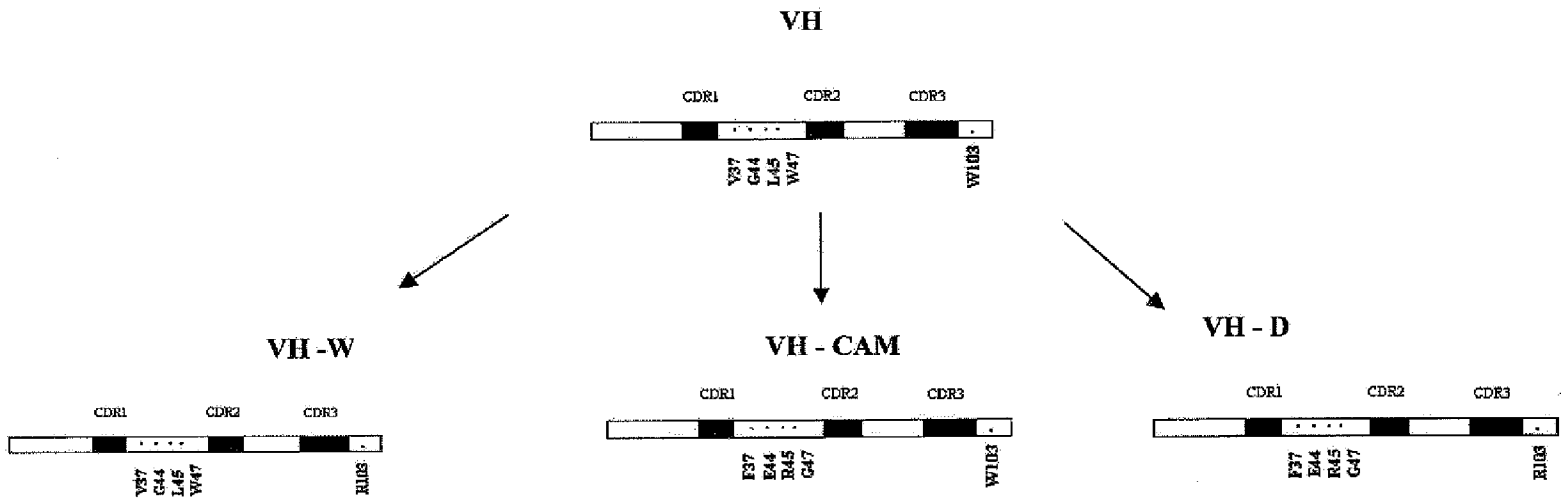

Figure 2A and B (*legend opposite*)

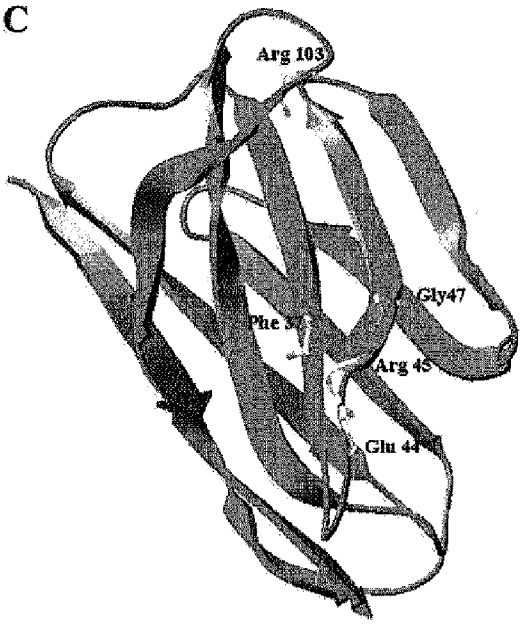

Figure 2. A, Amino acid sequence alignment of the rabbit anti-Vif VH domain, the camel Cab-Lys3 domain and the cAb-CA05 domain. The frameworks, CDRs and the amino acid numbering are as defined by Kabat *et al.*[58] The camel-specific antibody amino acids of framework 2 and 4 are in bold. The amino acids altered to camelize the rabbit VH anti-Vif domain are in bold and underlined. B, Schematic representation of the different anti-Vif VH constructs under investigation in this study. Single and multiple mutations were introduced into anti-Vif VH domain by protein engineering based on alignment with the camel Cab-Lys3 and the cAb-CA05 domains. In mutant VH-W, the highly conserved amino acid Trp in anti-Vif VH at position 103 was substituted by Arg. In mutant VH-CAM, Val37, Gly44, Leu45 and Trp47 (framework 2) were mutated to Phe37, Glu44, Arg45 and Gly47, respectively. In mutant VH-D, the five mutations described above (Val37F, G44E, L45R, W47G and W103R) were all introduced into the anti-Vif VH domain. C, Three-dimensional structure prediction of the camelized anti-Vif VH-D domain. The three-dimensional structure prediction of the VH domain from scFv 4BL was obtained by comparative protein modeling with SWISS-MODEL.[54–56] After introducing the mutated amino acids the refinement of overall protein structures was performed to achieve the model with lowest energy.[54] The amino acid mutations introduced into anti-Vif VH domain (Val37F, G44E, L45R, W47G and W103R) to mimic the VHH of *Camelidae* are shown on the exposed region contacting with putative VL domain.

showed near-background signals and lower non-specific binding of all single-domains to bovine serum albumin (BSA) and thyroglobulin, similar to that of anti-Vif scFv. Therefore, the decrease in the relative binding affinity of VH single-domains is not dramatic and still allows constant specific binding to HIV-1 Vif protein.

Expression of anti-Vif VH single-domains in mammalian cells

To determine the expression levels of single-domains in the reducing environment of the cytoplasm in mammalian cells, VH, VH-W, VH-CAM and VH-D were expressed in 293T cells and cell lyzates were prepared, centrifuged and the supernatant immunoprecipitated with the anti-HA monoclonal antibody matrix. Precipitated proteins were separated by SDS-PAGE, transferred to nitrocellulose membrane and analyzed by Western blot with HRP-conjugated anti-HA monoclonal antibody. As a negative control, lyzates of 293T cells not expressing antibody fragments were used in Western blot analysis and the total amount of single-domain proteins was assayed by comparison with cellular actin. The data in Figure 4 demonstrate that anti-Vif VH-CAM and VH-D antibody fragments were the most abundant intracellularly among the four single-domains. In mammalian cells, there was also a strong correlation between the improvement in protein solubility and the gradual increasing camelization (W → CAM → D). To further evaluate the expression level in the reducing environment of mammalian cells, turnover rates of intracellular single-domains were measured by pulse-chase analysis. After 36 hours post-transfection, cells were incubated with methionine/cysteine-free medium for two hours and then pulse-labeled with [^{35}S]methionine/cysteine for two hours. After labeling, medium was chased with excess amounts of methionine/cysteine and then harvested at several time-points. Labeled lyzates were immunoprecipitated with anti-HA affinity matrix, separated by SDS-PAGE and visualized by autoradiography. Figure 5 shows that anti-Vif VH-CAM and anti-Vif VH-D were the most stable, showing the higher steady-state accumulation and increased half-life, compared to VH and VH-W. Moreover, it should be noted that by overall comparison anti-Vif VH-D revealed a relatively higher steady-state accumulation at eight hours. In contrast, the overall steady-state levels of anti-Vif VH and VH-W were much less than VH-CAM and VH-D domains with a relatively short protein half-life of about two hours. These results were consistent with our observations using immunofluorescence microscopy where VH and VH-W consistently exhibited weaker fluorescence intensity than VH-CAM and VH-D, suggesting a lower concentration of those intrabodies within cells (data not shown). Therefore, protein accumulation at steady-state correlates significantly with differences in intracellular protein stability of VH-CAM and VH-D.

Camelized VH single-domains inhibit Vif function in a *trans*-complementation assay

To provide a qualitative and quantitative measure of the biological activity of the isolated

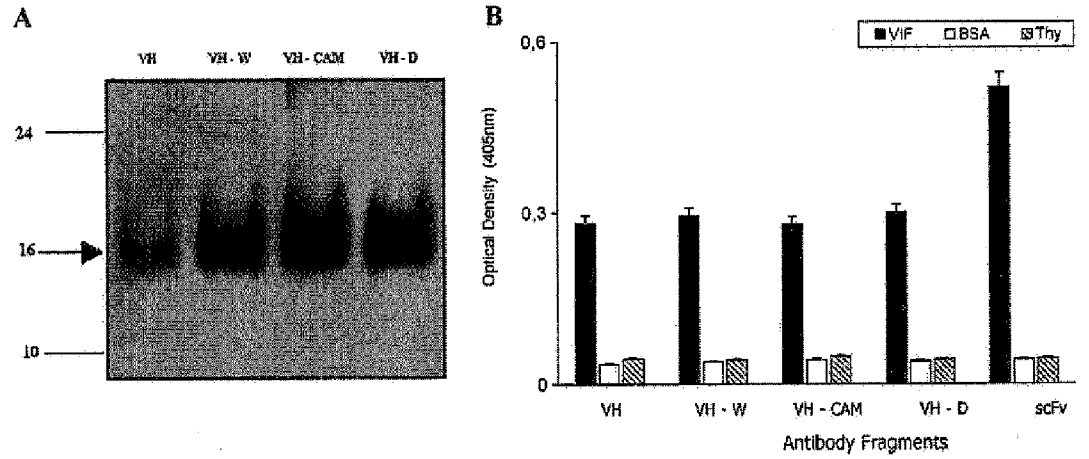

Figure 3. Expression and relative binding affinities of anti-Vif VH, VH-W, VH-CAM and VH-D domains. A, *E. coli* TOP10F bacteria expressing anti-Vif VH, VH-W, VH-CAM and VH-D single-domains after induction with 0.5 mM IPTG at 37 °C for 18 hours. Antibody fragments were extracted from the periplasmic space and purified as described in Materials and Methods. After separation on an SDS-PAGE 15% gel and blotting, single-domains were detected with HRP-conjugated anti-HA monoclonal antibody (Roche). Molecular mass is indicated in kDa. B, The anti-Vif VH, VH-W, VH-CAM and VH-D single-domains were used for evaluating relative binding affinities to 100 ng of Vif protein, thyroglobulin and BSA by ELISA. Results were obtained by measuring absorbance at 405 nm. Data represent results of three independent experiments; anti-Vif scFv 4BL was used as positive control. As shown, all VH domains have similar binding patterns to Vif antigen, but less than scFv 4BL. Background levels were detected using the control antigens BSA and thyroglobulin.

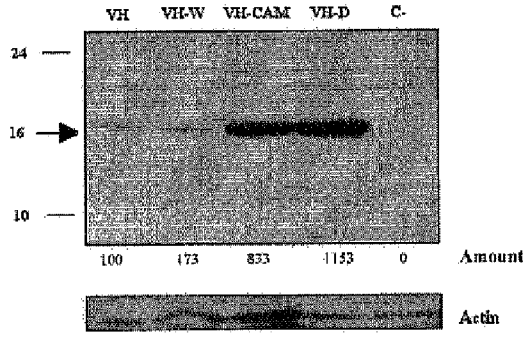

Figure 4. Expression of anti-Vif VH, VH-W, VH-CAM and VH-D single-domain intrabodies in eukaryotic cells. Anti-Vif VH intrabody expression vectors were transfected into 293T cells and after 48 hours cells were lyzed in 1 ml of buffer with 50 mM Tris (pH 8.0), 100 mM NaCl and 1% Nonidet P-40. The lyzate was cleared by centrifugation and immunoprecipitated with anti-HA affinity matrix (Roche). The proteins were separated by SDS-PAGE (15% gel) and visualized by Western blot probed with HRP-conjugated anti-HA monoclonal antibody. To control and normalize the transfection efficiency, mock lyzates of 293T cells were used as controls in Western blot analysis (C-) and the total amount of VH protein was assayed by comparison with cellular actin (anti-actin antibody, Santa Cruz). The amount of all proteins was determined by measurements of absorbance relative to the level of VH protein expression. Molecular mass is indicated in kDa.

single-domains, a transient *trans*-complementation assay in non-permissive cells that require Vif function for HIV-1 replication was used to examine the ability of the anti-Vif single-domains to inhibit a single round of HIV-1 replication. This complementation assay was previously shown to provide a quantitative measure of the ability of wild-type Vif to complement a single-round of HIV-1 replication *in trans*.[47] Non-permissive $H9_{38}$ LTR-CAT cells were cotransfected with pSVCATΔ*env*ΔVif, pVSVG, pSVL-Vif and plasmids encoding anti-Vif scFv 4BL, VH, VH-W, VH-CAM or VH-D domains. The HIV-1 virus particles produced in this assay result in only a single round of infection, as the packaged viral genome is defective for Env production. The efficiency of a single round of virus replication is quantified by measuring the level of chloramphenicol acetyl transferase (CAT) enzyme activity in the infected cultures after nine days, the minimum time for a detectable signal above background. Since our goal was to evaluate which VH single-domain has the strongest inhibitory activity when expressed intracellularly, the ability of the antibody fragments to inhibit a single round of HIV-1 replication *in trans* was examined. As shown in Figure 6, in the absence of Vif, replication of *vif*-negative virus was ~90-fold lower than that of *vif*-positive virus. Co-expression of anti-Vif VH-CAM and VH-D domains in $H9_{38}$ cells reduced *trans*-complementation to 30% and 10% of the wild-type level, respectively. In contrast, anti-Vif VH and VH-W domains, both expressed at low levels in mammalian cells, caused a much less significant reduction in *trans*-complementation to 5%

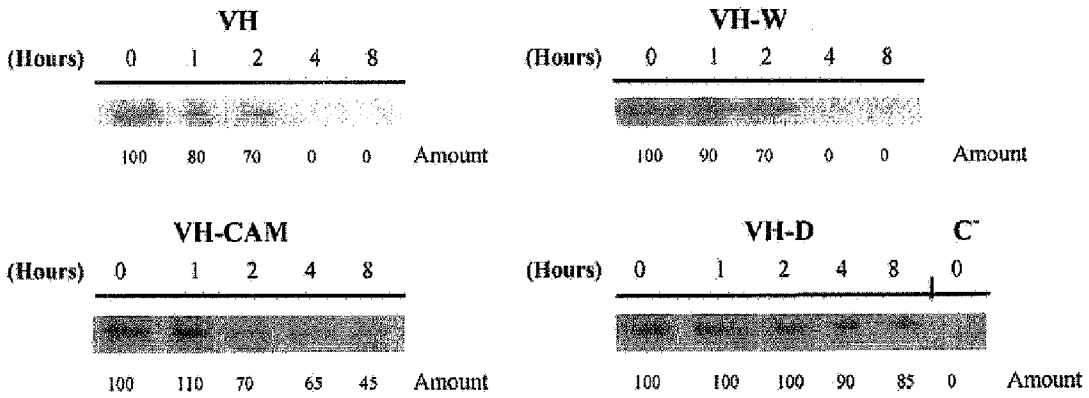

Figure 5. Pulse-chase analysis of anti-Vif VH single-domain intrabodies in transfected 293T cells. At 36 hours following transfection, 293T cells were pulse-labeled in [^{35}S]methionine/cysteine for two hours at 37 °C and chased for various times with DMEM medium supplemented with 40 × excess methionine (1.2 mg/ml) and 20 × cysteine (0.84 mg/ml). At each time-point, cells were lyzed in buffer with 50 mM Tris (pH 8.0), 100 mM NaCl, 1% Nonidet P-40 and immunoprecipitated with anti-HA affinity matrix (Roche). The proteins were separated by SDS-PAGE (15% gel) and visualized by autoradiography. Lyzates of 293T cells not expressing single-domains at time 0 were used in Western blot as a negative control (C^-). Chase times (in hours) are indicated on top. The amount of protein expressed at all time-points was determined by absorbance relative to the protein expressed at time 0. As shown, the steady-state levels of VH-D are higher compared to other VH domains. Nevertheless, the protein half-lifes of VH-D and VH-CAM are similar.

of the wild-type level. As a control, permissive cells (Jurkat) that do not require Vif function for HIV replication were cotransfected with pSVCAT-Δ*env*ΔVif, pVSVG, pSVL-Vif and plasmids encoding anti-Vif single-domains. Expression of single-domains in Jurkat cells had no inhibitory effect on HIV-1 replication. Thus, the biological activities of the anti-Vif VH fragments correlated directly with their solubility and increasing steady-state levels, indicating that the most highly camelized domain has the strongest anti-HIV-1 activity. Therefore, the intracellular solubility and stability of an intrabody is a critical factor that determines its efficiency in neutralizing intracellular antigens.

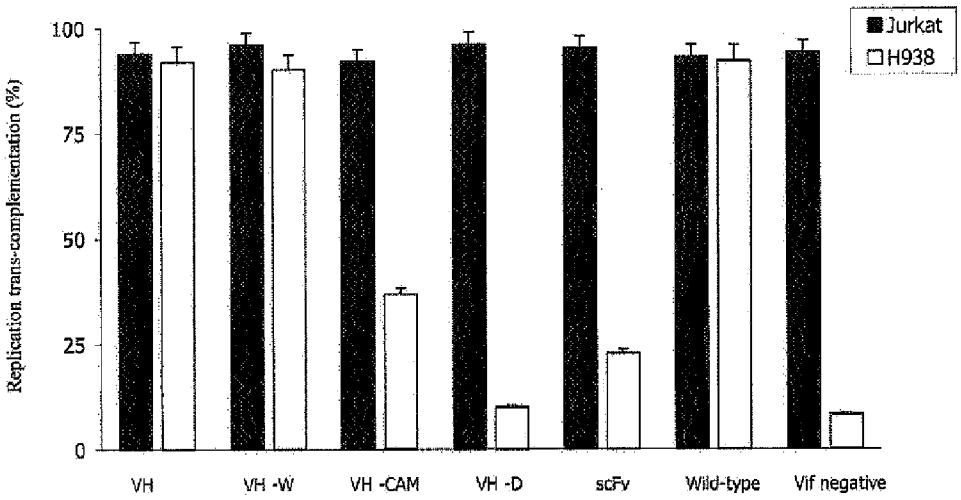

Figure 6. Neutralization of Vif function in a *trans*-complementation assay. Values shown represent the percentages of replication–complementation in non-permissive $H9_{38}$ cells (open bars) and permissive Jurkat cells (filled bars) relative to the value obtained for the wild-type. Cells were cotransfected with pSVCATΔ*env*ΔVif, pVSVG, psvlVif, and either anti-Vif scFv 4BL, VH, VH-W, VH-CAM, or VH-D expressor plasmids as described in Materials and Methods. The ability of anti-Vif antibody fragments to inhibit a single round of infection was measured by assaying for CAT activity in the cell cultures nine days after transfection. Background levels obtained when pVSVG was not cotransfected were 8(±2)%. Results shown are the means ± standard errors of two independent experiments.

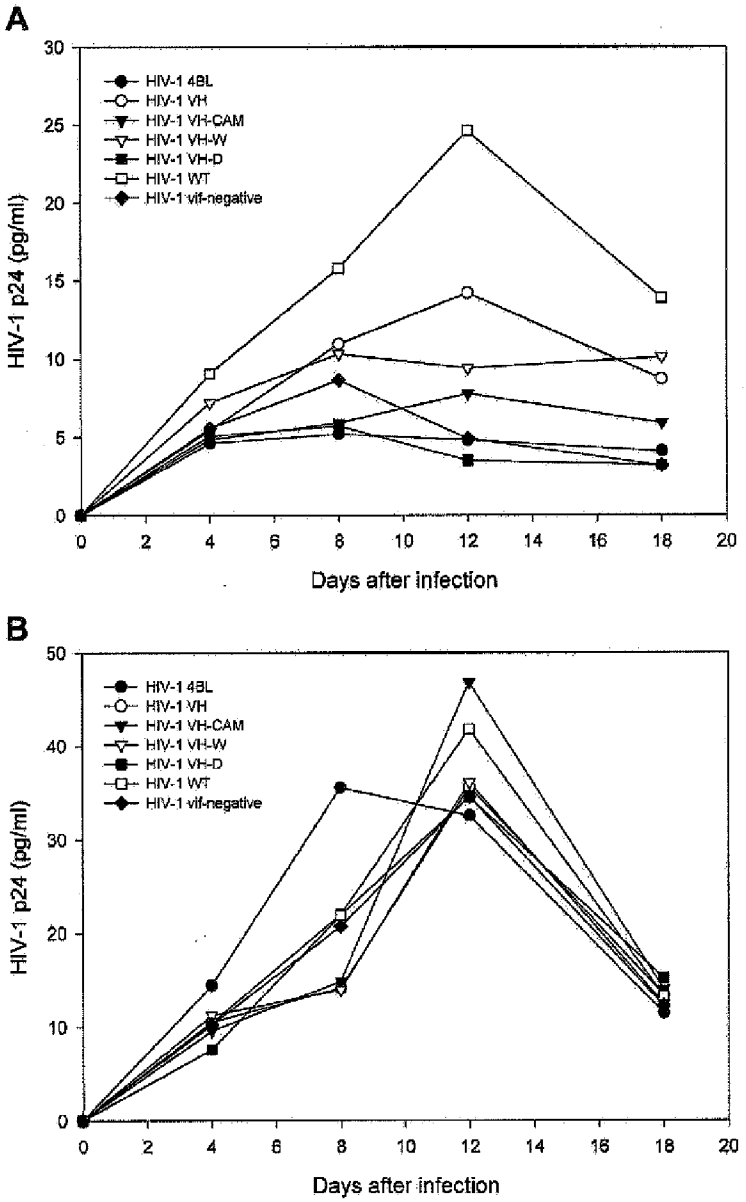

Figure 7. Cell-specific inhibition of HIV-1 replication in the presence of anti-Vif VH single-domains. Replication of HIV-1 encoding anti-Vif scFv 4BL, VH, VH-W, VH-CAM and VH-D antibody fragments was asseased in permissive and non-permissive cells. Cell-specific inhibition was started with HIV-1_{NL4-3} encoding anti-Vif single-domains produced after transfection of 293T cell lines with full-length proviral DNA as described in Materials and Methods. A, Non-permissive H9 cells were infected with HIV-4BL, HIV-VH, HIV-W, HIV-CAM and HIV-D. B, Permissive Jurkat cells were infected with HIV-4BL, HIV-VH, HIV-W, HIV-CAM and HIV-D. Infection of H9 and Jurkat cells with wild-type HIV-1_{NL4-3} and with HIV-1_{NL4-3} ΔVif were used as positive and negative controls, respectively. The cultures were maintained for up to 20 days, and to monitor infection aliquots were taken at the indicated time-points to determine p24 levels by ELISA. The data are representative of two independent experiments. C, H9 cells proliferation kinetics with WST-1 reagent. D, Jurkat cells proliferation kinetics with WST-1 reagent. The results of cellular proliferation and viability were measured according to the manufacturer's protocol (Roche) by absorption at 405 nm.

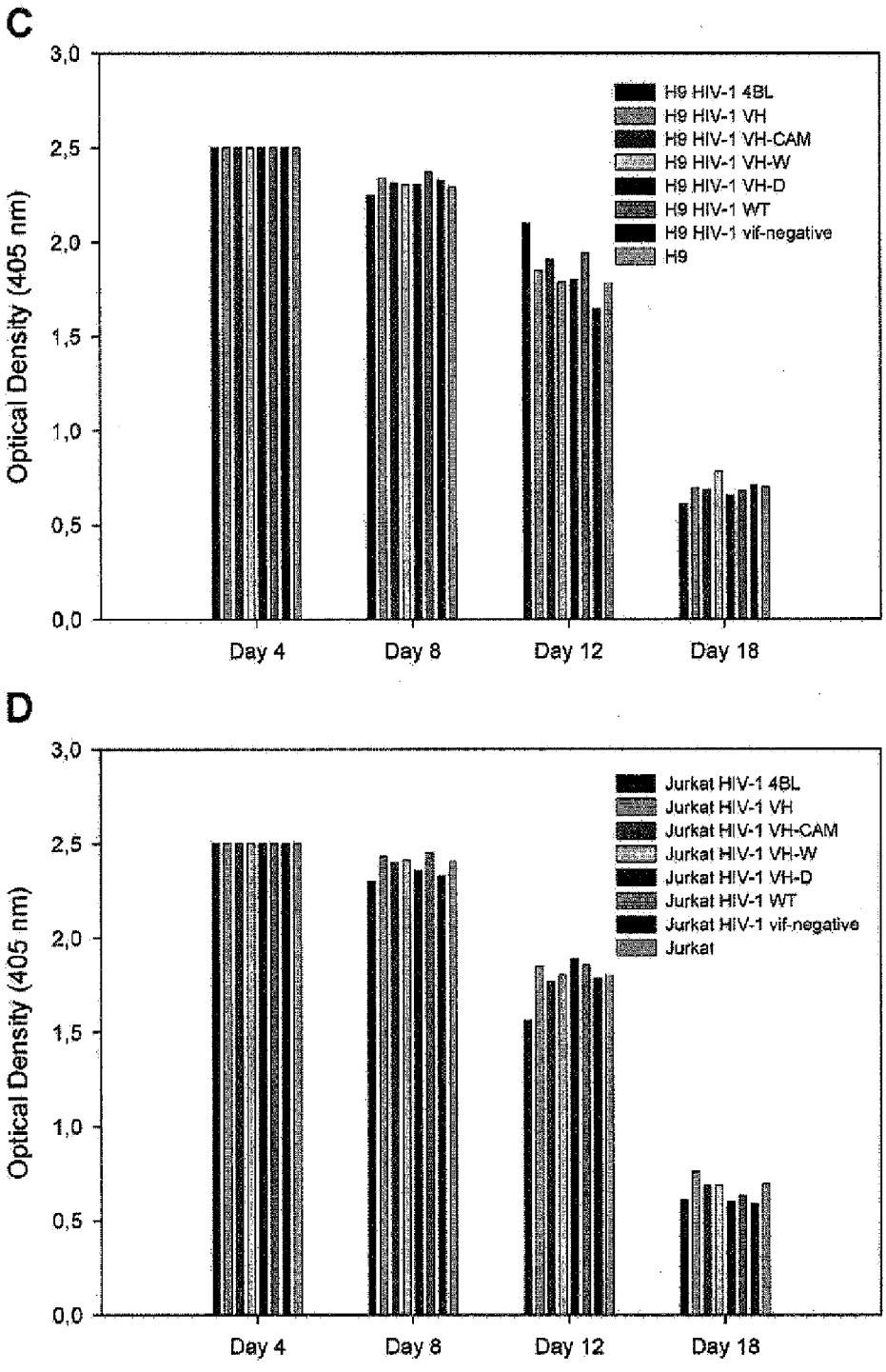

Figure 7 *(legend opposite)*

Inhibition of HIV-1 replication by anti-Vif single-domains is specific for non-permissive cells

The experiments described above examined the biological activity of anti-Vif antibody fragments in a transient assay under conditions in which most virus transmission occurs by cell-to-cell spread.[10,48] Vif modulates HIV-1 infection in cultured T-cell lines in a cell-dependent manner. To evaluate the specificity of viral inhibition in permissive and non-permissive cell lines, several recombinant HIV-1 viruses expressing each single-domain antibody *in cis* were generated. These recombinant HIV-1 viruses were derived from pHIVnPLAP-IRES-N +, by replacing the human placental alkaline phosphatase (PLAP) gene by scFv 4BL, VH, VH-W, VH-CAM and VH-D, generating pHIV-4BL, pHIV-VH, pHIV-W, pHIV-CAM and pHIV-D. In this experiment, 293T cells were transfected, and high-titer supernatants of HIV-4BL, HIV-VH, HIV-W, HIV-CAM and HIV-D were obtained. HIV-1 supernatants normalized for the same TCID50 were used to infect permissive cells (Jurkat) and non-permissive cells (H9) at a multiplicity of infection of 0.1 and their ability to replicate in these cells was assessed by performing standard virus growth curves. The cell cultures were maintained for up to 20 days and to monitor infection, aliquots were taken at the indicated time-points and HIV-1 p24 antigen levels were determined by ELISA. Two patterns of virus replication were obtained (Figure 7A and B). Non-permissive cells tested in this experiment did not support the spread of HIV-4BL, HIV-CAM and HIV-D. Similar results were obtained with HIVΔ*vif*. In contrast, the permissive cell line Jurkat supported replication of all viruses used in this experiment. In H9 cells, replication of HIV-VH and HIV-W exhibited an intermediate behavior. Previous studies have shown that intracellular antibody expression has no obvious negative effects on cell viability or proliferation.[10] Nevertheless, we quantified cell proliferation and cell viability of infected permissive and non-permissive cells compared with non-infected cells. The assay consists of a colorimetric assay based on the cleavage of the tetrazolium salt WST-1 by mitochondrial dehydrogenases in viable cells (Roche). The kinetics of WST-1 metabolism showed that H9 and Jurkat cells infected with HIV expressing anti-Vif antibody fragments have similar levels of proliferation compared with non-infected cell lines (Figure 7C and D). The same time-points were used for p24 antigen detection. As demonstrated previously in the transient assay, the replication of recombinant HIV expressing camelized VH domains shows that the specificity of Vif inhibition by intrabodies correlates with the cellular requirements for Vif function. The inhibition data confirm that only the highly soluble camelized fragments are able to fold correctly in sufficient amounts to be active as intrabodies.

Anti-Vif single-domain antibodies inhibit Vif's induced degradation of Apobec3G and avoid impairment of viral DNA synthesis

We next investigated the effect of VH single-domains on the fate of the viral reverse transcripts to further study the neutralization mechanism of HIV infectivity by single-domain constructs. It was previously suggested by the Landau laboratory that in the presence of Apobec3G, degradation of cDNA was more pronounced for ΔVif-defective virus.[39] A more dramatic effect was observed by quantification of integrated provirus. These data may be explained if the deamination by Apobec3G at the DNA minus-strand during reverse transcription does not strongly interfere with completion of cDNA, but instead the presence of uracyl results in degradation of the nucleic acid. To distinguish the role of different single-domains after viral entry in the target cell, cDNA was analyzed by quantitative real-time PCR in a single cycle of replication using primers specific for the early reverse transcripts, late reverse transcripts, and integrated proviruses[39,49] (Figure 8). Viruses were produced in the presence of Apobec3G together with constructs of antibody domains, and used for infection of target cells. Early reverse transcripts peaked with all antibody constructs between nine and 12 hours and decreased over time, similar to HIV-1 and HIV-1ΔVif in the presence of Apobec3G alone. The analysis of late reverse transcription showed differences between constructs. Two patterns emerged in comparison with Vif-positive and Vif-negative virus in the presence of Apobec3G. First, the VH and VH-W constructs showed no obvious differences compared to HIV-1 plus Apobec3G. Second, scFv 4BL, VH-D and VH-CAM showed less efficiency in late transcript synthesis similar to that of HIV-1 Vif-negative, with a decrease of 50% compared to VH. In contrast, quantification of integrated proviruses showed a stronger effect of all antibody constructs, except for the VH domain. All other constructs showed an effect between three- and sevenfold less provirus than HIV-1 wild-type. In particular, the VH-D and scFv 4BL show the more pronounced effect compared to other constructs, confirming our data where those antibody fragments were the more effective in inhibiting viral infectivity.

To determine whether these defects in reverse transcription and integration could be attributed to Vif inhibition alone or to downstream effect on Apobec3G, we cotransfected 293T with the cytidine deaminase expression vector, the Vif expression vector and different antibody constructs. Examination of resultant lyzates revealed that the amount of Vif used was sufficient to induce reduction in Apobec3G expression (Figure 9A). When antibody constructs were cotransfected together with similar amounts of Apobec3G and Vif, different profiles of cytidine deaminase expression were obtained. The VH construct caused no increase in Apobec3G

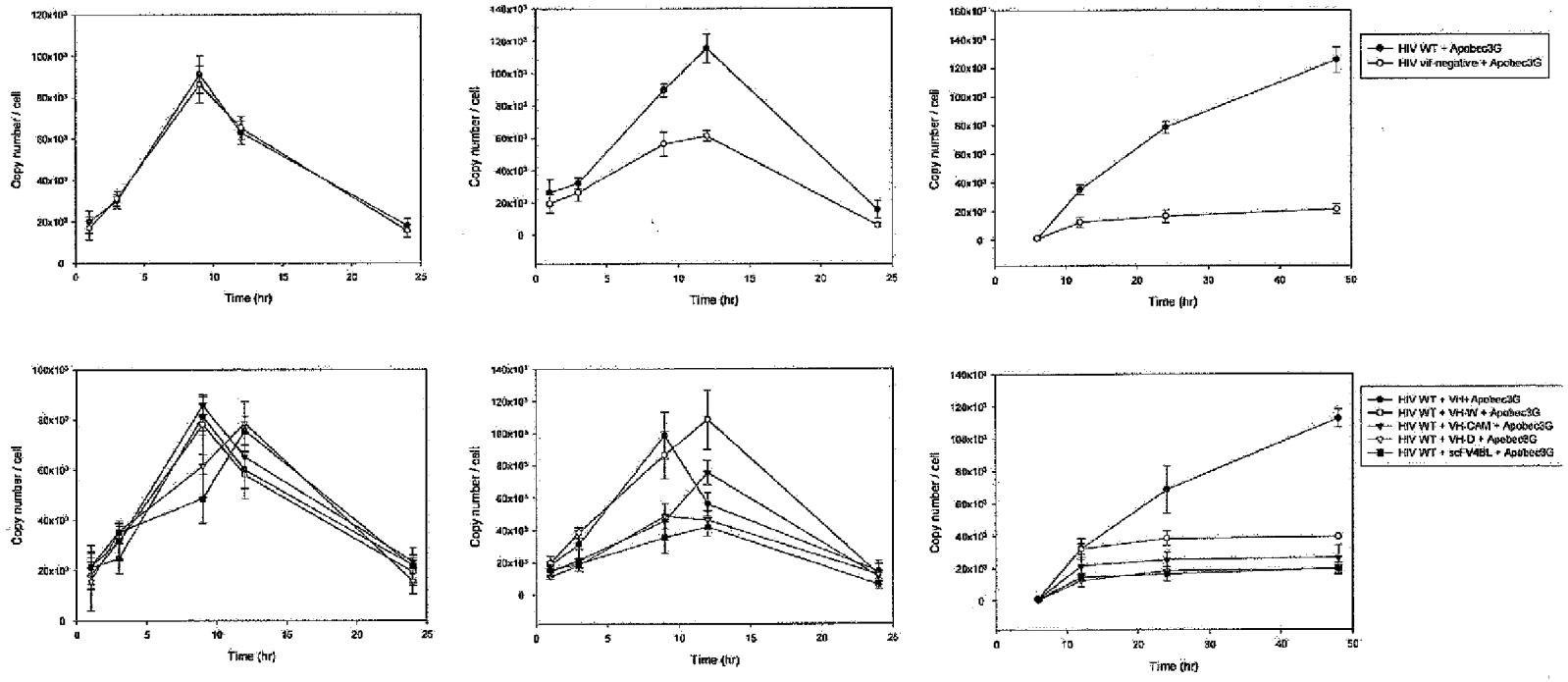

Figure 8. HeLa CD4 cells were infected in triplicate with DNase-treated HIV-1_{NL4-3} and HIV-1_{NL4-3} vif-negative virions produced by co-transfection of 293T cells with Apobec3G and different antibody constructs. Cell cultures were lyzed at indicated time-points post-infection and cellular DNA was prepared. Newly synthesized cDNA was measured by quantitative real-time PCR with primers specific for the early, late reverse transcripts or integrated proviruses as described by Butler *et al.*[40] Upper panels represent the cDNA synthesis and integration of HIV-1_{NL4-3} and HIV-1_{NL4-3} vif-negative virions in the presence of Apobec3G. Bottom panels represent the cDNA synthesis and integration of HIV-1_{NL4-3} and HIV-1_{NL4-3} vif-negative virions in the presence of Apobec3G, together with VH, VH-W, VH-CAM, VH-D and scFv 4BL. The results are representative of three independent experiments.

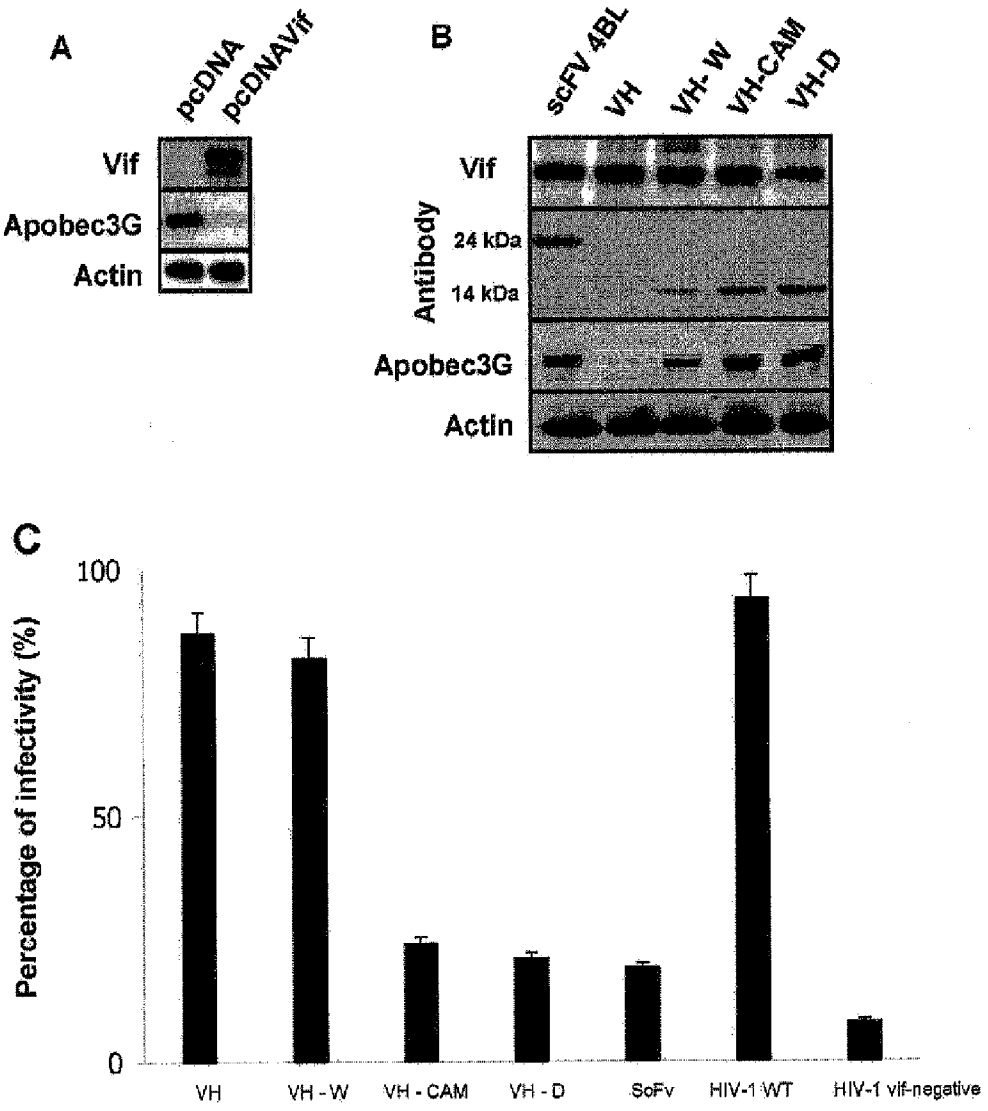

Figure 9. Single-domain antibodies increase expression of Apobec3G in the presence of Vif and reduce viral infectivity of HIV-1 wild-type. A, Sequential immunoblot analysis of cell lyzates co-transfected with 1 μg of pcDNA3.1-Vif and 1 μg of pcDNA3.1-Apobec3G-FLAG. Anti-Vif rabbit polyclonal antibody and anti-FLAG M2 mouse monoclonal antibody (Sigma) were used as primary antibodies. HRP-conjugated anti-rabbit IgG and anti-mouse IgG were used as secondary antibodies, respectively. Loading was controlled with anti-beta actin antibody (Abcam). B, Sequential immunoblot analysis of cell lyzates co-transfected with 1 μg of pcDNA3.1-Vif and 1 μg of pcDNA3.1-Apobec3G-FLAG, together with VH, VH-W, VH-CAM, VH-D and scFv 4BL. HRP-conjugated anti-HA monoclonal antibody was used to detect antibody constructs. As observed, VH-D and scFv 4BL have similar effectiveness to increase expression of Apobec3G in the presence of Vif. C, Single-cycle infectivity assay was performed with wild-type HIV-1_{NL4-3} virions, in the presence of Apobec3G and VH, VH-W, VH-CAM, VH-D and scFv 4BL constructs. The viruses were produced in 293T cells transfected with equal quantities of wild-type HIV-1_{NL4-3}, Apobec3G expression vector and antibody plasmids. Infectivity of the viruses normalized for p24 was measured in P4 LTR-β-Gal cells by quantification of the β-galactosidase activity in cell lyzates, using a colorimetric assay based on the cleavage of chlorophenolred-β-D-galactopyranoside(CPRG).

expression in the presence of Vif. In contrast, all other constructs increase the expression of Apobec3G and this result was dependent on the steady-state level of single-domain constructs and scFv 4BL. The higher expression of VH-D and scFv 4BL promoted the highest increase in Apobec3G expression (Figure 9B). To assess if the increased expression of Apobec3G in the presence

of different antibody constructs was reflected in a decreased viral infectivity, 293T cells were co-transfected with anti-Vif antibodies together with Apobec3G and HIV-1. Resultant viruses were collected and used to infect P4 LTR-β-Gal target cells, where the level of infectivity was measured by quantification of the β-galactosidase activity.[50,51] As shown in Figure 9C, a reduced effect in HIV infectivity was obtained with VH and VH-W. In contrast, VH-CAM, VH-D and scFv 4BL showed a pronounced reduction of 20–15% in viral infectivity compared to wild-type virus. These data are consistent with results of Apobec3G expression, reflecting an optimal inhibition of Vif. Taken together, these results suggest that the increased steady state of VH constructs optimally neutralize Vif and result in an increase stability of Apobec3G expression, favoring the inhibition of viral infectivity.

Discussion

The recombinant single-chain antibody fragment (scFv) is usually viewed as the suitable format for intracellular expression in eukaryotic cells. These intracellularly expressed antibodies have particular promise in the areas of functional genomics and gene therapy.[6,7] The purpose of these antibody fragments is to bind a specific protein and thereby inhibit a biological response. However, in the reducing environment of the cytoplasm the intrachain disulfide bridges cannot form and only very soluble and stably expressed antibody fragments will be able to fold correctly in sufficient amounts to be active as intrabodies.[21] Moreover, the interaction of single-domains VH and VL by the interface is weak and they may aggregate in the cytoplasm being targeted to proteosome degradation.

We recently developed an scFv from immunized rabbits that binds to HIV-1 Vif protein intracellularly and inhibits reverse transcription and viral replication.[10] The main function of Vif is to block the action of Apobec3G, a cytidine deaminase that renders HIV-1 non-infectivity by inducing G to A hypermutation in newly synthesised viral DNA.[39,40] Thus, Vif is an excellent target for therapeutic intervention.

Non-human antibodies are highly immunogenic in humans, thereby limiting their potential use for therapeutic applications. Nevertheless, in contrast to human antibodies derived from large naïve combinatorial antibody libraries that are selected *in vitro*, humanized antibodies derived from immune animals have been subjected to *in vivo* selection and, thus are more likely to recognize a given antigen selectively. Compared with other existing sources of human or humanized antibodies, immunized rabbits are an attractive alternative for several reasons. Humanized antibodies from immunized rabbits extend the accessible epitope repertoire of a given antigen. Epitopes that are not immunogenic in human or mice might be immunogenic in rabbits. This is of particular interest for the development of therapeutic scFv or VH single-domain antibodies that are to be evaluated in mouse models, and are required to recognize both the human antigen and its mouse homologues. Moreover, as was previously demonstrated, rabbit antibodies can be converted to humanized antibodies that retain both high specificity and affinity for the antigen.[52]

The results presented here strongly suggest the potential utility of rabbit VH single-domains as intrabodies. The use of scFv may be preferred due to its high affinity and diversity, implied by six CDR regions. However, its use as an intrabody is limited by low solubility in the reducing environment of the cytoplasm due to the lack of intrachain disulfide bonds that stabilize conformational structure. Therefore, the use of highly soluble and stable single-domains may obviate some of the technical obstacles responsible for the low efficacy of intracellular scFv.

Here, we evaluated rabbit single-domain antibody fragments as intrabodies against Vif protein. This constitutes a first step towards the design of a rabbit-derived minimal scaffold with intrabody properties, where the individual heavy chain variable domain (VH) of anti-Vif scFv was modified by protein engineering. To improve anti-Vif VH domain solubility, the hydrophobic surface area exposed in the absence of the light domain was mutated to mimic camelid heavy chain variable domains (VHH) naturally devoid of light chain.[27] The VH residues at positions 37, 44, 45 and 47 are all conserved, hydrophobic and are involved in interdomain contacts.[28,30] In camel VHH these residues are substituted by hydrophilic amino acid, and thus are more accessible to solvent, increasing the solubility of the isolated VHH domains. Trp103 is another amino acid that is crucial for the interaction with the VL domain, and is absolutely conserved in VH. Trp103 is maintained in all of the VHH reported structures. As reported by Desmyter *et al.*, Arg occupies position 103 in cAb-CA05, which is found in ~10% of VHH.[30] The mutation W103R drastically changes the nature of the VL surface interaction without disturbing the main chain conformation. It was proposed that W103R mutation might be a better choice than framework 2 mutations to render isolated VHs more soluble.[30] This would allow a soluble and more parental-related VH domain due to change of a crucial VL interaction residue. Therefore, it was inferred in our study that the W103R mutation on rabbit VH forms a supplementary choice to framework 2 mutants. Nevertheless, our results show an incremental role of framework 2 mutations, as the change of Trp103 alone slightly increased the solubility of VH from wild-type levels. Moreover, alterations in framework 2 were the major change responsible for increased rabbit VH domain solubility. This may be due to the different conformational structure of rabbit VH, in

which Trp103 may play a less crucial role for VL interaction. Other properties may be speculated, since this residue is strongly conserved in rabbit heavy-chain domains isolated from recombinant libraries (unpublished data). As demonstrated, intrabodies VH-CAM and VH-D are far more effective and exhibited increased steady-state expression levels compared to VH and VH-W. One possible explanation for low steady-state accumulation of intrabodies is attributed to intracellular protein stability. A VH single-domain with a long protein half-life would persist and potentially reach a much higher steady-state level than one with a very short protein half-life. Our data consistently show a strong correlation between targeting efficiency and the turnover rate, together with an increased steady-state accumulation of intrabodies in the cell. These results suggest that turnover rate, an index of overall protein stability, and steady-state accumulation of VH-CAM and VH-D are critical factors for the effectiveness of intrabodies. In the end, the concentration of intrabody inside the cell and the affinity for the antigen would govern the extent of its binding and consequent neutralization of function.

The mechanism of viral inhibition dissected here is consistent with Vif neutralization. As demonstrated by Mariani *et al.*, Apobec3G in the absence of Vif reduces the number of provirus copy number.[39] When single-domain antibodies are expressed, viral infectivity is predominantly affected during reverse transcription of the late cDNA and the effect is more pronounced at the integration step, probably caused by a decrease in the number of competent nucleic acid molecules. This is consistent with the results that show an increase in Apobec3G expression when the steady-state levels of anti-Vif VH domains and scFv become higher. It is conceivable that the increase of the intracellular level of Apobec3G will promote deamination resulting in a degradation of cDNA, as postulated before.[39,40] Our results of Vif's inhibition are consistent with this model, supported also by the corresponding decrease of viral infectivity.

The antibody library of scFv 4BL was derived previously from immunized rabbits with HIV-1 Vif protein.[10] The antibody diversity generated by V_HDJ_H rearrangements in rabbits is more limited than in mice and humans, since VH_1 is predominantly used out of more than 50 functional VH gene segments.[53] Somatic hypermutation and somatic gene conversion-like mechanisms are mostly responsible for the diversity in rearranged $V_{H1}DJ_H$ genes. Therefore, the limited diversity imposed by one VH family from rabbit-derived antibodies may result in the camelization process described in this study being extrapolated to other rabbit VH domains. Moreover, the camelization of rabbit antibody libraries may result in more effective VH domains, as maturation affinity by somatic hypermutation is dominant in these animals. This argument may invalidate the use of VH synthetic libraries by introducing CDR variability on a stable scaffold. Nevertheless, it should be noted that the discussion about effectiveness of intrabody and its half-life in the cytoplasm is still open. It is conceivable that less variability in the CDR of VH, or the lower affinity of these domains, can be compensated by superior steady-state levels of these proteins inside the cell.

In conclusion, camelization of rabbit single-domain VH framework does not affect antigen-neutralization capacity *in vitro* or *in vivo*, based on functional assays of HIV infectivity neutralization. In addition, camelization improves the solubility and stability of the VH domain, correlating with effects on inhibition of HIV infectivity. We may speculate that the improved stability and protein half-life of the VH single-domain in the cytoplasm may target more effectively the Vif antigen during HIV-1 production. Moreover, camelized VH domains retain a similar mechanism of action to inhibit Vif compared to scFv, which supports our conclusion that these modifications in the interface of the rabbit antibody VH framework may be preferable for intrabody development.

Materials and Methods

Cloning VH anti-Vif single-domain antibodies

A fragment encoding the anti-Vif VH domain was generated by PCR from the pComb3X phagemid vector containing the anti-Vif scFv gene (pComb3X-4BL).[10] The following primers were used: VHPiv-F 5′-AGGAGGCG CGGCCGCGGGGCCCAGGCGGCCAGATCTTCCCAG TCGGTGGAGGAG-3′ and RSC-B 5′-GAGGAGGAGGA GGAGGAGCCTGGCCGGCCTGGCCACTAGTG-3′. The resulting PCR fragment was gel-purified, digested with the restriction endonuclease SfiI, and cloned into the phagemid vector pComb3X. Plasmid pComb3X is derived from pComb3H.[16] For camelization, the anti-Vif VH domain was mutated into VH-CAM, VH-W and VH-D single-domains by protein engineering. The modifications tested in our study are summarized in Figure 2 and were based on sequences published for single-domain antibody fragments with high conformational stability and solubility[44] and on human camelization studies done by Davies & Reichmann.[43] For the VH-CAM mutant, specific oligonucleotide primers encoding point mutations V37F, G44E, L45R and W47G, were used for PCR-based mutagenesis. The following primers were used: VHPiv-F and VH CAM-B 5′-GTGTTACCAC TATAACTAATGATTCCGATTCCTTCTCTTTCCTTCCC GGGAGCCTGGCGGAA-3′; and VH CAM-F 5′-TTCC GCCAGGCTCCCGGGAAGGAAAGAGAAGGAATCG GAATCATTAGTTATAGTGGTAACAC-3′ and RSC-B. The PCR products were gel-purified and assembled in a further PCR reaction using the VHPiv-F and RSC-B primers. The resulting overlap PCR product was gel-purified, digested with the restriction endonuclease SfiI, and cloned into pComb3X vector. For construction of the VH-W mutant, specific oligonucleotide primers encoding point mutation W103R were used: VHPiv-F and W103R-B 5′-TGGAGGCTGAGGAGACGGTGACCAGG GTGCCCGGGCCCCTCAAGTTAATATCCGTATAAAA ATCTCTACC-3′. For the VH-D mutant, the same cloning

procedure for VH-W construction was applied but starting from the VH-CAM mutant. The mutants were verified by sequencing. After expression studies in *E. coli* TOP10F and analysis of binding activities, genes encoding VH single-domains were transferred into pCDNA3.1/Zeo$^+$ (Invitrogen). A methionine initiation codon was added into all VHs by PCR. The primers used for cloning in pCDNA3.1/Zeo$^+$ were: Babe ScFv5 5′-GGCATGGGGGCCCAGGCGGCCCAGCTC-3′ and Babe ScFv3 5′-GCCACCACCCTCCTAAGAAGC-3′. We introduced a sequence encoding the HA-tag sequence (YPYDVPDYA) at the C terminus, followed by a stop codon. The PCR products were cloned by NotI and XhoI into pCDNA3.1/Zeo$^+$. Anti-Vif single-domain genes were also cloned into pHIVnPLAP-IRES-N + in place of PLAP-IRES-nef. The primers used for cloning were VL-VH-NOT 5′-ATAAGAATGCGGCCGCTAAA CTATATGGGGGCCCAGGCGGCCGAGCTC-3′ and 4ScFv-HIV-Xho 5′-CCGCTCGAGCGGGCCACCACCCT CCTAAGAAGC-3′. Apobec3G was amplified from the H9 cell line cDNA using oligonucleotides 5′GAATTCA AGGATGAAGCCTCACTTCAGA3′ and 5′GACTGCAG CCCATCCTTCAGTTTTCCTG3′ and cloned in pcDNA3.1 (Invitrogen). The sequence of FLAG-tag was added at the C-terminal end of Apobec3G. The three-dimensional structure prediction of the VH domain from scFv 4BL was obtained by comparative protein modeling using SWISS-MODEL.[54–56] After introducing the mutated amino acids, the refinement of the overall protein structure was performed to achieve the model with lowest energy.[54]

Expression and purification of anti-Vif single-domains antibodies

To express and purify anti-Vif VH single-domains from the bacterial periplasmic space, phagemid DNA was transformed into non-suppressor *E. coli* strain TOP10F. A fresh colony of each VH clone was grown at 37 °C overnight in SOB medium containing 100 μg/ml of ampicillin. A 10 ml sample of cells was used to inoculate one liter of SOB medium containing 100 μg/ml of ampicillin. Cells were grown at 37 °C until $A_{550\ nm} = 0.9$, induced by the addition of 0.5 mM IPTG and growth was continued for 18 hours. After induction, the cell densities of the samples were analyzed and normalized to $A_{550\ nm} = 10$. Cultures were centrifuged for 30 minutes at 4000 *g* and bacterial pellets were disrupted by resuspending in 30 ml of 20 mM Tris–HCl buffer (pH 8.0), 0.7 M sucrose and supplemented with protease inhibitors (Roche). After one hour on ice, 5 ml of a 2 mg/ml lysozyme solution in 0.1 M EDTA (pH 8.0) was added. Cells were incubated for 30 minutes on ice and the soluble periplasmic extract was collected by 15 minutes centrifugation at 14,000 *g*. VH single-domains expressed in the periplasm were purified by nickel chelate affinity chromatography making use of the C-terminal His_6 of pComb3X. The eluted fraction was concentrated by Centricon columns (Millipore). Purified VH single-domains were analyzed by SDS-PAGE followed by Coomassie blue staining and Western blot with HRP-conjugated anti-HA monoclonal antibody (Roche). The concentration of proteins was determined, by the Bradford method by measuring the absorbance at 280 nm.

Vif expression and purification

The pD10Vif bacterial expression plasmid was described by Yang *et al.*[57] *E. coli* TOP10F strain was transformed with pD10Vif and expression of His_6-Vif was performed under 1 mM IPTG to log phase ($A_{550\ nm} = 0.6$–0.8). After induction for three hours at 37 °C, bacteria were lyzed in 6.5 M guanidine HCl, 0.05 M sodium phosphate (pH 7.8), 150 mM NaCl, at room temperature. Insoluble cell debris was removed by ultracentrifugation and the supernatant was loaded into a Zn-NTA-agarose column (Roche). The column was washed extensively with 6.5 M guanidine HCl, 0.05 M sodium phosphate (pH 6.5), 150 mM NaCl and sequentially loaded with on-column folding buffer: 0.05 M sodium phosphate (pH 6.5), 150 mM NaCl and left overnight at 4 °C. Elution of the refolded recombinant Vif protein was performed at room temperature with 500 mM imidazole, 0.05 M sodium phosphate (pH 6.5), 150 mM NaCl, 0.05% (w/v) sodium azide. Vif-containing fractions were pooled and concentrated by dialysis against 80% (v/v) glycerol. Aliquots were stored at 4 °C.

ELISA measurements

To analyze relative antigen binding affinities of each anti-Vif VH domain, ELISA plates (Nunc) were coated with 100 ng of purified recombinant HIV-1 Vif protein, thyroglobulin or BSA, overnight at 4 °C. Wells were blocked for one hour at 37 °C with 3% (w/v) BSA in phosphate-buffered saline (PBS). Purified anti-Vif VHs and anti-Vif scFv 4BL were added to the wells for further incubation and diluted at various concentrations starting at 10 μg/ml and 5 μg/ml, respectively. After washing the wells with PBS, HRP-conjugated anti-HA monoclonal antibody (Roche) was used for detection. The results were obtained from measurement of absorbance at 405 nm and were performed in triplicate.

Cell lines and transfections

The 293T and P4 LTR-β-Gal cells were maintained in Dulbecco's modified Eagles medium and H9, $H9_{58}$ LTR-CAT and Jurkat cells were maintained in RPMI 1640 medium. Media were supplemented with 10% (v/v) fetal calf serum (FCS), antibiotics (100 units/ml of penicillin and 100 μg/ml of streptomycin) and 2 mM glutamine. All cell cultures were maintained at 37 °C in 5% CO_2. Tissue culture media and reagents were from BioWhitaker. To produce large amounts of HIV-1 particles, 4×10^6–5×10^6 293T cells were transfected by Fugene (Roche) according to the manufacturer's protocol with 2 μg of wild-type HIV-1_{NL4-3}, pHIV-$1_{NL4-3}\Delta vif$ or pHIVn-PLAP-IRES-N expressing anti-Vif antibody fragments. The same procedure was followed for immunoprecipitations and Western blot analysis.

To evaluate expression of Apobec3G in the presence of Vif and antibody constructs, 293T cell lines were co-transfected where indicated with scFv 4BL, VH, VH-W, VH-CAM and VH-D, together with pcDNA3.1-APOBEC3G and pcDNA3.1-Vif. Cell lyzates were immunoblotted sequentially with anti-Vif rabbit polyclonal antibody, anti-FLAG M2 mouse monoclonal antibody (Sigma) and HRP-conjugated anti-HA monoclonal antibody (Roche). To control cell lyzate loading, beta-actin monoclonal antibody AC-15 was used (Abcam).

Expression of VH single-domain antibodies in eukaryotic cells

At 48 hours post-transfection, 293T cells were washed

with 5 ml of cold PBS. Cells were lyzed in 1 ml of 50 mM Tris (pH 8.0), 100 mM NaCl, 1% Nonidet P-40 containing protease inhibitors (Roche) for 60 minutes on ice. The lyzate was cleared by centrifugation for 30 minutes at 14,000 *g* and incubated overnight with anti-HA affinity matrix (Roche) at 4 °C. Immunoprecipitated proteins were separated by SDS/PAGE 15% (w/v) and transferred to nitrocellulose membrane. Western blot was performed with HRP-conjugated anti-HA monoclonal antibody (Roche). To control and normalize the transfection efficiency, mock lyzates of 293T cells were used in Western blot analysis and the total amount of VH protein was assayed by comparison with cellular actin (anti-actin antibody, Santa Cruz).

Pulse-chase

For pulse-chase experiments, 293T cells (1×10^6–2×10^6) were transfected by Fugene (Roche) with VH single-domain plasmids. At 36 hours post-transfection, cells were incubated with 1 ml of methionine/cysteine-free medium for two hours at 37 °C and metabolically labeled with similar medium containing 100 μCi of [^{35}S]methionine/cysteine for two hours at 37 °C. After labeling, cells were washed three times with 1 ml of DMEM supplemented with 40 × excess methionine (1.2 mg/ml) and 20 × excess cysteine (0.84 mg/ml) and incubated with the same medium for various times. At each time-point, cells were washed twice with cold PBS and lyzed on ice for one hour with 400 μl of lysis buffer containing protease inhibitors (Roche). Lyzates were cleared by centrifugation and supernatant incubated overnight at 4 °C with anti-HA affinity matrix (Roche). Immunoprecipitated proteins were analyzed by SDS-PAGE, and the gels were fixed before treatment with Autofluor Image Enhancer (National Diagnostics). The dried gels were subjected to autoradiography.

Replication complementation assay

A transient complementation assay was performed as previously described to provide a quantitative measure of the ability of wild-type Vif protein to complement a single-round of HIV-1 replication *in trans*.[47] Briefly, $H9_{38}$ LTR-CAT cells (10^6) and Jurkat (10^6) cells were cotransfected by Fugene (Roche), with 2 μg of pSVCAT-Δ*env*ΔVif, 2 μg of pVSVG, 2 μg of pSVLVif and either plasmids encoding anti-Vif scFv 4BL, VH, VH-W, VH-CAM or VH-D antibody fragments. The ability of antibody fragments to inhibit a single round of infection was measured by assaying for CAT activity in the transfected culture nine days after transfection. CAT assay was performed by the *Quan*-T-CAT system (Amersham Biosciences).

Cell-specific inhibition of HIV-1 replication

HIV-1 recombinant virus stocks encoding antibody fragments were prepared by transfection of 293T cells. At 48 hours post-transfection, the viral supernatants were normalized for the same TCID50 and used to infect permissive cells (Jurkat) and non-permissive cells (H9). Cell cultures were maintained for up to 20 days and to monitor infection, aliquots were taken at the indicated time-points to determine p24 levels by HIV-1 ELISA (Innotest). Permissive and non-permissive cells were infected with HIV-1_{NL4-3} and HIV-1_{NL4-3} ΔVif as positive and negative controls, respectively. Cellular proliferation and viability of infected H9 and Jurkat cells were analyzed with tetrazolium salt WST-1 (Roche) according to the manufacturer's protocol.

Infectivity assay

To further evaluate the inhibition of HIV-1 infectivity by VH domains and scFv, 293T cells (1×10^6–2×10^6) were cotransfected by Fugene (Roche), with 2 μg of pVSVG, 2 μg of HIV-1_{NL4-3}, 2 μg of pcDNA3.1-Apobec3G and either plasmids encoding anti-Vif scFv 4BL, VH, VH-W, VH-CAM or VH-D antibody fragments at 2 μg each. HIV-1_{NL4-3} ΔVif were used as negative control. At 48 hours post-transfection, the viral supernatants were normalized for the same TCID50 and used to infect subconfluent P4 LTR-β-Gal cells in 96-well plates. At 48 hours after infection, the ability of VH single-domains and scFv antibody fragments to inhibit HIV-1 infection was measured by quantification of the β-galactosidase activity in cell lyzates, using a colorimetric assay based on the cleavage of chlorophenolred-β-D-galactopyranoside (CPRG) by β-galactosidase.[50,51] Briefly, P4 LTR-β-Gal cells were washed with PBS and then lyzed with lysis buffer (50 mM Tris (pH 8.0), 100 mM NaCl, 1% Nonidet P-40). After incubation for 30 minutes on ice, CPRG reaction buffer (6 mM in lysis buffer) was added to the cell lyzates and incubated for two hours at 37 °C. The results were obtained by measuring absorbance at 570 nm and were performed in triplicate.

Real-time PCR quantification of HIV-1 cDNA synthesis and integration

Hela CD4 cells (1×10^6) were infected with DNase-treated viruses derived by 293T transfection. Target cells were lyzed and DNA was prepared from 0.5 hours to 24 hours postinfection. As described by Butler *et al.*, early HIV-1 reverse transcripts were quantified with primers ert2f (5′-GTG CCC GTC TGT TGT GTG AC) and ert2r (5′-GGC GCC ACT GCT AGA GAT TT) and the probe ERT2 [5′-(FAM)-CTA GAG ATC CCT CAG ACC CTT TTA GTC AGT GTG G-(TAMRA)-3′].[49] Late reverse transcripts were quantified with primers MH535, MH532, and the probe LRT-P.[49] Integrated proviruses were quantified using primers MH531 and MH704.

Data base accession numbers

The sequence reported here has been deposited in the GenBank data base (accession number AY369782).

Acknowledgements

We thank Carlos Barbas III for providing pComb3X and for helpful discussions. We thank Denise Champs and Patrick Medeiros for their help in real-time PCR. $H9_{38}$ cells, P4 LTR-β-Gal cells, plasmids HIV-1_{NL4-3}, HIV-1_{NL4-3} ΔVif and pHIVnPLAP-IRES-N were obtained from the AIDS Research and Reference Reagent Program. This work was supported by grants from the Fundação para a Ciência e Tecnologia (POCTI/33096/MGI/2000). F.A.S. was supported with a BI from Fundação para a Ciência e Tecnologia. A.F.V.

and M.S.M. are the recipients of doctoral fellowships from Fundação para a Ciência e Tecnologia. D.G. was supported by NIH grant AI36186.

References

1. Carter, P. & Merchant, A. M. (1997). Engineering antibodies for imaging and therapy. *Curr. Opin. Biotechnol.* **8**, 449–454.
2. Ewert, S., Honegger, A. & Plückthun, A. (2003). Structure-based improvement of the biophysical properties of immunoglobulin v(h) domains with a generalizable approach. *Biochemistry*, **42**, 1517–1528.
3. Cattaneo, A. & Biocca, S. (1999). The selection of intracellular antibodies. *Trends Biotechnol.* **17**, 115–121.
4. Bird, R. E., Hardmann, K. D., Jacobson, J. W., Johnson, S., Kaufman, B. M., Lee, T. *et al.* (1988). Single-chain antigen-binding proteins. *Science*, **242**, 423–426.
5. Huston, J. S., Levinson, D., Mudget-Hunter, M., Tai, M., Novotny, J., Margolies, M. N. *et al.* (1988). Protein engineering of antibody binding sites: recovery of specific activity in an anti-digoxin single-chain Fv analogue produced in *Escherichia coli*. *Proc. Natl Acad. Sci. USA*, **85**, 5879–5883.
6. Auf der Maur, A., Zahnd, C., Fischer, F., Spinelli, S., Honegger, A. & Cambillau, C. (2002). Direct *in vivo* screening of intrabody libraries constructed on a highly stable single-chain framework. *J. Biol. Chem.* **277**, 45075–45086.
7. Auf der Maur, A., Escher, D. & Barberis, A. (2001). Antigen-independent selection of stable intracellular single-chain antibodies. *FEBS Letters*, **508**, 407–412.
8. Tavladoraki, P., Benvenuto, E., Tinca, S., De Martinis, D., Cattaneo, A. & Galeffi, P. (1993). Transgenic plants expressing a functional single-chain Fv antibody are specifically protected from virus attack. *Nature*, **366**, 469–472.
9. Bai, J., Sui, J., Zhu, R. Y., Tallarico, A. S., Gennari, F., Zhang, D. & Marasco, W. A. (2003). Inhibition of Tat-mediated transactivation and HIV-1 replication by human anti-hCyclinT1 intrabodies. *J. Biol. Chem.* **278**, 1433–1442.
10. Goncalves, J., Silva, F., Freitas-Vieira, A., Santa-Marta, M., Malho, R., Yang, X. *et al.* (2002). Functional neutralization of HIV-1 Vif protein by intracellular immunization inhibits reverse transcription and viral replication. *J. Biol. Chem.* **277**, 32036–32045.
11. Marasco, W. A., La Vecchio, J. & Winkler, A. (1999). Human anti-HIV-1 tat sFv intrabodies for gene therapy of advanced HIV-1-infection and AIDS. *J. Immunol. Methods*, **231**, 223–238.
12. Paillard, F. (1999). Intrabodies to human immunodeficiency virus type 1. *Hum. Gene Ther.* **10**, 1425–1427.
13. Mhashilkar, A. M., Biswas, D. K., LaVecchio, J., Pardee, A. B. & Marasco, W. A. (1997). Inhibition of human immunodeficiency virus type 1 replication *in vitro* by a novel combination of anti-Tat single-chain intrabodies and NF-kappa B antagonists. *J. Virol.* **71**, 6486–6494.
14. Maciejewski, J. P., Weichold, F. F., Young, N. S., Cara, A., Zella, D., Reitz, M. S., Jr & Gallo, R. C. (1995). Intracellular expression of antibody fragments directed against HIV reverse transcriptase prevents HIV infection *in vitro*. *Nature Med.* **1**, 667–673.
15. Marasco, W. A., Haseltine, W. A. & Chen, S. Y. (1993). Design, intracellular expression, and activity of a human anti-human immunodeficiency virus type 1 gp120 single-chain antibody. *Proc. Natl Acad. Sci. USA*, **90**, 3793–7889.
16. Steinberger, P., Andris-Widhopf, J., Buhler, B., Torbett, B. E. & Barbas, C. F., 3rd (2000). Functional deletion of the CCR5 receptor by intracellular immunization produces cells that are refractory to CCR5-dependent HIV-1 infection and cell fusion. *Proc. Natl Acad. Sci USA*, **97**, 805–810.
17. Tanaka, T. & Rabbitts, T. H. (2003). Intrabodies based on intracellular capture frameworks that bind the RAS protein with high affinity and impair oncogenic transformation. *EMBO J.* **22**, 1025–1035.
18. Hyland, S., Beerli, R. R., Barbas, C. F., Hynes, N. E. & Wels, W. (2003). Generation and functional characterization of intracellular antibodies interacting with the kinase domain of human EGF receptor. *Oncogene*, **22**, 1557–1567.
19. Cohen, P. A., Mani, J. C. & Lane, D. P. (1998). Characterization of a new intrabody directed against the N-terminal region of human p53. *Oncogene*, **17**, 2445–2456.
20. Proba, K., Honegger, A. & Plückthun, A. (1997). A natural antibody missing a cysteine in VH: consequences for thermodynamic stability and folding. *J. Mol. Biol.* **265**, 161–172.
21. Wörn, A. & Plückthun, A. (2001). Stability engineering of antibody single-chain Fv fragments. *J. Mol. Biol.* **305**, 989–1010.
22. Proba, K., Wörn, A., Honegger, A. & Plückthun, A. (1998). Antibody scFv fragments without disulfide bonds made by molecular evolution. *J. Mol. Biol.* **275**, 245–253.
23. Visintin, M., Tse, E., Axelson, H., Rabbitts, T. H. & Cattaneo, A. (1999). Selection of antibodies for intracellular function using a two-hybrid *in vivo* system. *Proc. Natl Acad. Sci. USA*, **96**, 11723–11728.
24. Tse, E., Lobato, M. N., Forster, A., Tanaka, T., Chung, G. T. Y. & Rabbitts, T. H. (2002). Intracellular antibody capture technology: application to selection of intracellular antibodies recognising the BCR-ABL oncogenic protein. *J. Mol. Biol.* **317**, 85–94.
25. Tanaka, T., Chung, G. T. Y., Forster, A., Lobato, M. N. & Rabbitts, T. H. (2003). *De novo* production of diverse intracellular antibody libraries. *Nucl. Acids Res.* **31**, e23.
26. Desiderio, A., Franconi, R., Lopez, M., Villani, M. E., Viti, F., Chiaraluce, R. *et al.* (2001). A semi-synthetic repertoire of intrinsically stable antibody fragments derived from a single-framework scaffold. *J. Mol. Biol.* **310**, 603–615.
27. Hamers-Casterman, C., Atarhouch, T., Muyldermans, S., Robinson, G., Hamers, C., Songa, E. B. *et al.* (1993). Naturally occurring antibodies devoid of light chains. *Nature*, **363**, 446–448.
28. Muyldermans, S. (2001). Single domain camel antibodies: current status. *J. Biotechnol.* **74**, 277–302.
29. Tanha, J., Dubuc, G., Hirama, T., Narang, S. A. & MacKenzie, C. R. (2002). Selection by phage display of llama conventional V(H) fragments with heavy chain antibody V(H)H properties. *J. Immunol. Methods*, **263**, 97–109.
30. Desmyter, A., Decanniere, K., Muyldermans, S. & Wyns, L. (2001). Antigen specificity and high affinity binding provided by one single loop of a camel single-domain antibody. *J. Biol. Chem.* **276**, 26285–26290.
31. Conrath, K. E., Lauwereys, M., Wyns, L. &

Muyldermans, S. (2001). Camel single-domain antibodies as modular building units in bispecific and bivalent antibody constructs. *J. Biol. Chem.* **276**, 7346–7350.
32. Cortez-Retamozo, V., Lauwereys, M., Hassanzadeh, Gh G., Gobert, M., Conrath, K. & Muyldermans, S. (2002). Efficient tumor targeting by single-domain antibody fragments of camels. *Int. J. Cancer*, **98**, 456–462.
33. Frenken, L. G., van der Linden, R. H., Hermans, P. W., Bos, J. W., Ruuls, R. C., de Geus, B. & Verrips, C. T. (2000). Isolation of antigen specific llama VHH antibody fragments and their high level secretion by *Saccharomyces cerevisiae*. *J. Biotechnol.* **78**, 11–21.
34. Strebel, K., Daugherty, D., Clouse, K., Cohen, D., Folks, T. & Martin, M. A. (1987). The HIV "A" (sor) gene product is essential for virus infectivity. *Nature*, **328**, 728–730.
35. Fisher, A. G., Ensoli, B., Ivanoff, L., Chamberlain, M., Petteway, S., Ratner, L. *et al.* (1987). The sor gene of HIV-1 is required for efficient virus transmission *in vitro*. *Science*, **237**, 888–893.
36. Fan, L. & Peden, K. (1992). Cell-free transmission of Vif mutants of HIV-1. *Virology*, **190**, 19–29.
37. Sodroski, J., Goh, W. C., Rosen, C., Tartar, A., Portetelle, D., Burny, A. & Haseltine, W. (1986). Replicative and cytopathic potential of HTLV-III/LAV with sor gene deletions. *Science*, **231**, 1549–1551.
38. Gabuzda, D. H., Lawrence, K., Langhoff, E., Terwilliger, E., Dorfman, T., Haseltine, W. & Sodroski, J. (1992). Role of vif in replication of human immunodeficiency virus type 1 in CD4 + T lymphocytes. *J. Virol.* **66**, 6489–6495.
39. Mariani, R., Chen, D., Schrofelbauer, B., Navarro, F., Konig, R., Bollman, B. *et al.* (2003). Species-specific exclusion of Apobec3G from HIV-1 virions by Vif. *Cell*, **114**, 21–31.
40. Sheehy, A. M., Gaddis, N. C., Choi, J. D. & Malim, M. H. (2002). Isolation of a human gene that inhibits HIV-1 infection and is suppressed by the viral Vif protein. *Nature*, **418**, 646–650.
41. Wirtz, P. & Steipe, B. (1999). Intrabody construction and expression III: engineering hyperstable V(H) domains. *Protein Sci.* **8**, 2245–2250.
42. Tanaka, T., Lobato, M. N. & Rabbitts, T. H. (2003). Single domain intracellular antibodies: a minimal fragment for direct *in vivo* selection of antigen-specific intrabodies. *J. Mol. Biol.* **331**, 1109–1120.
43. Davies, J. & Riechmann, L. (1994). "Camelising" human antibody fragments: NMR studies on VH domains. *FEBS Letters*, **339**, 285–290.
44. Dumoulin, M., Conrath, K., Van Meirhaeghe, A., Meersman, F., Heremans, K., Frenken, L. G. *et al.* (2002). Single-domain antibody fragments with high conformational stability. *Protein Sci.* **11**, 500–515.
45. Martsev, S. P., Dubnovitsky, A. P., Stremovsky, O. A., Chumanevich, A. A., Tsybovsky, Y. I., Kravchuk, Z. I. & Deyev, S. M. (2002). Partially structured state of the functional VH domain of the mouse anti-ferritin antibody F11. *FEBS Letters*, **518**, 177–182.
46. Ward, E. S., Gussow, D., Griffiths, A. D., Jones, P. T. & Winter, G. (1989). Binding activities of a repertoire of single immunoglobulin variable domains secreted from *Escherichia coli*. *Nature*, **341**, 544–546.
47. Goncalves, J., Jallepalli, P. & Gabuzda, D. (1996). Subcellular localization of the Vif protein of human immunodeficiency virus type 1. *J. Virol.* **68**, 704–712.
48. Helseth, E., Kowalski, M., Gabuzda, D. H., Olshevsky, U., Haseltine, W. & Sodroski, J. (1990). Rapid complementation assays measuring replicative potential of human immunodeficiency virus type 1 envelope glycoprotein mutants. *J. Virol.* **64**, 2416–2420.
49. Butler, S. L., Hansen, M. S. & Bushman, F. D. (2001). A quantitative assay for HIV DNA integration *in vivo*. *Nature Med.* **7**, 631–634.
50. Mammano, F., Trouplin, V., Zennou, V. & Clavel, F. (2000). Retracing the evolutionary pathways of human immunodeficiency virus type 1 resistance to protease inhibitors: virus fitness in the absence and in the presence of drug. *J. Virol.* **74**, 8524–8531.
51. Eustice, D., Feldman, P., Colberg-Poley, A., Buckery, R. & Neubauer, R. (1991). A sensitive method for the detection of β-galactosidase in transfected mammalian cells. *BioTechniques*, **11**, 739–743.
52. Rader, C., Ritter, G., Nathan, S., Elia, M., Gout, I., Jungbluth, A. A. *et al.* (2000). The rabbit antibody repertoire as a novel source for the generation of therapeutic human antibodies. *J. Biol. Chem.* **275**, 13668–13676.
53. Popkoy, M., Mage, R. G., Alexander, C. B., Thundivalappil, S., Barbas, C. F., III & Rader, C. (2003). Rabbit immune repertoires as sources for therapeutic monoclonal antibodies: the impact of kappa allotype-correlated variation in cysteine content on antibody libraries selected by phage display. *J. Mol. Biol.* **325**, 323–335.
54. Guex, N. & Peitsch, M. C. (1997). SWISS-MODEL and the Swiss-PdbViewer: an environment for comparative protein modeling. *Electrophoresis*, **18**, 2714–2723.
55. Schwede, T., Kopp, J., Guex, N. & Peitsch, M. C. (2003). SWISS-MODEL: an automated protein homology-modeling server. *Nucl. Acids Res.* **31**, 3381–3385.
56. Peitsch, M. C. (1995). Protein modeling by E-mail. *Bio/Technology*, **13**, 658–660.
57. Yang, X., Goncalves, J. & Gabuzda, D. (1996). Phosphorylation of Vif and its role in HIV-1 replication. *J. Biol. Chem.* **271**, 10121–10129.
58. Kabat, E., Wu, T.T., Perry, H.M., Gottesman, K.S., Foeller, C. (1991). *Sequence of Proteins of Immunological Interest*, Publication 91-3242 US Public Health Services, National Institutes of Health, Bethesda, MD.

Edited by M. Yaniv

(Received 21 January 2004; received in revised form 14 April 2004; accepted 16 April 2004)

doi:10.1016/S0022-2836(03)00836-2 J. Mol. Biol. (2003) 331, 1109–1120

JMB Available online at www.sciencedirect.com SCIENCE DIRECT®

Single Domain Intracellular Antibodies: A Minimal Fragment For Direct *In Vivo* Selection of Antigen-specific Intrabodies

Tomoyuki Tanaka, M. Natividad Lobato and Terence H. Rabbitts*

MRC Laboratory of Molecular Biology, Hills Road, Cambridge CB2 2QH, UK

There is a major need in target validation and therapeutic applications for molecules that can interfere with protein function inside cells. Intracellular antibodies (intrabodies) can bind to specific targets in cells but isolation of intrabodies is currently difficult. Intrabodies are normally single chain Fv fragments comprising variable domains of the immunoglobulin heavy (VH) and light chains (VL). We now demonstrate that single VH domains have excellent intracellular properties of solubility, stability and expression within the cells of higher organisms and can exhibit specific antigen recognition *in vivo*. We have used this intracellular single variable domain (IDab) format, based on a previously characterised intrabody consensus scaffold, to generate diverse intrabody libraries for direct *in vivo* screening. IDabs were isolated using two distinct antigens and affinities of isolated IDabs ranged between 20 nM and 200 nM. Moreover, IDabs selected for binding to the RAS protein could inhibit RAS-dependent oncogenic transformation of NIH3T3 cells. The IDab format is therefore ideal for *in vivo* intrabody use. This approach to intrabodies obviates the need for phage antibody libraries, avoids the requirement for production of antigen *in vitro* and allows for direct selection of intrabodies *in vivo*.

Keywords: single VH domain antibody; cancer therapy; intrabody; *in vivo* selection; library

*Corresponding author

Introduction

Antibodies and their derivative fragments are used in research, in biotechnology and in clinical settings for diagnostic and therapeutic applications. In the field of cancer therapy, monoclonal anti-tumour antibodies have been targeted to cancer cells and have had some success for direct neutralisation[1] or triggering anti-cancer immune responses[2] but such uses are restricted to extracellular antigens. However, most oncogenic proteins, for instance fusion proteins resulting from chromosomal translocations,[3] are intracellular and thus not amenable to conventional antibody-based therapy. Further, putative target molecules, such as those identified from genome sequencing programmes like the Human Genome Project,[4] can be based on open reading frames (ORFs) derived from DNA sequence alone. Reagents which can interfere with function are key components of the functional genomics arm of genome projects.

Techniques that can elucidate the function of gene products are important in biological research. A number of approaches are available to define gene function, such as knock-out technologies which rely on developing a phenotype from loss of gene activity in embryonic stem (ES) cells, or in mutant mice. Recently, RNA interference (RNAi) has been developed to ablate specific mRNA species.[5] This approach is limited by incomplete RNA cleavage, inaccessible RNA sequences and proteins with a long half-life. In addition, RNAi cannot be used to specifically target individual protein–protein interactions or

Abbreviations used: Ab, antibody; AD, activation domain; β-gal, β-galactosidase; CDR, complementarity determining region; DBD, DNA-binding domain; FR, framework region; IAC, intracellular antibody capture; IDab, intracellular single domain antibody fragment; PBS, phosphate-buffered saline; scFv, single chain Fv fragment; VL, immunoglobulin light chain variable domain; VH, immunoglobulin heavy chain variable domain.

E-mail address of the corresponding author: thr@mrc-lmb.cam.ac.uk

post-translational modifications of proteins. Intracellular antibodies (intrabodies) with specific and high-affinity binding properties have potential in therapy of human diseases and in functional genomics[6,7] in which the target proteins or protein interactions are only found inside the cell. Intrabodies are usually single chain variable fragments (scFv) comprising a heavy (H) and a light (L) chain variable (V) domain held together by a flexible linker peptide, to create a single polypeptide chain[8,9] and have been effective against target proteins *in vivo*.[7,10,11] There are, however, rather few scFv which work efficiently as intrabodies because antibodies are usually made in the endoplasmic reticulum and in the reducing environment of the cell, e.g. in the cytoplasm, scFv cannot form disulphide bonds, which are critical in folding of almost all antibodies, and thus often exhibit insolubility, instability and/or incorrect protein folding.

A number of approaches have been devised to overcome the limitation imposed by the cellular environment.[12–14] Intracellular antibody capture (IAC) technology is an approach based on selecting intrabodies starting with diverse scFv phage antibody libraries, which are initially screened with antigen *in vitro*, and subsequently screening the selected scFv in a yeast *in vivo* antibody–antigen interaction assay.[15,16] IAC has proved successful in allowing the selection of intrabodies recognising a diverse set of antigens and has helped to define a scaffold of immunoglobulin V-region residues which are particularly advantageous for in-cell function.[17] The generality and speed of IAC is currently limited by the initial screen of a phage antibody library and also by the need to prepare purified antigen for this initial screening step. For high-throughput screening purposes, an approach is needed for direct screening of intrabodies *in vivo*. Further, a numerical limitation of scFv intrabodies is the combinatorial effect of heavy and light chains and the subsequent diversity required to include antigen-specific intrabodies.

Current IAC screening protocols require scFv phage antibody libraries of greater than 10^9 diversity to facilitate the isolation of a small number (around 10–50) of intracellular antibodies.[15–17] It is possible that single variable region domains, which are the smallest immunoglobulin-based recognition units (Dabs),[18] could prove more efficacious as a source of intrabodies, since the overall complexity for screening should be lower than scFv.[19,20] We describe here a simple procedure for direct *in vivo* selection of intrabodies which utilises a single domain format based on the intrabody consensus sequence.[15] Single domain libraries have been made from which intrabodies (IDabs) have been successfully isolated against different epitopes on two different antigens; viz. the oncogenic protein RAS and the cAMP/calcium-dependent transcription factor ATF-2. The anti-RAS IDabs can inhibit mutant RAS-induced NIH3T3 cell oncogenic transformation, illustrating that IDabs can be functional *in vivo*.

Results

Single domain antibody fragments can function as intrabodies *in vivo*

In our previous study,[17] intracellular scFv antibodies were isolated by an IAC method[15] and their *in vivo* effectiveness for antigen binding was improved using step-by-step mutagenesis of the scFv framework to a consensus sequence.[21] We have now tested the ability of the individual domains of the anti-RAS scFv intrabodies (i.e. the single VH domain or the single VL domain) to bind antigen *in vivo*. Various expressed antibody fragments (indicated in Figure 1A) were tested in a luciferase reporter assay which comprised transfecting COS7 cells with a minimal luciferase reporter plasmid together with a vector encoding RAS antigen linked to the Gal4 DNA-binding domain (DBD) and one encoding an antibody fragment linked to the VP16 transcriptional activation domain (AD). The expression of the intrabody–VP16 fusions was assessed by detection of proteins using Western blotting. All the clones support the expression of their respective proteins in COS7 cells (Figure 1B) and it is evident that both scFv and single domain intrabody fusions (VH and VL) are equivalently and well expressed.

The ability of the intrabodies to interact with their respective antigen *in vivo* was tested using a luciferase reporter gene assay. Figure 1C shows the levels of luciferase resulting from transcriptional activation of the reporter following interaction of the Gal4 DBD–RAS and the intrabody–VP16. It is significant that the best luciferase activation was achieved with the anti-RAS VH single domain formats. For instance, the VH from intrabody anti-RAS scFv33 (Figure 1, 33VH) stimulates the reporter activity about five times more than the parental scFv clone (Figure 1(C), 33). The anti-RAS VL single domain, however, did not activate at all (33VL). As we described previously,[17] conversion of scFv33 to a consensus format (here we used the I21R33 version) had increased *in vivo* function in terms of antigen binding. The single domain VH derived from this intrabody also performed better than the parental molecule (Figure 1, I21R33VH) in this reporter assay. Finally, mutation of the cysteine residues, which are involved in the intra-domain disulphide bonds of the VH domains, had no substantial effect on *in vivo* expression or function (clones I21R33VH-C22S and I21R33VH-C92S). Thus single domain intrabodies (IDabs) can function without the intra-domain disulphide bond. We conclude that binding of the anti-RAS scFv33 to antigen can occur through the VH domain alone and an important corollary is that single domains appear to be excellent mediators of intracellular antibody function.

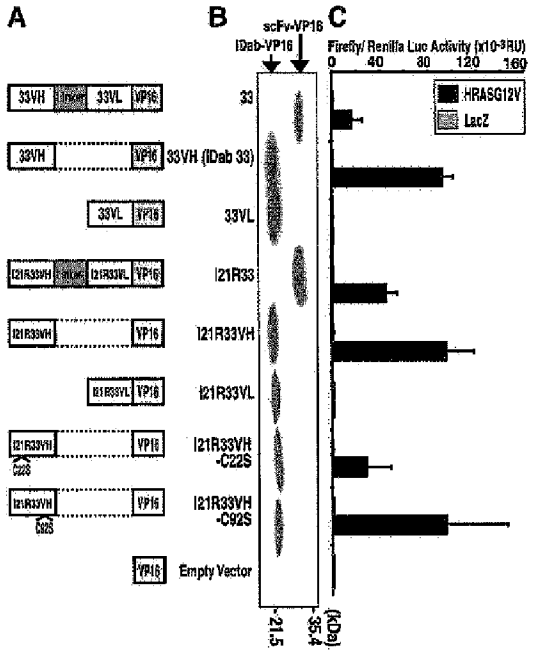

Figure 1. Interaction of anti-RAS scFv or single domain derivatives with RAS protein in mammalian cells. COS7 cells were transiently co-transfected with various scFv or single domain (IDab) derivatives fused with the VP16 AD together with the Gal4-DBD RAS bait plasmid pM1-HRASG12V or pM1-β-gal (lacZ). Two reporter plasmids were also included in each transfection; viz. the firefly luciferase reporter plasmid pG5-Luc and an internal *R. luciferase* constitutive expression control plasmid pRL-CMV. The luciferase activities were measured 48 hours after transfection using the Dual Luciferase Assay System (Promega). A, Diagrammatic representation of the intrabody-VP16 fusions expressed in COS7. Anti-RAS scFv33 (33) and I21R33 have been described before.[17] Intrabodies 33VH and 33VL are the VH and VL single domains, respectively, from scFv33; I21R33VH and I21R33VL are the VH and VL single domains, respectively, from scFvI21R33; I21R33VH-C22S is the VH single domain from scFvI21R33 with a Cys to Ser mutation at position 22 (23 according to the IMGT unique numbering for V-DOMAINs[39,40]) and I21R33VH-C92S is the VH single domain from scFvI21R33 with a Cys to Ser mutation at position 92 (104 according to the IMGT unique numbering for V-DOMAIN[39,40]). B, Western blot of COS7 cell extracts after the expression of scFv-VP16 or IDab-VP16 fusions. ScFv or IDab-VP16 fusion proteins were detected using anti-VP16 (14-5, Santa Cruz Biotechnology) monoclonal antibody and horseradish peroxidase (HRP)-conjugated anti-mouse IgG antibody. C, The normalised activities are shown for firefly luciferase signals compared to the *R. luciferase* activity (used as internal control for the transfection efficiency). Results with the Gal4 DBD-RAS bait pM1-HRASG12V are shown in black boxes and with pM1-β-gal (lacZ) in grey boxes (in all cases, the signal obtained with the pM1-β-gal bait was negligible).

Direct screening of synthetic single domain intracellular antibody libraries in yeast

The observed functioning of single VH domains in mammalian cells suggested that the IDab format could be generally useful for production of intracellular antibody libraries with sufficient diversity for isolation of antigen-specific IDabs directly by yeast antibody–antigen interaction procedures.[14] This idea was tested by generating IDab libraries, based on the previously described intrabody consensus framework,[15,17] for direct *in vivo* screening in yeast.[22] Two IDab libraries were made by cloning diversified VH domains into the pVP16* vector to encode IDab–VP16 fusion proteins. The sizes of the libraries were around 3×10^6 (IDab library 1) and 5×10^7 (IDab library 2, estimated diversity $\sim 3 \times 10^7$), which were complexities compatible with direct yeast screening.

The IDab libraries were screened with two different antigens (viz. HRASG12V and ATF-2) to ascertain their general utility. Yeast cells, which have *his3* and *lacZ* reporter genes, were transfected the IDab libraries together with antigen bait clones encoding the antigen fused to the LexA DBD. In excess of a hundred clones showed histidine independent growth with either antigen bait (Table 1), suggesting the intracellular interaction of the antigen and VH single domain intrabodies. These clones were picked and assessed using a β-galactosidase (β-gal) filter assay and the ten causing most rapid colour development were selected and sequenced. Figure 2A shows the derived amino acid sequences from the VH complementarity determining region (CDR) regions, compared with the parental CDR regions of IDab 33. Among the selected clones, several identical sequences were found with IDabs selected against the different antigens suggesting that these clones bind with LexA DBD portion of the bait protein. This was assessed by re-assaying histidine-independent growth and β-gal activation of each IDab clone

Table 1. IDab library screening data

Bait (antigen)	Library	No. clones screened	No. clones HIS- growth	No. clones β-gal positive
HRASG12V	IDab library 1	7.86×10^7	454	374
	IDab library 2	1.65×10^8	510	488
ATF-2	IDab library 1	1.18×10^7	314	277

Two different IDab-VP16 libraries were screened with two antigen baits (HRASG12V and ATF-2) as LexA–DBD fusions. Library 1 had randomised VH CDR 2 and 3, while library 2 had randomised VH CDR1, 2 and 3. The primary screening results are shown as the initial number of clones screened in yeast L40 with the antigen bait and the numbers of colonies growing on histidine-deficient plates (HIS-growth) and the corresponding proportion causing β-gal activation (β-gal positive).

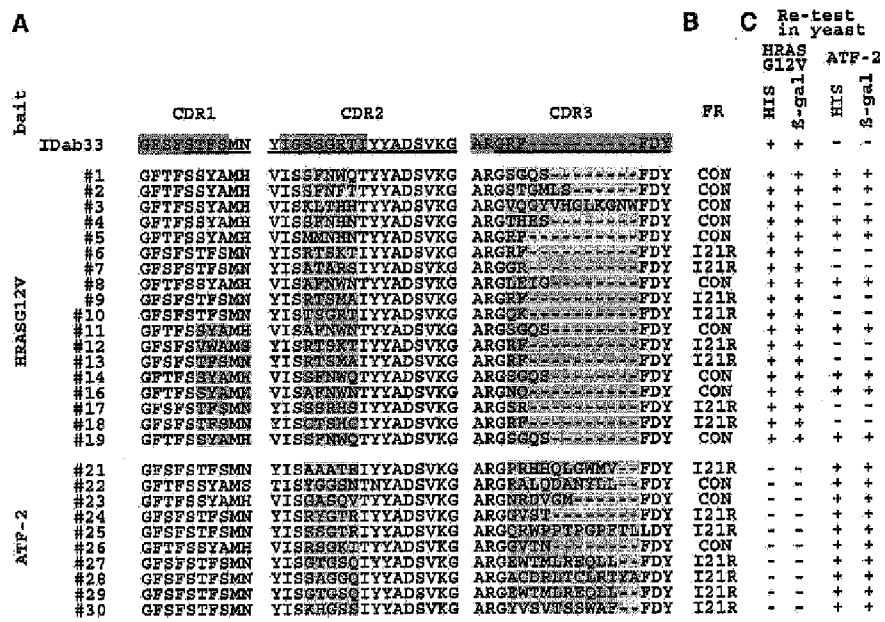

Figure 2. VH CDR protein sequences of IDabs isolated from intrabody library screening. Alignment of derived protein sequences of CDRs of selected IDab intrabody clones obtained by screening the single domain libraries with two protein baits; viz. HRASG12V and ATF-2 proteins. A, The nucleotide sequences of the IDab clones were obtained and the derived protein translations (shown in the single-letter code) were aligned. The IDab CDRs are aligned and compared with those of IDab33 (the highlighted CDR regions of the VH domain are defined by IMGT (the International ImMunoGeneTics, information system at http://imgt.cines.fr)[41] (grey highlighted in IDab33, top line) and by Kabat *et al.* (underlined in IDab33, top line)[42]). In the sequences of the IDabs selected from the libraries, only those regions which were randomised by the PCR mutagenesis are highlighted with grey. Note that the anti-RAS IDabs clones 11 to 19 originated from IDab library 2 and these have all three CDRs mutated and hence the highlighted region of CDR1 as well as CDR2 and 3 in the sequences derived from those clones. B, The middle panel shows which VH framework each selected IDab originates from. CON, framework from the scFv625 which carries the canonical IAC consensus.[15] I21R, framework from the scFvI21R33 which has a sequence very close to the canonical consensus.[17] C, Each selected IDab was re-tested in the yeast assay with either the starting bait or the heterologous bait using both histidine dependence (HIS) or β-gal activation assays (β-gal) and scored positive (+) or negative (−) in those assays.

with the heterologous bait (Figure 2C). In this way, we found that nine of the anti-RAS IDabs showed interaction not only with the cognate bait but also with the non-relevant ATF-2 bait (clones #1, #2, #4, #5, #8, #11, #14, #16, #19), consistent with these IDabs being anti-LexA intrabodies. The remaining ones were confirmed to have specificity against the RAS antigen. All the selected anti-ATF-2 IDabs were specific for the cognate antigen. Significant length variation of the VH CDR3 was found, especially in the anti-ATF-2 clones, consistent with the method of CDR3 randomisation, which included length variation from two to 12 codons.

Library selected IDabs can function in mammalian cells

Our results show that it is possible to select IDabs by directly screening a library in yeast, thus avoiding the *in vitro* phage antibody library screening required in the original IAC method.[16,22] The efficacy of these IDabs in mammalian cells was tested using three different transcriptional transactivation assays (Figure 3). First, we tested the IDab clones in the COS7-based luciferase reporter assay.[17] The IDab sequences were cloned into a mammalian expression vector to express the IDab fused with the VP16AD at the C terminus. COS7 cells were transfected with IDab–VP16 constructs and either a specific bait expressing as a Gal4 DBD–antigen fusion or a bait comprising Gal4 DBD–LexA fusion (Figure 3A and B). We observed a degree of variability in the activation of luciferase, with some clones giving a high stimulation of reporter activity, for instance anti-RAS clones #6 and #10 (Figure 3(A)), while some only produced a moderate stimulation, for instance anti-RAS clone #3 or the anti-ATF-2 clones #27 and #29 (Figure 3(B)). Interestingly, anti-RAS clone #3 not only has a long CDR3 compared to other anti-RAS IDabs (Figure 2), but only stimulated luciferase activation when co-expressed with HRAS, but not with KRAS and NRAS, whereas the anti-RAS IDab clones #6, #7, #9, #10, #12, #13, #17 and #18 stimulated luciferase activation when

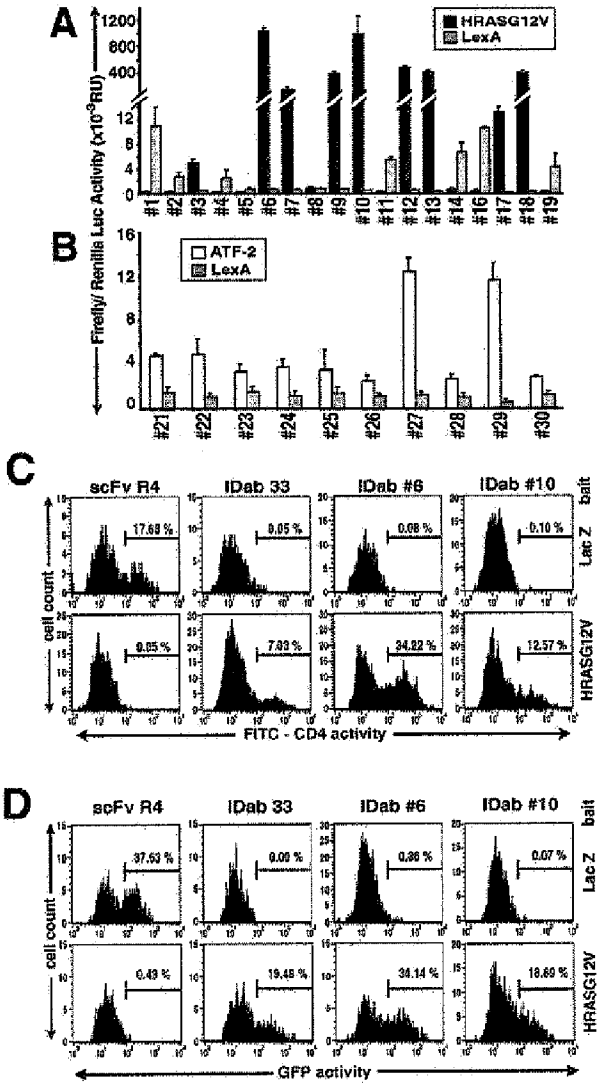

Figure 3. Mammalian intracellular two-hybrid IDab antibody–antigen interaction assays. Mammalian two-hybrid antibody-antigen interaction assays were performed with three independent methods. A and B, Luciferase reporter assay. COS7 were transfected with the pEF-IDab-VP16 vectors and one of three bait vectors, viz. pM1-HRASG12V (black boxes), pM1-ATF-2 (open boxes) or pM1-LexA (grey boxes) together with pG5-luc (firefly luciferase) and pRL-CMV (*R. luciferase*) reporter plasmids. Luciferase levels were determined as described in Materials and Methods. Each histogram represents the firefly luciferase signal normalised to the *R. luciferase* signal (used as internal control for the transfection efficiency). A, Results with HRASG12V-selected IDabs. B, Results with ATF-2 selected IDabs. C, FACS analysis to detect CD4 expression. The CHO-CD4 cell line, which has a chromosomal CD4 reporter gene regulated *via* the Gal4 upstream activating sequence (UAS),[23] was co-transfected with the bait vector pM1-HRASG12V, expressing RAS protein, or a bait vector pM1-lacZ, expressing β-gal protein, together with the indicated pEF-scFv-VP16 or pEF-IDab-VP16 vectors. Induction of cell surface CD4 expression was assayed at 48 hours after transfection using anti-human CD4 antibody and FITC-conjugated anti-mouse Ig antibody. The indicated percentages of CD4 expressing cells were measured with a FACSCalibur. ScFvR4 is an anti-β-gal antibody.[24] D, FACS analysis to detect GFP expression. The CHO-GFP cell line was constructed as described in Materials and Methods using a GFP reporter regulated *via* the Gal4 UAS site.[22] The CHO-GFP cell line was co-transfected with the bait vectors pM1-HRASG12V or pM1-lacZ together with the various indicated pEF-VP16-scFv or pEF-IDab-VP16 vectors. GFP expression was measured with a FACSCalibur 48 hours after transfection.

co-expressed with all three RAS antigens (data not shown). These data indicate that the anti-RAS intrabody #3 recognises a different epitope on the RAS molecule from the other IDabs. Clones #1, #2, #4, #11, #14, #16 and #19 stimulated significant reporter activity with LexA as a bait which, taken together with the finding that these IDabs bind both to LexA-RAS and LexA-ATF-2 baits (Figure 2C), shows that they are anti-LexA DBD intrabodies.

Validation of mammalian cell activity of the anti-RAS IDabs was obtained using Chinese hamster ovary (CHO) cells which carry either chromosomal CD4[25] or GFP reporters. When these reporters are stimulated by transient expression of a complex between Gal4 DBD–antigen and IDab–VP16 fusion proteins, either the CD4 molecule in expressed at the surface of the CHO cells (CHO-CD4) or green fluorescent protein is produced in the cells (CHO-GFP). The results obtained with anti-RAS IDabs in CHO-CD4 and CHO-GFP cells are shown in Figure 3C and D, respectively. When a non-relevant intrabody, anti-β-gal scFvR4,[24] was expressed with the RAS bait, no reporter activation was observed for either CHO-CD4 (Figure 3C) or CHO-GFP (Figure 3D). However, around 15–40% of cells displayed CD4 or GFP expression when scFvR4 and a lacZ

bait were co-transfected (Figure 3C and D). The bait specificity was reversed when anti-RAS IDab33 (the original IDab sub-cloned from the anti-RAS scFv33[17]) or anti-RAS IDab #6 or #10 were co-expressed with the baits, since activation was only observed with the RAS bait (Figure 3C and D). These results indicate that the yeast IDab library screening approach can select IDabs with sufficiently good *in vivo* properties to facilitate binding to relevant antigen within mammalian cells.

Single domain intracellular antibodies are expressed as soluble proteins *in vivo*

The IDab intrabodies that we have used in these reporter assays are expressed as fusions with the VP16 AD and are well expressed. However, the VP16 domain of the fusion proteins could be a major determinant of solubility and stability in mammalian cells and it is possible that the single domains alone would not be well tolerated *in vivo*, as these antibody fragments do have a tendency to aggregate *in vitro*.[25] Indeed, unmodified human VH domains, in the absence of the VL domain (i.e. with the hydrophobic VL interface exposed) are only monomeric at low protein concentrations *in vitro* and begin to aggregate with the increase in concentration.[25,26] We have assessed IDab characteristics *in vivo* by expressing anti-RAS IDabs in NIH3T3 cells by transiently transfecting clones encoding either scFv or IDab antibody fragments and detection of expressed intrabodies by Western analysis using anti-FLAG tag antibody. This expression analysis was performed in the presence or absence of antigen expression and proteins were extracted from detergent lysed cells either in the soluble fraction or as post-lysis insoluble material collected by centrifugation. IDab and scFv intrabody proteins appeared in both the cellular fractions in this analysis (Figure 4A and B) and no significant differences were observed whether or not antigen was co-expressed. Significantly, anti-RAS IDab clones #6 and #10 seemed to be expressed as soluble proteins better than scFv formats. These results suggest that IDabs can be more stable in cells than the scFv format, perhaps because scFv have a peptide linker, which may lead to proteolysis susceptibility, following poor association of VH and VL *in vivo*.

Single domain intracellular antibodies can bind antigen *in vitro* with high affinity

Determinants of "intracellular affinity" in the complex milieu of the mammalian cell are binding affinity, expression levels and stability of the intrabody in presence and absence of antigen. It is not possible to determine binding affinity *in vivo* or to carry out studies of thermodynamic (or kinetic) stability or aggregation tendencies. However, to assess a parameter of intracellular affinity, we have determined the *in vitro* binding affinity of

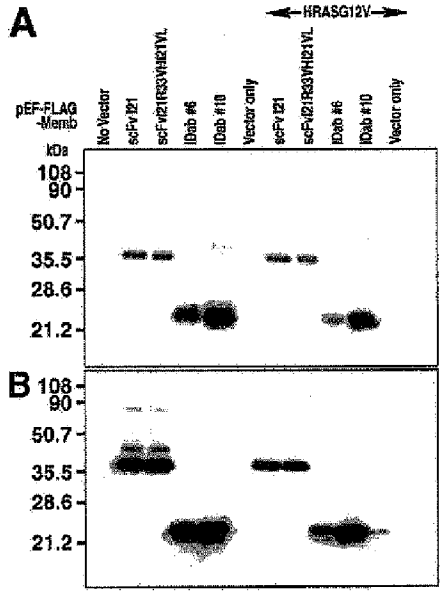

Figure 4. Expression of intrabodies in NIH3T3 cells. NIH3T3 clone D4 were transiently transfected with the expression vector pEF-FLAG-Memb encoding either scFv or IDab proteins with an N-terminal FLAG tag for detection purposes. Transfections were carried with or without the RAS antigen expression vector pZIP-neoSV(X)-HRASG12V as indicated. Soluble and "insoluble" proteins were extracted from NP40 lysed cells, separated as described[17] and fractionated on SDS-14% PAGE. After electrophoresis, proteins were transferred to membranes and detected with a anti-FLAG tag monoclonal antibody (M2, Sigma) and HRP-conjugated anti-mouse Ig antibody. The migration pattern of molecular mass markers (in kDa) is indicated on the left. A, Soluble fraction; B, insoluble fraction.

four selected anti-RAS IDab clones #3, #10, #12, compared to the original IDab 33. The Dab proteins were expressed in bacteria but the final yields of purified Dab proteins were rather low (up to 0.5 mg per litre of culture), presumably because purification and concentration invokes the stickiness and aggregation of Dabs at high concentration *in vitro*.[26]

We measured the RAS antigen-binding affinities of the IDabs using a biosensor. The K_d of scFv33 was found to be about 10 nM (Table 2) which is consistent with our previous study.[17] The mutated scFvI21R33VHI21VL (in which the framework of anti-RAS scFv33 is mutated to the I21 consensus VH but retains the I21 VL sequence) maintains the affinity of scFv33 (K_d about 18 nM) consistent with the importance of the VH–antigen interaction. Loss of affinity was observed when the VH of scFv33 was made into the IDab format (Table 2; K_d of about 90 nM), being about one order of magnitude weaker than original scFv33. The K_d of anti-RAS IDab clones #3, #10, and #12 were around 180 nM, 120 nM, 26 nM, respectively. Thus, there

Table 2. Affinity measurements of anti-RAS IDab proteins using a BIAcore

scFv/IDab	k_{on} (M^{-1} s^{-1})	k_{off} (s^{-1})	K_d (nM)
scFv33	$1.76(\pm 1.41) \times 10^5$	$1.13(\pm 1.16) \times 10^{-3}$	9.97 ± 8.82
scFvI21R33VHI21VL	$4.78(\pm 1.95) \times 10^4$	$8.65(\pm 0.78) \times 10^{-4}$	18.19 ± 1.85
IDab 33	$1.25(\pm 0.12) \times 10^4$	$1.44(\pm 0.68) \times 10^{-2}$	90.13 ± 9.70
IDab anti-RAS #3	$5.66(\pm 0.18) \times 10^5$	$1.04(\pm 0.01) \times 10^{-3}$	182.98 ± 7.19
IDab anti-RAS #10	$2.32(\pm 1.17) \times 10^4$	$2.54(\pm 0.34) \times 10^{-3}$	121.45 ± 46.6
IDab anti-RAS #12	$2.73(\pm 1.12) \times 10^4$	$7.05(\pm 2.28) \times 10^{-4}$	26.65 ± 2.90

His-tagged antibody fragments were produced by expression in bacteria and purified by Ni-NTA agarose affinity chromatography. Biosensor measurements were made using a BIAcore 2000. The Table summarises the values of association (k_{on}) and dissociation rates (k_{off}) together with calculated equilibrium dissociation constants (K_d) using BIA-evaluation 2.1 software. At high IDab concentrations, non-specific interactions between IDab and antigen were detected. scFv33[17]; scFvI21R33VHI21VL is an scFv derivative of scFv33 with VH framework regions of scFvI21, VH CDR1, 2 and 3 of scFv33 and VL of I21;[17] IDabs #3, #10 and #12 are intrabodies isolated from the IDab libraries using HRASG12V as a bait.

is no obvious correlation between the *in vitro* affinity of the anti-RAS IDabs (which is a measure of real antigen–antibody interaction) and *in vivo* activity (where the total *in vivo* antigen–antibody interaction involves several factors). These data suggest that it is worthwhile evaluating IDabs in both *in vivo* and *in vitro* assays but nonetheless the binding affinity component of the selected IDabs is within a suitable range for *in vivo* function as antigen-binding moieties.

Oncogenic transformation of NIH3T3 cells can inhibited by IDab intrabodies

The purpose of intrabodies is to ablate or otherwise interfere with the function of proteins inside cells, for instance to block an abnormal function in a cancer cell. The function of oncogenic RAS is mediated through constitutive signalling in tumours and this can be emulated by introducing mutant RAS (HRASG12V; with a glycine to valine mutation at codon 12) into NIH3T3 cells, resulting in loss of contact inhibition and focus formation in confluent cell cultures. We have shown that scFv intrabodies, which have been selected by IAC, can inhibit the RAS-mediated transformation.[17] We have evaluated the utility of IDabs to inhibit transformation, by carrying out RAS transformation assays in the presence or absence of these antibody fragments (Figure 5).

When an expression clone encoding mutant HRASG12V was transfected into NIH3T3 cells, growth of transformed, non-contact inhibited foci was detected (Figure 5A), whereas cells into which vector alone was introduced, retained their contact inhibition. This defined 100% and 0% relative transformation, respectively (Figure 5B). When the HRASG12V clone was co-transfected with scFvI21 (an scFv which has no detectable RAS binding in mammalian assays, although it is expressed efficiently[17]), the transforming ability of the mutant RAS was unaffected, since the numbers of foci observed with HRASG12V alone or HRASG12V plus scFvI21 were approximately the same (Figure 5A and B). Conversely, we observed an ablation of transforming activity when HRASG12V was co-expressed with anti-RAS scFv (scFvI21R33VHI21VL in which the scFv comprises VH of anti-RAS scFv33 with VL of I21[17]), with only around 20% of focus formation compared with the HRASG12V control alone (Figure 5B). Two anti-RAS IDabs were tested in this assay (IDab #6 and #10) which were chosen because of their excellent stimulation in the mammalian reporter assays (Figure 3) and their good expression characteristics in NIH3T3 cells (Figure 4). These behaved in a similar way to the anti-RAS scFv, showing a dramatic effect on the transformation index. Anti-RAS IDab #6 and #10 reduced the transforming activity of oncogenic HRASG12V to below10% of the transfected cells expressing HRASG12V alone (Figure 5B). Thus, these IDabs can be expressed in mammalian cells and in sufficient quantity and quality to inhibit tumorigenic transformation. The data indicate that the IDab selection procedure will be generally useful for generating reagents with sufficiently good *in vivo* properties to interfere with protein function in mammalian cells.

Discussion

Single domain antibody fragments are effective intrabodies

The purpose of using intracellular antibodies is to bind to target proteins *in vivo* and elicit a biological response. We have shown here that single domains (in this case, VH alone but VL alone should possess the same property) can be effective intracellular reagents showing excellent solubility and stability, and thus are ideal for binding specifically and with high affinity to antigen *in vivo*.

Several considerations make single domains attractive as intrabodies compared to scFv and other formats. The association of VH and VL domains is weak in scFv[27] and the dissociated form can be predominant becoming a target for aggregation and proteolysis inside cells. An alternative form of VH–VL heterodimer is the disulphide-stabilised Fv fragment (dsFv),[28] but this in not a good option for intrabodies because

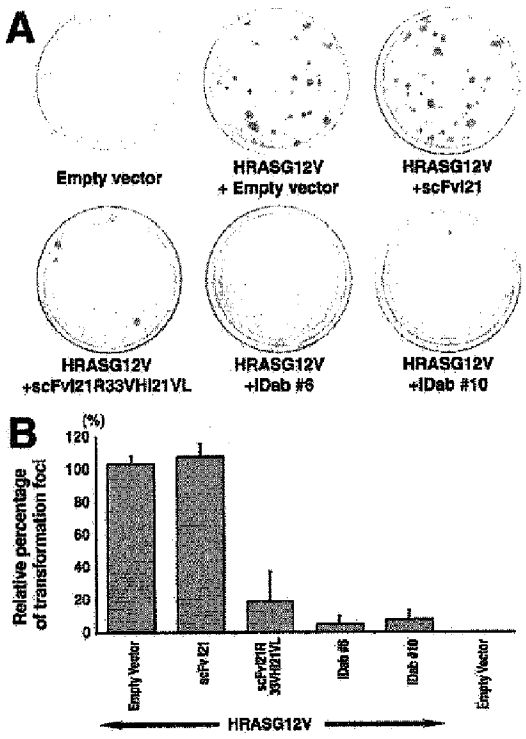

Figure 5. Inhibition of mutant RAS-mediated oncogenic transformation of NIH3T3 cells by anti-RAS IDabs. Mutant HRASG12V cDNA was cloned into the mammalian expression vector pZIPneoSV(X) and anti-RAS scFvs or IDabs were cloned into the pEF-FLAG-Memb vector (this encodes a protein with a plasma membrane targeting signal fused at the C terminus of each scFv or IDab and a FLAG-tag fused at the N terminus). pZIPneoSV(X)-HRASG12V (100 ng) and pEF-FLAG-Memb-scFv (2 μg) or pEF-FLAG-Memb-IDab were co-transfected into low passage NIH3T3 D4 cells using LipofectAMINE™ (Invitrogen). Two days later, the cells were transferred to 10 cm plates. After reaching confluence, cells were maintained for 14 days in DME medium containing 5% donor calf serum and the plates were stained with crystal violet to allow foci of transformed cells to be quantified. A, Photographs of representative NIH3T3 growth plates showing transformed foci. Empty vector in the top left panel indicates co-transfection with the pZIPneoSV(X) vector without cloned RAS together with the pEF-FLAG-Memb vector without cloned scFv or IDab. The other plates show cultures after transfections of cells with pZIPneoSV(X)-HRASG12V plus the indicated scFv or IDab pEF-FLAG-Memb expression vector. B, A histogram showing relative percentage of transformed foci, estimated as the number of foci normalised to the focus formation induced by pZIPneoSV(X)-HRASG12V together with the pEF-FLAG-Memb empty vector only (the value set at 100%). Results shown represent one experiment, in which each transfection was performed in duplicate (two additional experiments yield similar results).

the disulphide bond is not formed inside cells. Natural H chain antibodies are found in camel and related species in the absence of light chains and these are effective for binding and specificity *in vitro*.[29] *In vitro* VH libraries have been described[19,20,25] in which the VL interface of the VH domain was mutated to mimic the camel VH domain.[19,25,30] Camelisation of the VH framework of the anti-RAS VH IDabs (mutations G44E, L45R, W47G or W47I[19,25]) destroyed antigen-binding activity *in vivo* as judged by the luciferase reporter assay (data not shown). However, the IDabs described here, based on the IAC consensus scaffold, are expressed well as soluble proteins in cells and non-specific interactions with non-relevant antigen have not been detected. This suggests that modifications may not be useful for IDab intrabody applications. Rather, the employment of pre-defined immunoglobulin framework scaffolds is likely to be more useful, as these can exhibit properties attuned to the intracellular environment.[17] IDabs based on the IAC consensus[15,17] fulfil this prerequisite for function. Thus, single domain intracellular antibodies are the smallest antibody fragment known at present with potential for in cell use.

A robust, rapid and simple procedure is needed to identify effective intrabodies and our approach has taken advantage of direct screening in the *in vivo* milieu to facilitate the isolation of those intrabodies which can fold adequately, have sufficient stability and can function *in vivo*. Specially designed, diverse intrabody libraries have an advantage for this objective as the process of deriving antigen-specific intrabodies would be greatly simplified and success more likely. The single domain intrabody format provides the means to achieve this since libraries using the scFv format are limited by the complexity of the VH and VL combination where there are six random CDR loops. The maximum diversity using single domain libraries (only three CDR loops) is lower than scFv. Moreover, IDabs composed of monomeric domains may be advantageous for interaction with antigen as the contact area between antigen and antibody occurs over a small area, which could target small, hidden epitopes not accessible conventional scFv intrabodies. In these settings, IDabs might, for instance, recognise clefts formed by fusion of two protein domains which can result from chromosomal translocations in cancers.

Single domain intrabody library screening: IAC[2]

A key feature which increases the effectiveness of IDab libraries is the use of a pre-defined intrabody consensus VH framework sequence[15,17] as a scaffold for library diversification, since these sequences display ideal properties for intracellular function, such as expression, solubility and functionality without the requirement for the conserved

intra-domain disulphide bonds.[17] Furthermore, diverse IDab libraries are readily screened *in vivo* to generate sets of antigen-specific molecules. This approach is the second generation of the IAC method (IAC^2). The IAC^2 strategy comprises screening for IDabs in a yeast antibody–antigen interaction assay followed by verification of activity in mammalian cells using primarily a reporter assay, followed by an antigen-specific biological assay. The IAC^2 obviates the need for the preliminary selection of diverse phage scFv libraries *in vitro*, which in turn obviates the need for production of antigen *in vitro*, as the first step in the first generation IAC.[14] We have used consensus scaffold VH domain sequences[15,17] as frameworks for the construction of VH IDab libraries, so the effective "intracellular" diversity is greater than could realistically be achieved with scFv whilst requiring more limited physical diversity than if using all the VH subgroups.

In conclusion, single domain intrabodies (IDabs) can be isolated directly from *in vivo* bespoke intrabody libraries using a second generation IAC approach (IAC^2) and this new simple approach to derivation of functional intrabodies relies only on expertise of two-hybrid screening methods. Thus, IDabs can readily be obtained with IAC^2 and are good candidates to serve as a lead tools for therapeutics and functional genomics research.

Materials and Methods

Plasmids

Reporter plasmids

The reporter plasmids pG5-Luc[15,31] and pG5GFP-hyg[32] have been described. pRL-CMV was obtained from Promega Ltd.

Bait expression clones

The plasmids pM1-HRASG12V, pM1-LacZ[17] and pBTM-ATF-2[33] have been described. pM1-ATF-2 was made by sub-cloning the *Sma*I-*Bam*HI fragment from pBTM-ATF-2 into the pM1 vector.[34] For production of pM1-LexA, a LexA–DBD fragment was amplified from pBTM116[35] using BLEXAF2, 5′-CGCGGATCCTGAAA GCGTTAACGGCCAGG-3′ and BAMLEXAR, 5′-CGC GGATCCAGCCAGTCGCCGTTGC-3′, and cloned into the *Bam*HI site of pM1.

Intrabody expression clones

The intrabody expression plasmids pEF-scFv33-VP16 (anti-RAS), pEF-scFvI21R33-VP16 (anti-RAS)[17] and pEF-scFvR4-VP16 (anti-β-gal)[24,21] have been described. The clones pEF-33VH-VP16, pEF-I21R33VH-VP16, pEF-I21R33VH-C22S-VP16 and pEF-I21R33VH-C92S-VP16 were made by PCR amplification of the VH domain fragments from the parental pEF-scFv-VP16 (using the oligonucleotides EFFP, 5′-TCTCAAGCCTCAGA CAGTGGTTC-3′ and NotVHJR1′ 5′-CATGATGATGT GCGGCCGCTCCACCTGAGGAGACGGTGACC-3′; the latter introduces a *Not*I cloning site) and cloning into the *Sfi*I-*Not*I sites of pEF-VP16.[21] The pEF-33VL-VP16 and pEF-I21R33VL-VP16 domain fragments were amplified from the parental pEF-scFv-VP16 using VLF1 5′-ATCATGCCATGGACATCGTGATGACCCAGTC-3′ (this introduces a *Nco*I cloning site) plus VP162R, 5′-CAA CATGTCCAGATCGAA-3′ and sub-cloned into the *Nco*I-*Not*I sites of pEF-VP16.[21]

pHEN2-scFv or IDab (for bacterial periplasmic expression) were made by cloning the *Sfi*I-*Not*I fragments of the appropriate pEF-scFv-VP16 or pEF-IDab-VP16 into pHEN2 phagemid. The pZIPneoSV(X)-HRASG12V was made by cloning the coding sequence of HRASG12V mutant cDNA from pEXT-HRAS into the pZIPneoSV(X) vector.[36] The pEF-FLAG-Memb-IDab clones were made by inserting the appropriate *Sfi*I-*Not*I fragments of the pEF-IDab-VP16 clones into pEF-FLAG-Memb.[17]

All the above constructs were verified by sequencing.

Construction of yeast IDab libraries

The construction of the IDab libraries in the yeast prey expression vector pVP16* is described in detail elsewhere.[21] Two IDab libraries were made (designated IDab library 1 and 2; Table 1). For library 1 preparation, the VH templates were from the previously described scFv, viz. scFvI21R33 or scFv625, which have intrabody VH consensus frameworks, of which the scFv625 has the canonical consensus.[17,21] The VH CDR2 and CDR3 regions of these scFvs were randomised by PCR mutagenesis[21,37] using NNM for codon redundancy in the CDRs (where N = A, G, C or T and M = T or G) and the products cloned into pVP16*, to encode VH–VP16 AD fusion proteins. This produced two diverse sets of clones with variability in the VH CDR2 and CDR3 regions. The total number of clones for the I21R33-derived library was approximately 2×10^6 and of the scFv625 consensus-derived library was approximately 1.4×10^6. These were combined to give a total of approximately 3.4×10^6 clones (IDab library 1).

For the preparation of IDab library 2, the templates were the libraries described above. The CDR1 regions were randomised by mutagenesis[21,37] and cloned into pVP16*. This generated two diverse sets of clones with variability in the VH CDR1, CDR2 and CDR3 regions. The total number of clones obtained for the I21R33-derived library was approximately 3×10^7 and approximately 2.2×10^7 from the scFv625 consensus-derived library. These were combined to give a total of approximately 5.2×10^7 clones (IDab library 2). The diversity of the libraries was estimated by determination of the total number of colony forming units and sequencing randomly picked clones to verify both the presence of VH segments (~100% of clones had VH inserts) and the randomisation of CDRs. The latter showed that ~57% of clones in the I21R33-derived library and ~63% of clones in the scFv625 consensus-derived library had fully ORFs in VH and VP16 fusions; the other clones had stop codons in either CDR1, CDR2 or CDR3, introduced during the randomisation process (for the I21R33-derived library ~17%, ~13% and ~9% had stop codons in CDR1, CDR2 or CDR3, respectively; for the scFv625 consensus-derived library ~5%, ~26% and ~5% had stop codons in CDR1, CDR2 or CDR3, respectively) and thus the diversity in each library could be estimated at $\sim 1.7 \times 10^7$ and $\sim 1.4 \times 10^7$ for I21R33- and scFv625 consensus-derived libraries respectively (i.e. combined library 2 of $\sim 3 \times 10^7$).

Intracellular antibody capture (IAC) screening of IDab libraries

The screening of synthetic IDab libraries was performed according to the protocol of IAC technology, as described.[15,17] A detailed protocol is available†.

In outline, 500 μg of pBTM-antigen (bait) and 1 mg of the pVP16*-IDab library 1 or the pVP16*-IDab library 2 (preys) were co-transfected into *S. cerevisiae* L40. Positive clones were selected using the auxotrophic markers Trp, Leu and His. Positive clones were selected for his prototrophy and confirmed using β-gal filter assays. For the selected clones, true positive clones were confirmed by re-testing histidine dependent growth and β-gal activation, using relevant and non-relevant baits. Ten double positive clones causing the most rapid colour development in β-gal filter assays were selected and sequenced. More efficient selections can be achieved by first creating a yeast strain stably expressing the bait of interest (see also website indicated above).

Luciferase assays and Western blots

The luciferase reporter assay procedure has been described previously.[15,17] scFv or IDab intrabodies were cloned into the pEF-VP16 expression vector and the antigen into the pM1 vector. COS7 cells (2×10^5) were transiently co-transfected with 500 ng of pG5-Luc, 50 ng of pRL-CMV, 500 ng of pEF-scFv-VP16 or pEF-IDab-VP16 and 500 ng of pM1-antigen bait using 8 μl LipofectAMINE™ transfection reagent (Invitrogen), according to the manufacture's instructions. Forty-eight hours after transfection, the cells were washed, lysed and assayed using the Dual-Luciferase Reporter Assay System (Promega). Transfection efficiency was normalised to *Renilla luciferase* activity, which was obtained by co-transfection of pRL-CMV. The data represent two experiments, each performed in duplicate.

To confirm the expression of scFv-VP16 or IDab–VP16 fusion proteins, whole protein extracts were prepared by directly adding SDS-PAGE buffer to the transfected COS7 cell pellets. The lysates were analysed by SDS-PAGE, followed by Western detection using an anti-VP16 monoclonal antibody (14-5, Santa-Cruz Biotechnology) as the primary antibody and an HRP-conjugated rabbit anti-mouse IgG antibody (Amersham-Pharmacia Biotech, APB) as the secondary antibody. The blots were visualised using an ECL detection kit (APB). Analysis of expression of scFv or IDab intrabodies in NIH3T3 cells (D4 line, a kind gift from Dr C. Marshall) was carried out as described.[17] D4 cells were transfected with pEF-FLAG-Memb-scFv or pEF-FLAG-Memb-IDab with or without pZIPneoSV(X)-HRASG12V. Forty-eight hours after transfection, the cells were washed once with PBS, lysed in ice-cold lysis buffer (10 mM Hepes (pH 7.6), 250 mM NaCl, 5 mM EDTA, 0.5% (w/v) NP-40, 1 μg/ml of leupeptin, 1 μg/ml of pepstatin A, 0.1 mg/ml of aprotinin, 1 mM phenylmethanesulfonyl fluoride) and the cells recovered by centrifugation at 4 °C. The pellets ("insoluble" fraction) and the supernatants ("soluble" fraction) were analysed by SDS-PAGE, followed by Western detection using an anti-FLAG monoclonal antibody (M2, Sigma) as primary antibody.

† http://www2.mrc-lmb.cam.ac.uk/PNAC/Rabbitts_T/group/

Mammalian two-hybrid assays using CD4 or GFP reporter cells

CHO cells were grown in minimal essential medium alpha (MEM-α, Invitrogen) supplemented with 10% (v/v) foetal calf serum, penicillin and streptomycin. FACS analyses of the CHO-CD4 line[23] were performed essentially as described before.[38] The CHO-GFP line was established by transfecting the pG5GFP-Hyg vector into CHO cells using LipofectAMINE™ and selecting transfected cells for seven days in MEM-α containing 0.3 mg/ml of hygromycin B (Sigma). The CHO-GFP stable clone 39a was chosen for further assays. For FACS assays, 3×10^5 CHO-CD4 or CHO-GFP cells were seeded in six-well plates 24 hours before transfection. pM1-antigen (0.5 μg) and 1 μg of pEF-scFv-VP16 or pEF-IDab-VP16 were co-transfected into the cells. Forty-eight hours after transfection, cells were washed, dissociated and re-suspended in PBS. For the CHO-CD4 assay, induction of cell surface CD4 expression was detected by using an anti-human CD4 antibody (RPA-T4, Pharmingen) and FITC-conjugated anti-mouse IgG antibody (Pharmingen). The fluorescence of CHO-CD4 or of CHO-GFP cells was measured with a FACSCalibur (Becton Dickinson) and the data were analysed by the CELLQuest software.

Purification of IDab fragments *in vitro* and BIAcore affinity measurement

For *in vitro* assays, scFvs and IDabs were expressed and isolated from the bacterial periplasm as previously described.[17] IDab fragments were cloned into the pHEN2 vector containing the pelB leader sequence with a His-tag and a myc-tag. IDabs were induced with 1 mM isopropyl-β,D-thiogalactopyranoside (IPTG) in 1 l culture for four hours at 30 °C. The cells were harvested and periplasmic fractions extracted in 10 ml of cold TES buffer (0.2 M Tris–HCl (pH 7.5), 0.5 mM EDTA, 0.5 M sucrose). After dialysis against 2.5 l of PBS, including 10 mM imidazole at 4 °C, scFv and IDab fragments were purified using Ni-NTA agarose (QIAGEN), according to the manufacture's instructions, concentrated using Centricon concentrators (YM-10, Amicon) and aliquots were stored at −70 °C. Protein concentration was measured using a Bio-Rad Protein assay kit according to the manufacture's instructions. *In vitro* affinities of scFvs and IDabs were determined using surface plasmon resonance on a BIAcore 2000 instrument (Pharmacia Biosensor). The kinetic rate constants, k_{on} and k_{off}, were calculated using the software supplied by the manufacturer. K_d values were calculated from k_{off} and k_{on} rate constants ($K_d = k_{off}/k_{on}$). All measurements were performed in duplicate.

Transformation assays in NIH3T3 cells

Low passage NIH3T3 clone D4 cells were seeded at 2×10^5 cells per well in six-well plates, 24 hours before transfection. For transfection, 2 μg of pEF-FLAG-Memb-scFv or IDab vector and 100 ng of pZIPneoSV(X)-HRASG12V vector were used with 12 μl of LipofectAMINE™. Two days after transfection, the cells were transferred into 10 cm plates and grown at 37 °C. After reaching confluence, the cultures were kept for two weeks in Dulbecco's modified Eagle's (DME) medium containing 5% (v/v) donor calf serum (Invitrogen) with penicillin and streptomycin. Focus formation, due to

loss of contact inhibition, was scored by staining the plates with crystal violet.

Acknowledgements

This work was supported by the Medical Research Council. T.T. was supported partly by the Medical Research Council, by Kyoto University and by the National Foundation for Cancer Research. N.L. was supported by the Kay Kendall Leukaemia Fund. We thank Professor Antonino Cattaneo for pBTM-ATF-2, Dr Chris Marshall for NIH3T3 D4 clone cells, Dr Lawrence A. Quilliam for the pZIPneoSV(X) vector, Drs Roger Williams and Michael Pacold for the HRASG12V cDNA clone, Dr Chi Van Dang for CHO-CD4 cells and Dr Toshi Shioda for the pG5GFP-Hyg vector.

References

1. Trail, P. A. & Bianchi, A. B. (1999). Monoclonal antibody drug conjugates in the treatment of cancer. *Curr. Opin. Immunol.* **11**, 584–588.
2. Segal, D. M., Weiner, G. J. & Weiner, L. M. (1999). Bispecific antibodies in cancer therapy. *Curr. Opin. Immunol.* **11**, 558–562.
3. Rabbitts, T. H. & Stocks, M. R. (2003). Chromosomal translocation products engender novel intracellular therapeutic technologies. *Nature Med.* **9**, 383–386.
4. Collins, F. S. *et al.* (1998). New goals for the US Human Genome Project: 1998–2003. *Science*, **282**, 682–689.
5. Tuschl, T. (2002). Expanding small RNA interference. *Nature Biotechnol.* **20**, 446–448.
6. Cattaneo, A. & Biocca, S. (1999). The selection of intracellular antibodies. *Trends Biotechnol.* **17**, 115–121.
7. Rondon, I. J. & Marasco, W. A. (1997). Intracellular antibodies (intrabodies) for gene therapy of infectious diseases. *Annu. Rev. Microbiol.* **51**, 257–283.
8. Bird, R. E., Hardman, K. D., Jacobson, J. W., Johnson, S., Kaufman, B. M., Lee, S-M. *et al.* (1988). Single-chain antigen-binding proteins. *Science*, **242**, 423–426.
9. Huston, J. S., Levinson, D., Mudgett-Hunter, M., Tai, M-S., Novoty, J., Margolies, M. N. *et al.* (1988). Protein engineering of antibody binding sites: Recovery of specific activity in an anti-digoxin single-chain Fv analogue produced in *Escherichia coli*. *Proc. Natl Acad. Sci. USA*, **85**, 5879–5883.
10. Biocca, S., Pierandrei-Amaldi, P. & Cattaneo, A. (1993). Intracellular expression of anti-p21ras single chain Fv fragments inhibits meiotic maturation of xenopus oocytes. *Biochem. Biophys. Res. Commun.* **197**, 422–427.
11. Tavladoraki, P., Benvenuto, E., Trinca, S., De Martinis, D., Cattaneo, A. & Galeffi, P. (1993). Transgenic plants expressing a functional single-chain Fv antibody are specifically protected from virus attack. *Nature*, **366**, 469–472.
12. Proba, K., Worn, A., Honegger, A. & Pluckthun, A. (1998). Antibody scFv fragments without disulfide bonds made by molecular evolution. *J. Mol. Biol.* **275**, 245–253.
13. Worn, A. & Pluckthun, A. (1998). Mutual stabilization of VL and VH in single-chain antibody fragments, investigated with mutants engineered for stability. *Biochemistry*, **37**, 13120–13127.
14. Visintin, M. *et al.* (1999). Selection of antibodies for intracellular function using a two-hybrid *in vivo* system. *Proc. Natl Acad. Sci. USA*, **96**, 11723–11728.
15. Tse, E., Lobato, M. N., Forster, A., Tanaka, T., Chung, G. T. Y. & Rabbitts, T. H. (2002). Intracellular antibody capture technology: application to selection of single chain Fv recognising the BCR-ABL oncogenic protein. *J. Mol. Biol.* **317**, 85–94.
16. Visintin, M., Settanni, G., Maritan, A., Graziosi, S., Marks, J. D. & Cattaneo, A. (2002). The intracellular antibody capture technology (IACT): towards a consensus sequence for intracellular antibodies. *J. Mol. Biol.* **317**, 73–83.
17. Tanaka, T. & Rabbitts, T. H. (2003). Intrabodies based on intracellular capture frameworks that bind the RAS protein with high affinity and impair oncogenic transformation. *EMBO J.* **22**, 1025–1035.
18. Ward, E. S., Gussow, D., Griffiths, A. D., Jones, P. T. & Winter, G. (1989). Binding activities of a repertoire of single immunoglobulin variable domains secreted from Escherichia coli. *Nature*, **341**, 544–546.
19. Davies, J. & Riechmann, L. (1996). Single antibody domains as small recognition units: design and *in vitro* antigen selection of camelized, human VH domains with improved protein stability. *Protein Eng.* **9**, 531–537.
20. Reiter, Y., Schuck, P., Boyd, L. F. & Plaksin, D. (1999). An antibody single-domain phage display library of a native heavy chain variable region: isolation of functional single-domain VH molecules with a unique interface. *J. Mol. Biol.* **290**, 685–698.
21. Tanaka, T., Chung, G. T. Y., Forster, A., Lobato, M. N. & Rabbitts, T. H. (2003). *De novo* production of diverse intracellular antibody libraries. *Nucl. Acids Res.* **31**, e23..
22. Tse, E., Chung, G. & Rabbitts, T. H. (2000). Isolation of antigen-specific intracellular antibody fragments as single chain Fv for use in mammalian cells. In *Methods in Molecular Biology and Medicine* (Turksen, K., ed.), pp. 433–446, Humana Press, Totawa.
23. Fearon, E. R., Finkel, T., Gillison, M. L., Kennedy, S. P., Casella, J. F., Tomaselli, G. F. *et al.* (1992). Karyoplasmic interaction selection strategy: a general strategy to detect protein–protein interaction in mammalian cells. *Proc. Natl Acad. Sci. USA*, **89**, 7958–7962.
24. Martineau, P., Jones, P. & Winter, G. (1998). Expression of an antibody fragment at high levels in the bacterial cytoplasm. *J. Mol. Biol.* **280**, 117–127.
25. Davies, J. & Riechmann, L. (1995). Antibody VH domains as small recognition units. *Biotechnology (NY)*, **13**, 475–479.
26. Riechmann, L. & Muyldermans, S. (1999). Single domain antibodies: comparison of camel VH and camelised human VH domains. *J. Immunol. Methods*, **231**, 25–38.
27. Glockshuber, R., Malia, M., Pfitzinger, I. & Pluckthun, A. (1990). A comparison of strategies to stabilize immunoglobulin Fv-fragments. *Biochemistry*, **29**, 1362–1367.
28. Reiter, Y. & Pastan, I. (1996). Antibody engineering of recombinant Fv immunotoxins for improved targeting of cancer: disulfide-stabilized Fv immunotoxins. *Clin. Cancer Res.* **2**, 245–252.
29. Muyldermans, S., Cambillau, C. & Wyns, L. (2001). Recognition of antigens by single-domain antibody

fragments: the superfluous luxury of paired domains. *Trends Biochem. Sci.* **26**, 230–235.
30. Muyldermans, S., Atarhouch, T., Saldanha, J., Barbosa, J. A. & Hamers, R. (1994). Sequence and structure of VH domain from naturally occurring camel heavy chain immunoglobulins lacking light chains. *Protein Eng.* **7**, 1129–1135.
31. de Wet, J. R., Wood, K. V., DeLuca, M., Helinski, D. R. & Subramani, S. (1987). Firefly luciferase gene: structure and expression in mammalian cells. *Mol. Cell. Biol.* **7**, 725–737.
32. Shioda, T., Andriole, S., Yahata, T. & Isselbacher, K. J. (2000). A green fluorescent protein-reporter mammalian two-hybrid system with extrachromosomal maintenance of a prey expression plasmid: application to interaction screening. *Proc. Natl Acad. Sci. USA*, **97**, 5220–5224.
33. Portner-Taliana, A., Russell, M., Froning, K. J., Budworth, P. R., Comiskey, J. D. & Hoeffler, J. P. (2000). *In vivo* selection of single-chain antibodies using a yeast two-hybrid system. *J. Immunol. Methods*, **238**, 161–172.
34. Sadowski, I., Bell, B., Broad, P. & Hollis, M. (1992). GAL4 fusion vectors for expression in yeast or mammalian cells. *Gene*, **118**, 137–141.
35. Hollenberg, S. M., Sternglanz, R., Cheng, P. F. & Weintraub, H. (1995). Identification of a new family of tissue-specific basic helix-loop-helix proteins with a two-hybrid system. *Mol. Cell. Biol.* **15**, 3813–3822.
36. Cepko, C. L., Roberts, B. E. & Mulligan, R. C. (1984). Construction and applications of a highly transmissible murine retrovirus shuttle vector. *Cell*, **37**, 1053–1062.
37. Hoogenboom, H. R. & Winter, G. (1992). By-passing immunisation. Human antibodies from synthetic repertoires of germline VH gene segments rearranged *in vitro*. *J. Mol. Biol.* **227**, 381–388.
38. Tse, E. & Rabbitts, T. H. (2000). Intracellular antibody-caspase mediated cell killing: a novel approach for application in cancer therapy. *Proc. Natl Acad. Sci. USA*, **97**, 12266–12271.
39. Lefranc, M. P. (2002). IMGT, the international ImMunoGeneTics database: a high-quality information system for comparative immunogenetics and immunology. *Dev. Comp. Immunol.* **26**, 697–705.
40. Lefranc, M. P., Pommie, C., Ruiz, M., Giudicelli, V., Foulquier, E., Truong, L. *et al.* (2003). IMGT unique numbering for immunoglobulin and T cell receptor variable domains and Ig superfamily V-like domains. *Dev. Comp. Immunol.* **27**, 55–77.
41. Lefranc, M.-P. & Lefranc, G. (2001). *The Immunoglobulin FactsBook*, Academic Press, London.
42. Kabat, E. A., Wu, T. T., Perry, H. M., Gottesman, K. S. & Foeller, C. (1991). *Sequences of Proteins of Immunological Interest*, 5th edit., National Institutes of Health, Bethesda.

Edited by J. Karn

(Received 22 May 2003; received in revised form 23 June 2003; accepted 23 June 2003)